The University Of Sheffield.

Thesis Title

The role of shear stress and NF-κB in regulating endothelial dysfunction and atherosclerosis

By:

Neil P Bowden

A thesis submitted in partial fulfilment of the requirements for the degree of Doctor of Philosophy

The University of Sheffield
Faculty of Medicine, Dentistry & Health
Department of Infection, Immunity and Cardiovascular Disease

18/07/17

Acknowledgements

The last three and half years of work that have gone into this PhD thesis have been the most difficult yet rewarding time in my life. I couldn't have done it without the help of the wonderful friends, family and colleagues that have supported me.

Firstly, I would like to thank Paul Evans and Sheila Francis for their supervision, and the British Heart Foundation for funding my PhD. I'd also like to thank all the other members of the Evans' group and the rest of the O floor research office for being great company, giving great advice and setting all of the chocolate and cakes next to me for three years! Many members of the group and office have come and gone while I've been here, and I don't want to leave anyone out by mentioning specific names. Suffice it to say, those that have been my closest friends (I hope) know who they are. You've made my time in the lab a delight, and I'll miss you all.

I'd like to thank my parents, Jeremy and Karen, for their unending support throughout my life. I can credit my interest in biology to the day my dad brought an old microscope home, and my mum pricked her finger so that I could have a blood specimen to look at. There have been some tough times since I moved away to Sheffield, but your support and encouragement have helped me get to this point.

Lastly, I give the utmost thanks to my partner Natalie. I know your eyes glaze over when I talk about science, but you listened anyway. You've been by my side through the highs and lows of the last three years and I genuinely could not have done it without you.

Abstract

Atherosclerotic plaques are predominantly localised to bends and branches of arteries, where low shear stress causes altered gene expression in endothelial cells, leading to enhanced proliferation, apoptosis, inflammation and lesion development. A central regulator of these events is NF-κB signalling, comprising a family of transcription factors which can be subdivided into two pathways – canonical and non-canonical. While the canonical pathway is known to promote atherogenesis, investigation of the role of its negative regulator Cezanne (OTUD7B), has not been undertaken. Cezanne also inhibits the non-canonical NF-κB pathway, which has not been studied in the context of ECs exposed to shear stress. The hypothesis that Cezanne expression was regulated by shear stress and consequently modify NF-κB activity and lesion development was tested. In addition, the expression and role of non-canonical NF-κB was investigated in endothelial cells exposed to shear stress, and the contribution of Cezanne to this pathway also tested.

Immunofluorescence staining for Cezanne in the murine aortic arch revealed elevated expression at an atheroprone site. Exposure of human cells to shear stress in two complimentary flow systems *in vitro* showed enhanced expression under low shear stress. Following silencing of Cezanne, NF-κB phosphorylation was found to be enhanced, but no effect was detected on NF-κB target genes, or on non-canonical NF-κB. *Otud7b*$^{-/-}$ mice were also found to have no difference in NF-κB target gene expression or proliferation as measured by immunofluorescence staining; moreover, lesion size in *Otud7b*$^{-/-}$*Ldlr*$^{-/-}$ animals was unaltered.

The expression of non-canonical NF-κB subunits p100/p52 and RelB were also found be enhanced by low shear stress, in RNA isolated from porcine aortas as well as *in vitro*. Silencing and immunofluorescence staining revealed that the pathway promoted proliferation specifically at sites of low shear stress *in vitro*, via repression of p21. Analysis of proliferation in the aortic arches of *Nfkb2*$^{-/-}$ recapitulated this finding, with decreased proliferation at the inner curvature of the aortic arch, measured by Ki-67 positivity.

The conclusions were that Cezanne expression was elevated by low shear stress, and is responsible for inhibition of NF-κB phosphorylation, but does not affect target gene expression or the development of atherosclerosis. The non-canonical NF-κB pathway is also elevated by low shear stress. Cezanne did not alter its activity, which was to promote proliferation by inhibiting the expression of p21. This reveals a novel mechanism for the control of low shear stress proliferation, as well as identifying the role of non-canonical NF-κB in endothelial cells.

List of Figures

List of Tables

List of Abbreviations

ATF2	activating transcription factor 2
ACAT1	acyl-coenzyme A:cholesterol acyltransferase 1
B2M	β2 microglobulin
BAFF	B-cell-activating factor
BAFFR	BAFF receptor
BCA	bicinchoninic acid
BCL2	B-cell lymphoma 2
BSA	bovine serum albumin
cAMP	cyclic adenosine monophosphate
CBP	cAMP response element-binding protein binding protein
CD40	cluster of differentiation 40
CD40L	cluster of differentiation 40 ligand
CDK	cyclin-dependant kynase
Cezanne	cellular zinc-finger anti-NF-κB
CFD	computational fluid dynamics
ChIP	chromatin immunoprecipitation
cIAP	cellular inhibitor of apoptosis
CYLD	cylindromatosis tumour suppressor
DAPI	4,6-Diamidino-2-phenylindole
Dlk1	delta-like 1 homolog
DMEM	Dulbecco's modified Eagle's medium
DMOG	dimethyloxaloglycine
DPX	di-N-butylphthalate polystyrene xylene
DTT	dithiothreitol
DUB	deubiquitinating enzyme
E-selectin	endothelial selectin
EC	endothelial cell
ECM	extracellular matrix
EDTA	ethylenediaminetetraacetic acid
ENO2	enolase 2
eNOS	endothelial nitric oxide synthase
GADD45β	growth arrest and DNA-damage-inducible beta
HDAC	histone deacetylase
HIF	hypoxia inducible factor
HUVEC	human umbilical vein ECs
ICAM-1	intracellular adhesion molecule-1
IKK	IκB kinase
IL	interleukin
IL-1R	interleukin-1 receptor
IRAK	IL-1R-associated kinase
IκB	inhibitor of kappa B
JAMM	JAB1/MPN/MOV34 metalloenzyme
JNK	c-Jun N-terminal kinase
KLF2	Krüppel-like factor 2
LDL	low density lipoprotein
LPS	lipopolysaccharides
LT-β	lymphotoxin-β
LTβR	LT-β receptor
M-CSF	macrophage colony stimulating factor
MAP3K	MAPK kinase kinase
MAPK	mitogen activated protein kinase
MCP-1	monocyte chemoattractant protein 1
MEF	mouse embryonic fibroblast

MKP-1	MAPK phosphatase-1
MMP	matrix metalloproteinase
MyD88	myeloid differentiation primary response protein-88
NEMO	NF-κB essential modulator
NES	nuclear export sequence
NF-κB	nuclear factor κ-light-chain-enhancer of activated B cells
NIK	NF-κB-inducing kinase
NLS	nuclear localisation sequence
NO	nitric oxide
OTU	ovarian tumour protease
OTUD7B	OTU domain 7B
ox-LDL	oxidised LDL
PBS	phosphate buffered saline
PCNA	proliferating cell nuclear antigen
PCSK9	proprotein convertase subtilisin/kexen type 9
PECAM-1	platelet endothelial cell adhesion molecule
PFKFB3	6-Phosphofructo-2-kinase/fructose-2,6-biphosphatase 3
PVDF	polyvinylidene fluoride
RHD	Rel homology domain
RING	really interesting new gene
RIP1	receptor-interacting serine/threonine-protein kinase 1
ROS	reactive oxygen species
RSK1	ribosomal S6 kinase 1
SCF	Skp1-Culllin-1/Cdc53-F-box protein
SOD2	superoxide dismutase 2
T75	75 cm^2 growth area flask
TAB2	TAK1 binding protein 2
TAD	transactivation domain
TAE	Tris-acetate EDTA
TAK1	transforming growth factor-β-activated kinase-1
TBS	Tris-buffered saline
TBST	TBS Tween-20
TLR	Toll-like receptor
TNFR	TNFα receptor
TNFα	tumour necrosis factor α
TOLLIP	Toll interacting protein
TRADD	TNFR-associated death domain protein
TRAF	TNFR-associated factor
UCH	ubiquitin C-terminal hydrolase
USP	ubiquitin-specific protease
UXT	ubiquitously expressed transcript protein
VCAM-1	vascular cell adhesion molecule 1
VE-cadherin	vascular endothelial cell cadherin
VEGF	vascular endothelial growth factor
VEGFR2	vascular endothelial growth factor receptor 2
VHL	von Hippel-Lindau tumour suppressor
VSMC	vascular smooth muscle cell
ZA20D1	zinc finger A20 domain-containg protein 1
βTrCP	β-transducin repeat containing protein

Table of Contents

1. Introduction

Atherosclerosis is a chronic disease of the vascular system which can lead to angina pectoris, myocardial infarction or stroke, together responsible for over 400,000 hospital episodes in the UK each year (British Heart Foundation, 2016), and in 2015 accounted for 27% of all deaths (Townsend et al., 2015). It is not a modern disease, having been identified in ancient Egyptian remains (Zimmerman, 1993) and documented for hundreds of years. Leonardo da Vinci, who performed various autopsies on blood vessels of the young and old in the early sixteenth century, remarked that in the vessels of the old "the coat thickens so much that they close themselves up and stop the movement of the blood" (Boon, 2009). Indeed, this is a simplified definition of the pathology of atherosclerosis. The arterial thickening described by da Vinci is in fact development of fatty lesions on the inner wall of arteries.

These atherosclerotic plaques are a complex arrangement of various cell types, extracellular matrix and lipids, the development of which takes place over the lifetime of an individual. Plaque development is outlined in Figure 1.1. They begin as early "fatty-streak" type lesions which have been detected even in foetal aortas (Napoli et al., 2005). Endothelial cells (ECs) which line the lumen of blood vessels secrete chemokines such as monocyte chemoattractant protein 1 (MCP-1) when they are activated, which attract circulating leukocytes to the endothelium. These cells then attach to the vessel wall, aided by the presence of adhesion molecules like vascular cell adhesion molecule 1 (VCAM-1) and endothelial selectin (E-selectin). Subsequently, monocytes transmigrate through the endothelium into the subendothelial space, in part driven by enhanced endothelial junctional permeability at disease sites (Jaipersad et al., 2013; Libby, 2002).

Within the intima, monocytes differentiate into macrophages as a result of macrophage colony stimulating factor (M-CSF) and other molecules, and begin to take up low density lipoprotein (LDL) (Weber and Noels, 2011). The permeable endothelium allows transport of circulating LDL into the intima, where it can become oxidised (ox-LDL) through exposure to transition metal ions or via the oxidative actions of enzymes expressed by ECs, vascular smooth muscle cells (VSMCs) or macrophages (Yoshida and Kisugi, 2010). Scavenger receptors such as CD36 and scavenger receptor A on the surface of macrophages are responsible for the majority of ox-LDL uptake. Within the cell, acyl-coenzyme A:cholesterol acyltransferase 1 (ACAT1) activity results in the esterification of LDL cholesterol, which subsequently is stored in cytoplasmic lipid droplets (Yu et al., 2013). These lipid-laden macrophages are referred to as foam cells due to the appearance of the lipid droplets within the cytoplasm.

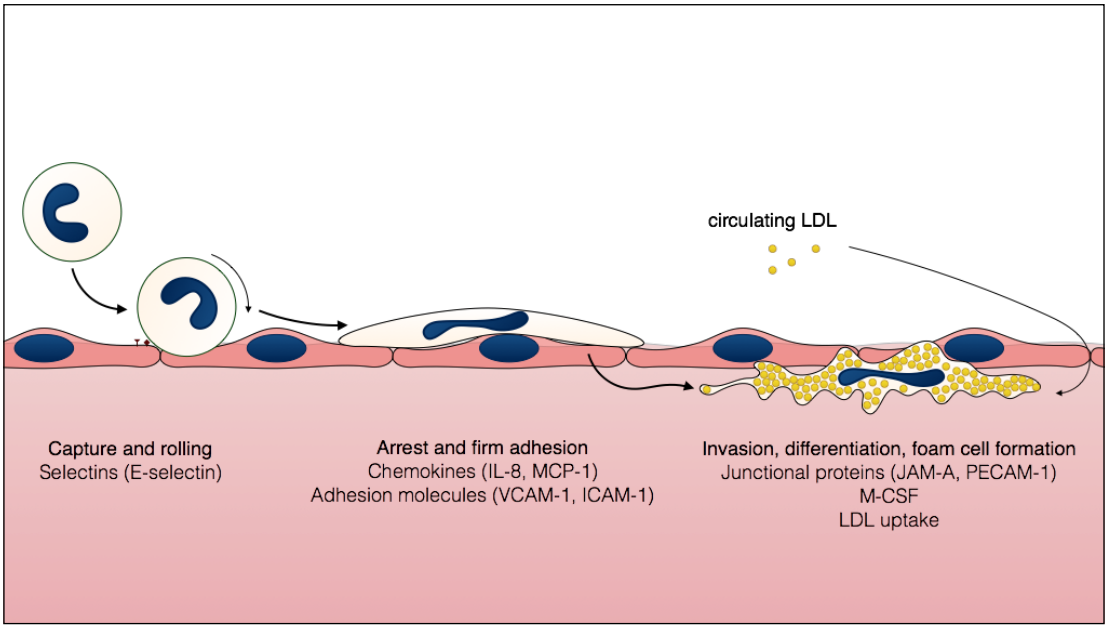

Figure 1.1: The mechanism of atherogenesis. Monocytes circulating in the blood weakly adhere to activated endothelial cells through the action of selectins including E-selectin. The weak adhesion causes the monocyte to 'roll' along the endothelial surface, driven by chemokines like IL-8 and MCP-1 until interaction with the adhesion molecules VCAM-1 or ICAM-1 cause firm adhesion. Adherent monocytes then invade the endothelium, interacting with junctional proteins, and differentiate into macrophages. These macrophages take up LDL which has been oxidised in the intima, causing a build-up of lipid bodies within their cytoplasm. These lipid-laden 'foam cells' are responsible for early fatty-streak lesions, and their continued growth and apoptosis lead to the formation of plaques.

Further inflammatory and growth-factor signalling from ECs, foam cells and other invading leukocytes like T cells and neutrophils (Döring et al., 2015) causes infiltration of more monocytes and proliferation of foam cells. In addition, circulating progenitor cells can infiltrate the subendothelial space and differentiate into VSMCs which further proliferate, leading to intimal thickening (Sata et al., 2002). VSMCs from the arterial wall can also play a role in pathogenesis; these cells become phenotypically altered, changing from a contractile to synthetic phenotype, and migrating into the intima, where they too begin to proliferate and lay down collagen to create a fibrous cap (Bennett et al., 2016; Lopes et al., 2013). Cytokine release and oxidative stress within the intima leads to apoptosis of foam cells, which deposit their lipid contents into the extracellular matrix while also further enhancing inflammatory signalling (Seimon and Tabas, 2009).

Over a period of years, this process continues and the lesion grows in size until it begins to occlude the blood vessel. When a lesion partially blocks a vessel, it gives rise to conditions such as angina pectoris or peripheral arterial disease, whereby impaired oxygen availability as a result of poor circulation causes pain in the affected area. In some cases, this is a stable condition; a higher degree of lesion fibrosis is associated with stable angina pectoris which has a low cardiovascular event rate (Bando et al., 2015).

In contrast, a thin fibrous cap can lead to plaque rupture (Stone et al., 2011). In part driven by the action of matrix metalloproteinases (MMPs) which degrade the cap (Agewall, 2006), plaque rupture results in the core of the plaque being exposed to the bloodstream. The presence of thrombogenic stimuli within the core generates thrombus formation on the surface of the plaque, which can serve to completely occlude blood flow if arterial narrowing is already severe (Libby, 2002). These cases can result in myocardial infarction if in a coronary artery, stroke if in an artery supplying the brain or ischaemia of the affected limb or organ if in another artery. The prognosis for these conditions is worse; myocardial infarction and stroke can be fatal as a result of loss of oxygen to these critical organs, and survival rates are largely dependent on the length of time before a patient can be treated (Martin et al., 2014). Due to the rate of disease incidence associated with atherosclerosis, it represents a significant burden to the health service and therefore research into preventative medicine is critical; understanding how the disease develops may aid in finding a method to reduce its prevalence.

There are several medical and environmental risk factors which play large roles in the development of atherosclerosis. Blood cholesterol and cigarette smoking are two of the most important risk factors; elevated cholesterol increases the amount of LDL available for uptake by foam cells, while cigarette smoking increases reactive oxygen species (ROS) concentrations in the blood which can oxidise this LDL and promote inflammation

(Csordas and Bernhard, 2013). Obesity, poor diet and physical inactivity also play roles in increasing an individual's risk of developing the disease (Dod et al., 2010; Hjermann et al., 1981; Yusuf et al., 2004). However, while these factors are systemic in nature, applying throughout the vasculature, the development of atherosclerotic lesions is focal, occurring predominantly at bends and branches within the arteries.

Lining the inner wall of the blood vessels, ECs provide an interface between the circulating blood and the tissues of the vessel wall. These cells are responsible for a variety of physical and biochemical functions which act in concert to maintain vascular health. These functions, reviewed by Michiels (2003) include acting as a barrier between blood components and VSMCs; contributing to vasodilation through nitric oxide (NO) signalling to VSMCs; the development of new blood vessels through angiogenesis; and regulation of inflammation. Quiescent ECs maintain the health of the vasculature, however at sites prone to atherosclerosis, disease development is promoted through the dysregulation of EC physiology. The resulting changes include morphological differences, with ECs adopting rounded, cobble-stone shapes rather than aligning with the direction of the arterial blood flow (Reidy and Langille, 1980). At atheroprone sites, ECs also exhibit elevated turnover (Davies et al., 1986), rates of proliferation (Akimoto et al., 2000) and apoptosis (Choy et al., 2001). Furthermore there is increased inflammatory signalling activity through the mitogen activated protein kinase (MAPK) and nuclear factor kappa-light-chain-enhancer of activated B cells (NF-κB) pathways (Warboys et al., 2011), the latter of which will be focused on in more detail in this report. A great deal of research has been carried out to determine the particular factors at the bends and branch points of the vascular system leading to this observed endothelial dysfunction and thus atherosclerosis.

1.1 Vessel haemodynamics contribute to plaque localisation and progression

The environment in which a plaque develops is not only governed by biochemical processes which occur within and between cells, but also through physical forces which shape the cellular response. Blood flowing through the vasculature exerts several forces on the cells, including hydrostatic pressure, cyclic stretch across the cardiac cycle and shear stress. Caro et al. (1969) proposed that the focal nature of atherosclerosis results from these mechanical properties of blood flow. Contrary to literature at the time which assumed that sites prone to atherosclerosis would be subject to mechanical damage from rapid flow, Caro identified that atherosclerosis was preferentially located at sites where the wall shear stress of blood against the endothelium is locally decreased. This was confirmed using glass-blown models of the human aorta and correlation to regions of

atherosclerosis in human tissue samples (Caro et al., 1971). Shear stress is the frictional force exerted on a surface by the movement of another substance across it, in the case of haemodynamics it is exerted on ECs by the movement of blood. It is a function of blood velocity, blood viscosity and vessel diameter, defined by the equation:

$$Wall\ shear\ stress = \frac{4\mu Q}{\pi r^3}$$

Where μ is viscosity, Q is flow rate and r is vessel radius (Cunningham and Gotlieb, 2005). Since Caro's initial publications, more sophisticated computational fluid dynamics (CFD) models have been generated which can more precisely map and characterise the forces generated by blood flow at these regions in different species (Chatzizisis et al., 2011; Feintuch et al., 2007; Lantz et al., 2012; Samady et al., 2011; Serbanovic-Canic et al., 2016).

Although the specific haemodynamics can be an order of magnitude apart in different species, sites of lesion development tend to have similar features. In these models, blood flow at regions prone to atherosclerosis is complex, characterised by flow recirculation, oscillation, lower velocity and shear stress while regions protected from atherosclerosis are more ordered, possessing higher velocity and shear stress with a unidirectional flow (Figure 1.2).

Elegant *in vivo* studies have solidified the causative link of low shear stress in the development of atherosclerosis by utilising murine models of atherosclerosis along with techniques to alter shear stress within the vasculature (Figure 1.3). Implantation of a flow-restricting cuff is one method of carrying this out, whereby a cast with fixed internal geometry is placed around a carotid artery, altering the shape of the vessel to create regions of low shear stress, high shear stress and oscillating shear stress. The development of atherosclerosis was found to be induced specifically at the low and oscillating shear stress regions, and not in high shear stress or in the contralateral artery with no cuff (Cheng et al., 2006). A similar result was found with a different method of inducing low shear stress. Nam et al. (2009) found that partial ligation of one carotid artery resulted in low, oscillating shear stress in that vessel, with an increase in shear in the other. Again, analysis of lesion development showed a localisation to the low shear stress region. This difference in lesion development determined by the biomechanical forces exerted on ECs reveals the crucial role that these cells play in altering vessel susceptibility to disease.

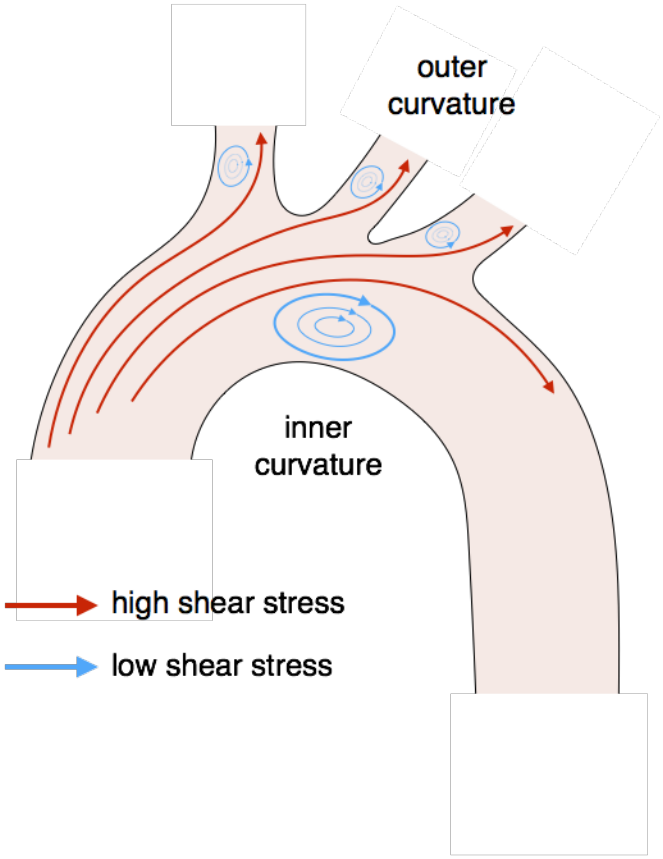

Figure 1.2: Simplified shear stress dynamics of the aortic arch. Blood flowing through the vasculature is not uniform, illustrated by this diagrammatic representation of an aortic arch. At branch points, shear stress is high (red arrow) on the downstream wall of the branch, while on the upstream wall the shear stress is lower (blue arrow) and the flow pattern is more complex, including oscillations. Similarly at bends in the vessels, the outer wall of the bend experiences unidirectional flow with high shear, while shear stress at the inner wall is lower and recirculation zones are present.

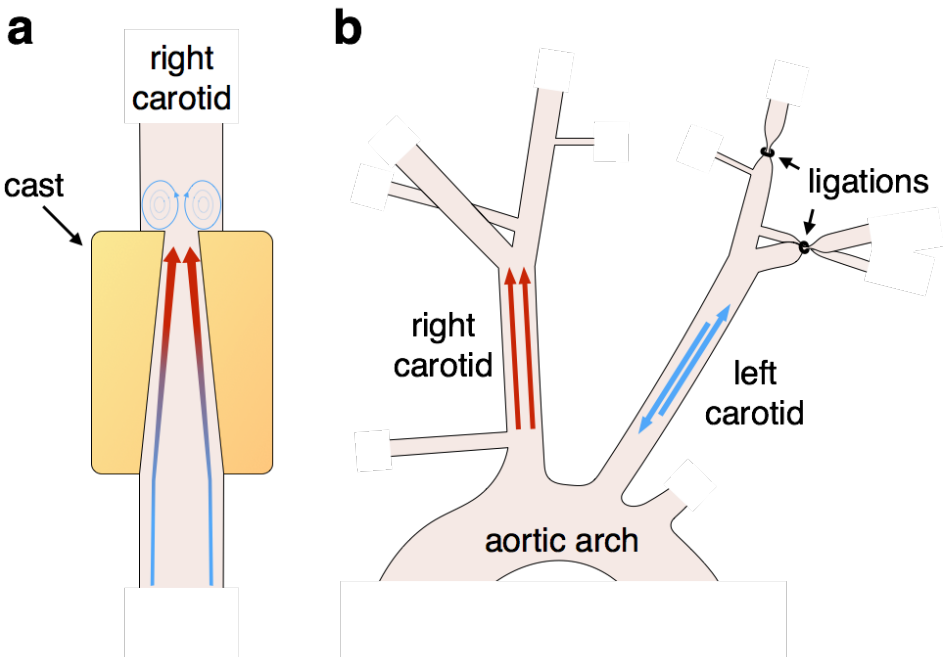

Figure 1.3: Methods to alter shear stress *in vivo*. This illustration shows two methods which have been successfully used to alter the natural shear stress experienced by ECs in the murine vasculature. **(a)** The right carotid artery after placement of a constrictive cuff. Shear stress is relatively low upstream, but the gradual narrowing of the cast interior causes an increase. Upstream of the cast, regions of oscillatory shear stress form. **(b)** Partial carotid ligation of the left carotid artery induces oscillatory flow. Ligation of three of the four branching arteries (external carotid artery, internal carotid artery and occipital artery) of the left carotid artery causes reciprocal flow of low shear stress in that artery, while increasing the shear stress in the right carotid artery.

1.1.1 Exposure to different shear stress patterns regulates EC gene expression and phenotype

Differences in shear stress can potentially lead to EC dysfunction via two mechanisms. The first is that due to a decrease in flow velocity and an increase of recirculation at sites of low shear stress, there is an increase in the transport of blood molecules into the endothelium (Tarbell, 2003). There are various data which support this hypothesis, suggesting that not only biologically inert molecules like albumin (Staughton et al., 2001), but also LDL may show an increased rate of transport into the subendothelial space (Wada and Karino, 2002). Additionally, at atheroprone sites, a low oxygen environment is generated (Santilli et al., 1995), explained by an increase in oxygen uptake and consumption but a decrease in oxygen replacement due to flow stagnation. This can activate hypoxic signalling (Akhtar et al., 2015), and lead to a further increase in LDL uptake through inducing apoptosis, creating gaps in the endothelium at so-called leaky junctions (Weinbaum et al., 1985), as well as generation of ROS which can activate ECs (Heo et al., 2011).

The second mechanism by which shear stress can regulate EC dysfunction is via direct sensing of the mechanical force, transducing this into biochemical signals. Evidence which points specifically to mechanosensing as a mechanism of physiological changes in ECs comes primarily from *in vitro* studies, where it is possible to introduce artificial flow conditions to cultured cells. In these systems, unidirectional flow has been shown to suppress inflammatory activation (Chiu et al., 2005; Partridge et al., 2007; Surapisitchat et al., 2001), proliferation (Akimoto et al., 2000) and apoptosis (Dimmeler et al., 1996), observations which are also supported *in vivo* at sites protected from atherosclerosis.

The phenotypic changes observed in ECs as a result of differences in shear stress arise from significant shifts in gene expression profiles. Several unbiased screens have been carried out to date, investigating differences in EC gene expression between samples exposed to different shear stress patterns (Dunn et al., 2014; Ni et al., 2010; Passerini et al., 2004; Serbanovic-Canic et al., 2016). Combined, these studies show that cells exposed to high and low shear stress display differential expression of hundreds of genes, in pathways including inflammation, proliferation, apoptosis and development. Modification of gene expression may result from altered molecular transport, mechanosensing, or perhaps a combination of both. Oxidised LDL – and other circulating molecules such as interleukin-1β (IL-1β) and cluster of differentiation 40 ligand (CD40L) – can stimulate expression of inflammatory target genes such as VCAM-1 and E-selectin (Collins et al., 1995; Cominacini et al., 2000; Henn et al., 1998). However, expression of these molecules can also be altered by shear stress alone, with

ECs exposed to low shear stress *in vitro* displaying similar phenotypes to those at disease prone sites *in vivo* (Dardik et al., 2005). This may be mediated by the function of mechanosensory complexes such as the platelet endothelial cell adhesion molecule (PECAM)-1, vascular endothelial cell cadherin (VE-cadherin) and vascular endothelial growth factor receptor 2 (VEGFR2) complex (Tzima et al., 2005). This complex is able to transduce mechanical signals of blood flow to invoke physiological changes under laminar flow. Cells deficient in either VE-cadherin or PECAM-1 were found to not align under flow as wild-type cells do, furthermore as well as impaired EC alignment in the aorta, PECAM-$1^{-/-}$ mice showed reduced inflammatory activity at atheroprone sites.

Regulation of the expression of such a large number of genes is possible through modification of the expression or activity of transcription factors or transcriptional coactivators such as Krüppel-like factor 2 (KLF2), histone deacetylases (HDACs) or NF-κB (Hajra et al., 2000; Lee et al., 2012), which can act alone or together to promote or repress the expression of many genes. Of particular interest in this thesis is the shear stress modulation of NF-κB signalling, pathway members of which have been implicated in playing a key role in regulating EC inflammation, apoptosis and proliferation (Van der Heiden et al., 2010). Understanding how this pathway functions to regulate these key markers of endothelial dysfunction may give insight into the development of atherosclerosis.

1.2 NF-κB signalling

The NF-κB family is a group of transcription factors which regulate many cellular processes, including immune cell activation, differentiation, cell growth and survival, and tissue inflammation. There are five subunits which make up the family, illustrated in Figure 1.4: RelA, RelB, c-Rel, p50 and p52 (Hayden and Ghosh, 2008). These combine by homo- or heterodimerisation to form active transcription factors. NF-κB subunits are characterised by the presence of a well conserved Rel homology domain (RHD; (Vallabhapurapu and Karin, 2009). This domain folds into two distinct subdomains (Figure 1.5) with a short linker region between. The carboxy-terminal subdomain is responsible for the dimerisation of NF-κB subunits while the amino-terminal subdomain wraps around a DNA helix, bringing the linker region into contact with the major groove of DNA and thus permitting transcription factor activity through the transactivation domain (TAD) found only on RelA, RelB and c-Rel (Müller and Harrison, 1995). The p50 and p52 subunits require activation by proteasomal processing from their respective precursors p105 and p100. The mature proteins may still bind DNA but can only serve to inhibit transcription without interaction with a cofactor activator (Beinke and Ley, 2004).

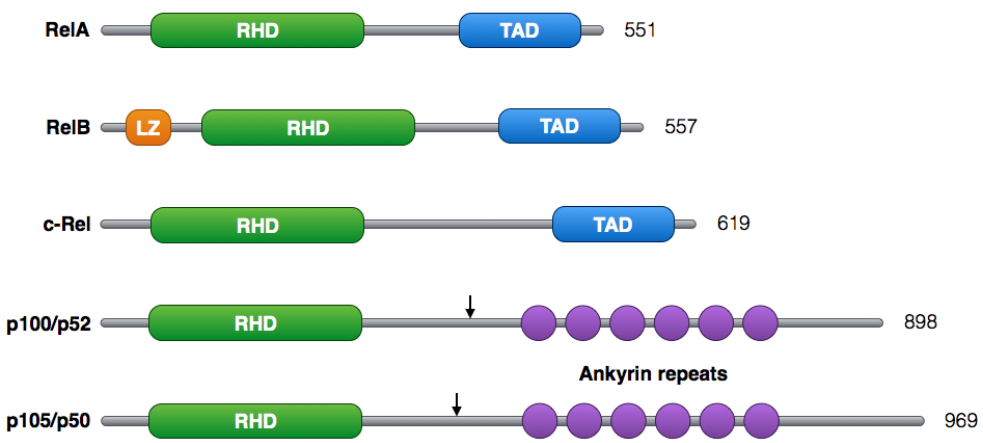

Figure 1.4: Domain structures of the five NF-κB family subunits. The five subunits of the NF-κB family show varying amounts of similarity to each other. All five possess the Rel homology domain (RHD) responsible for DNA binding activity. Only RelA, RelB and c-Rel possess the C terminal transactivation domain (TAD) that confers the ability to activate transcription of target genes. The remaining subunits – p52 and p50 – are processed from larger precursors by proteasomal processing, with the cleave site shown as an arrow in each. The precursors can act as inhibitors of NF-κB activation through their ankyrin repeats; the mature forms require heterodimerisation with another subunit to activate gene transcription.

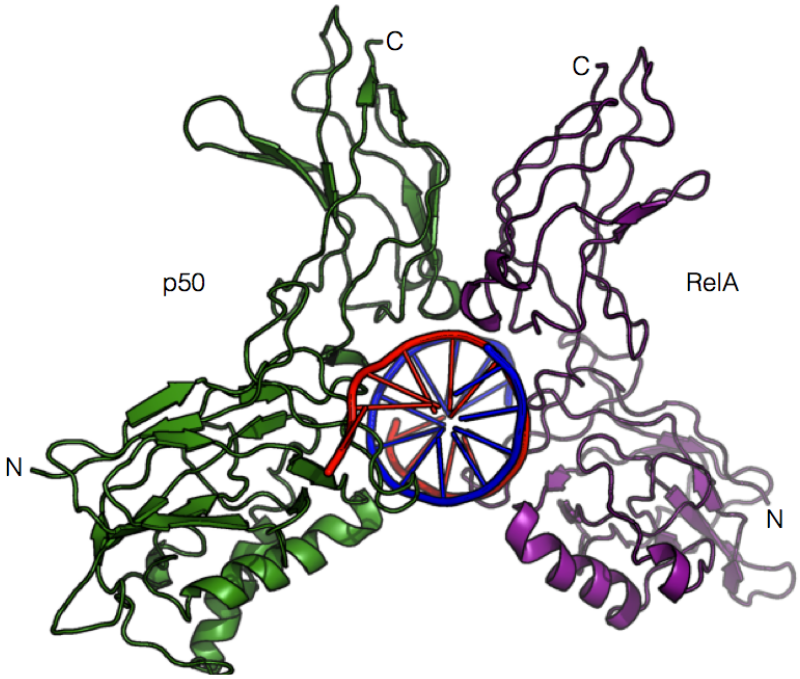

Figure 1.5: Structure of NF-κB bound to DNA. The structure of the p50/RelA dimer bound to DNA reveals the distinct subdomain structure of the RHD. The C terminal mediates dimerisation through β-sheet interactions, while the link between the N and C termini is responsible for binding DNA in the major groove.
Structure downloaded from the Protein Data Bank, solved by Chen et al., 1998.

NF-κB activation can be initiated by a diverse range of stimuli (discussed further below), and the pathway exhibits stimulus-dependent and cell-type-dependent regulation of gene expression (reviewed by Sen and Smale, 2009). In part this may be due to cofactors such as cyclic adenosine monophosphate response element binding protein (CREB) binding protein (CBP)/p300 and ubiquitously expressed transcript protein (UXT) (Vanden Berghe et al., 1999; Sun et al., 2007), which can bind to NF-κB and enhance its transcriptional activity. In addition, post-translational modification of NF-κB subunits can alter their activity and consensus sequence (Perkins, 2006). Phosphorylation at the serine 276 residue of RelA by protein kinase A regulates binding to the transcriptional coactivators CBP and p300, a change which results in an induction of NF-κB activity (Zhong et al., 1998), while phosphorylation at serine 536 may alter turnover from promoter regions and target gene specificity (Bohuslav et al., 2004; Lawrence et al., 2005; Moles et al., 2013; Sasaki et al., 2005).

Perhaps the most important mechanism by which NF-κB signalling is regulated is in the combination of subunits which make up the active dimer. The consensus sequence of members of the NF-κB family is usually written as a variant of 5' GGGRNNYYCC 3', where 'R' represents a purine, 'Y' a pyrimidine and 'N' any nucleotide (Natoli et al., 2005). However, due to the heterogeneity of the total population of NF-κB dimers this is only an approximation. There are 15 possible homo- or heterodimeric combinations, 12 of which have been confirmed *in vivo* (Hoffmann et al., 2006). Certain dimers are more common; RelA and c-Rel preferentially dimerise with p50 – indeed the most abundant NF-κB dimer is RelA/p50 – but RelB instead shows preference for p52 dimerisation (Vallabhapurapu and Karin, 2009). These two groups of dimers have almost entirely different mechanisms of upstream activation and are responsible for the activation of distinct genes, although the mechanism for this is not yet fully understood. Thus, NF-κB activation is separated into two pathways; the canonical and non-canonical pathways.

1.3 Activation of NF-κB signalling

NF-κB activity relies on its ability to bind DNA (Figure 1.5). In unstimulated cells, NF-κB dimers are retained in the cytoplasm through blocking of the nuclear localisation sequence (NLS) - found at the C-terminal end of the RHD - by inhibitory molecules of the family of inhibitor of κB (IκB) of which there are three typical molecules: IκBα, IκBβ and IκBε. Multiple ankyrin repeats present on IκB molecules are responsible for binding to the NLS of one or both of the subunits of the NF-κB dimer. This results in either a flux of NF-κB across the nuclear membrane through the action of a free NLS (Jacobs and Harrison, 1998) and opposing nuclear export sequence (NES) on the C terminus of IκBα or –ε (Arenzana-Seisdedos et al., 1997; Lee and Hannink, 2002), or constitutive

cytoplasmic localisation of the NF-κB:IκBβ complex through blocking of both NLSs (Malek et al., 2001). IκBα can additionally provide a dampening mechanism of negative feedback; its expression is induced by NF-κB and it is subsequently able to transport cytoplasmic dimers back to the cytoplasm, creating oscillations of nuclear NF-κB as a hallmark of the response (Nelson et al., 2004). In addition to the typical IκBs, unprocessed p100 and p105 can act as inhibitors through the ankyrin repeat domain present in place of the TAD (Basak et al., 2007; Beinke and Ley, 2004). In all cases, inactive NF-κB is primarily localised to the cytoplasm; however, the mechanism of cytoplasmic release differs between the canonical and non-canonical pathways.

1.3.1 Canonical NF-κB

The canonical NF-κB pathway (Figure 1.6) is responsible for activation of p50, RelA and c-Rel dimers. Its main characteristic is proteasomal degradation of IκB as a means to release NF-κB from its cytoplasmic retention and allow translocation to the nucleus. Various receptors are responsible for the initial stimulus to activate the canonical NF-κB pathway. TNFR (tumour necrosis factor α (TNFα) receptor), TLRs (Toll-like receptors) and IL-1R (interleukin-1 receptor) have all been discovered to be involved, among others (de Winther et al., 2005). Each receptor differs slightly in its mechanism of activation but these feed into the same pathway downstream. Different pathways can be categorised broadly by the signal adaptors which perpetuate the activation of each receptor. Signalling through TNFα to TNFR first recruits the adaptor protein TNFR-associated death domain protein (TRADD), which binds to TNFR (Hsu et al., 1995), then secondly TNFR-associated factor 2 (TRAF2) (Hsu et al., 1996a), and finally receptor-interacting serine/threonine-protein kinase 1 (RIP1) (Hsu et al., 1996b). TLRs and IL-1R function in an analogous manner, utilising the adaptors MyD88 (myeloid differentiation primary-response protein-88), TOLLIP (Toll interacting protein) and IRAK (IL-1R-associated kinase) family proteins in place of TRADD. These proteins activate another TRAF family protein, TRAF6.

Both RIP1 and TRAF6 are then involved in a complex polyubiquitin signalling network, which unites the different upstream signals into a single pathway. RIP1 becomes ubiquitinated by lysine-63 (K63) or -11 (K11)-linked ubiquitin chains (Dynek et al., 2010; Lee et al., 2004). As TRAF2 possess E3 ubiquitin ligase activity, which is the enzymatic reaction responsible for the addition of the first ubiquitin molecule to a specific site of the target protein, it was thought that it was directly responsible for catalysing ubiquitination of RIP1. In fact, two more proteins known as cellular inhibitors of apoptosis 1 and 2 (cIAP1 and -2) also associate with TRAF2 to carry out E3 ubiquitin ligase function as a complex (Bertrand et al., 2008; Vince et al., 2009). TRAF6 may

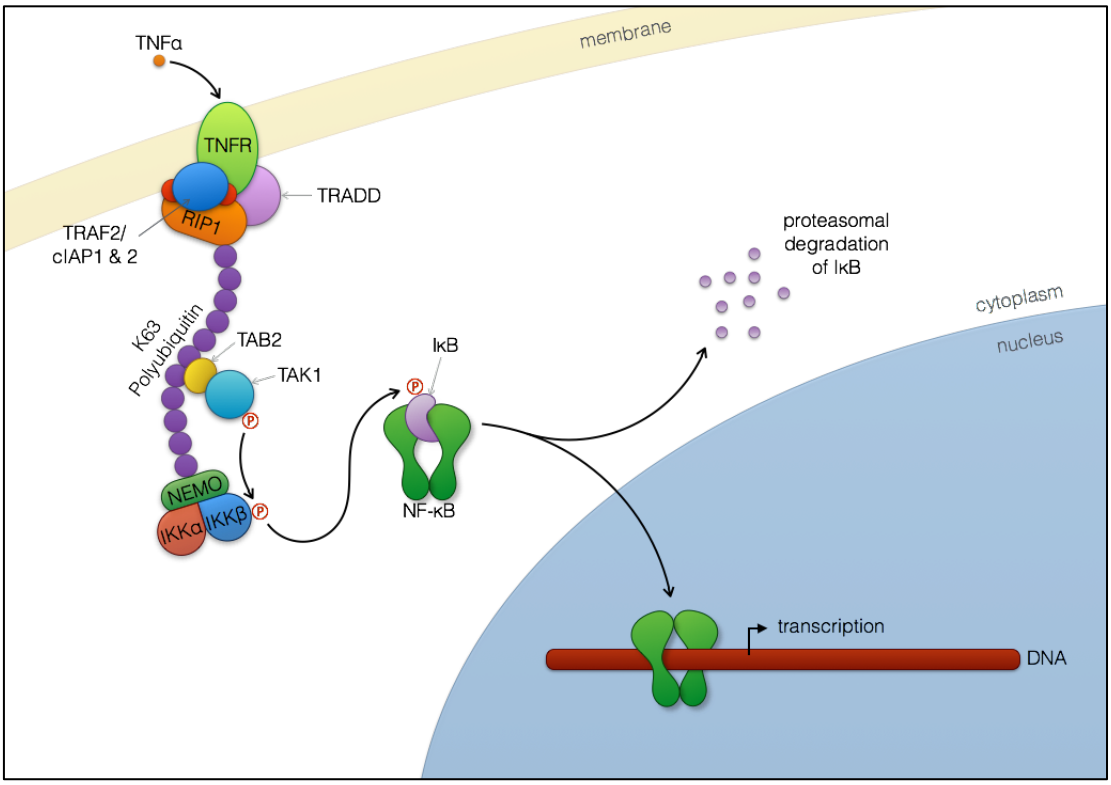

Figure 1.6: The canonical pathway of NF-κB activation. Activation of the membrane receptor (TNFR illustrated, see text for differences with other receptors) causes lysine-63-linked polyubiquitination of RIP1, mediated by the TRAF2/cIAP1/cIAP2 complex. The kinase TAK1 associates with this polyubiquitin chain via the adaptor TAB2, as does its target – NF-κB essential modifier (NEMO). In this conformation, TAK1 is able to phosphorylate IκB kinase β (IKKβ), which forms the IKK complex together with IKKα and NEMO. Activated IKK phosphorylates the inhibitor of κB (IκB), which recruits a ubiquitin ligase complex to mark it for proteasomal degradation by lysine-48-linked polyubiquitination. This releases NF-κB from its sequestration in the cytoplasm, allowing it to enter the nuclear and activate transcription.

become autopolyubiquitinated with K63-linked ubiquitin chains when activated (Lamothe et al., 2007) and as such would be analogous to the TRAF2-mediated ubiquitination of RIP1, although this is unclear at present, as TRAF6 autoubiquitination-independent activation has been reported (Walsh et al., 2008).

The polyubiquitin chains extend and act as a scaffold, linking to the NF-κB essential modulator (NEMO) (Ea et al., 2006), part of the IκB kinase (IKK) complex, also comprising IKKα and IKKβ (Krappmann et al., 2000). Linear ubiquitin chains (linked by methionine 1) have also been found to link NEMO to the TNFR complex independently of RIP1, and this is required for efficient progression of signalling (Haas et al., 2009). The presence of the polyubiquitin scaffold between the receptor and IKK complex allows recruitment of the mitogen-activated protein kinase kinase kinase (MAP3K) molecule TAK1 (transforming growth factor-β-activated kinase-1) via the adaptor molecule TAK1 binding protein 2 (TAB2) (Chen et al., 2006). By binding to the polyubiquitin scaffold, TAK1 is brought into proximity of its target, IKKβ. TAK1 phosphorylates serines 177 and 181 of IKKβ, thus activating the IKK complex (Delhase et al., 1999). The IKK complex possesses serine/threonine protein kinase activity through the combined activity of IKKα and -β (Zandi et al., 1997) and is responsible for phosphorylating IκB proteins at conserved serine residues in the DSGXXS motif (Hayden and Ghosh, 2008). This phosphorylation creates a binding site for β-transducin repeat containing protein (βTrCP). βTrCP is a variable 'F-box' component of the larger SCF (Skp1-Cullin-1/Cdc53-F-box protein) E3 ubiquitin ligase complex (reviewed by Cardozo and Pagano, 2004). $SCF^{\beta TrCP}$ ubiquitinates two lysine residues upstream of the phosphorylation site with K48-linked ubiquitin to mark it for proteasomal degradation (Perkins, 2006), thus freeing the NF-κB dimer to enter the nucleus and carry out its transcription factor activity.

The function of the canonical NF-κB pathway is primarily in the regulation of inflammatory signalling. Activation of NF-κB signalling is crucial in the cellular response to injury and infection; affected sites produce inflammatory molecules – such as ILs and MCP-1 – and adhesion molecules as a result of active NF-κB which attract leukocytes to the area to resolve the infection or initiate tissue repair (Caamaño and Hunter, 2002; Wang et al., 2013b). Additional canonical NF-κB functions include regulation of cell survival via the upregulation of anti-apoptotic and antioxidative genes like B-cell lymphoma 2 (*BCL2*) and superoxide dismutase 2 (*SOD2*), which can have a profound role in promoting tumour survival (Baldwin, 2012).

1.3.2 Non-canonical NF-κB

The non-canonical pathway (Figure 1.7) is responsible predominantly for activation of p52/RelB dimers. In contrast to the canonical pathway, the non-canonical does not rely on degradation of IκB to promote NF-κB activation, but instead relies on the processing of p100 into p52 (Sun and Ley, 2008). The unprocessed p100 is able to dimerise with and stabilise RelB through multiple domain interactions, including the dimerisation domain and C terminal ankyrin repeat domain (Fusco et al., 2009). The p100/RelB complex is transcriptionally inactive due to predominant localisation to the cytoplasm. In a similar fashion to NF-κB/IκBα, a NES present on the N-terminus of p100 combats the NLS of RelB thus causing a shuttling of the complex across the nuclear membrane, with a bias towards export (Solan et al., 2002).

The NF-κB-inducing kinase (NIK) is responsible for activating p100 processing. This serine/threonine MAP3K is necessary for non-canonical NF-κB activity (Xiao et al., 2001), and is able to specifically phosphorylate IKKα independent of the trimeric IKK complex in canonical activation (Ling et al., 1998). Serines 866 and 870 on the C terminus of p100 form a phosphorylation site for IKKα which bears similarity to the IκBα site responsible for ubiquitin-mediated degradation. Sure enough, phosphorylation of these serines on p100 allows recruitment of $SCF^{\beta TrCP}$ to this site (Fong and Sun, 2002). Bound to p100, $SCF^{\beta TrCP}$ is then able to catalyse polyubiquitination at lysine 855 (K855) approximately 10 residues upstream of the binding site (Amir et al., 2004), marking p100 for proteolytic processing into p52.

Processing of p100 to p52 is a tightly regulated process; in the absence of activation, p100 is much more abundant than p52, and even overexpressed p100 has extremely low rates of processing to p52 in comparison to p105 to p50 processing which is constitutive (Sun, 2011). Downregulation is achieved by a multi-component degradative pathway upstream of NIK. Cellular abundance of NIK is maintained at low levels in spite of its constitutive expression, through continued proteasomal degradation. Another ubiquitin ligase complex, consisting of TRAF2 and -3, and cIAP1 and -2 constitutively interacts with NIK to mark it for proteasomal degradation. TRAF3 binds to the N-terminal binding motif ISIIAQA on NIK (Liao et al., 2004) and to TRAF2, acting as a bridge between NIK and cIAP1/2 (Zarnegar et al., 2008b); while cIAPs possess E3 ubiquitin ligase activity through a RING domain (Yang et al., 2000) and conjugate ubiquitin onto NIK to mark it for proteasomal degradation and thus maintain a low NIK concentration (Skaug et al., 2009). Zarnegar et al. illustrated the importance of this control of NIK accumulation with an elegant rescue experiment in mice. *Traf3*$^{-/-}$ mice were found to die within weeks of birth due to elevated NIK leading to overactive p100 processing and constitutive non-

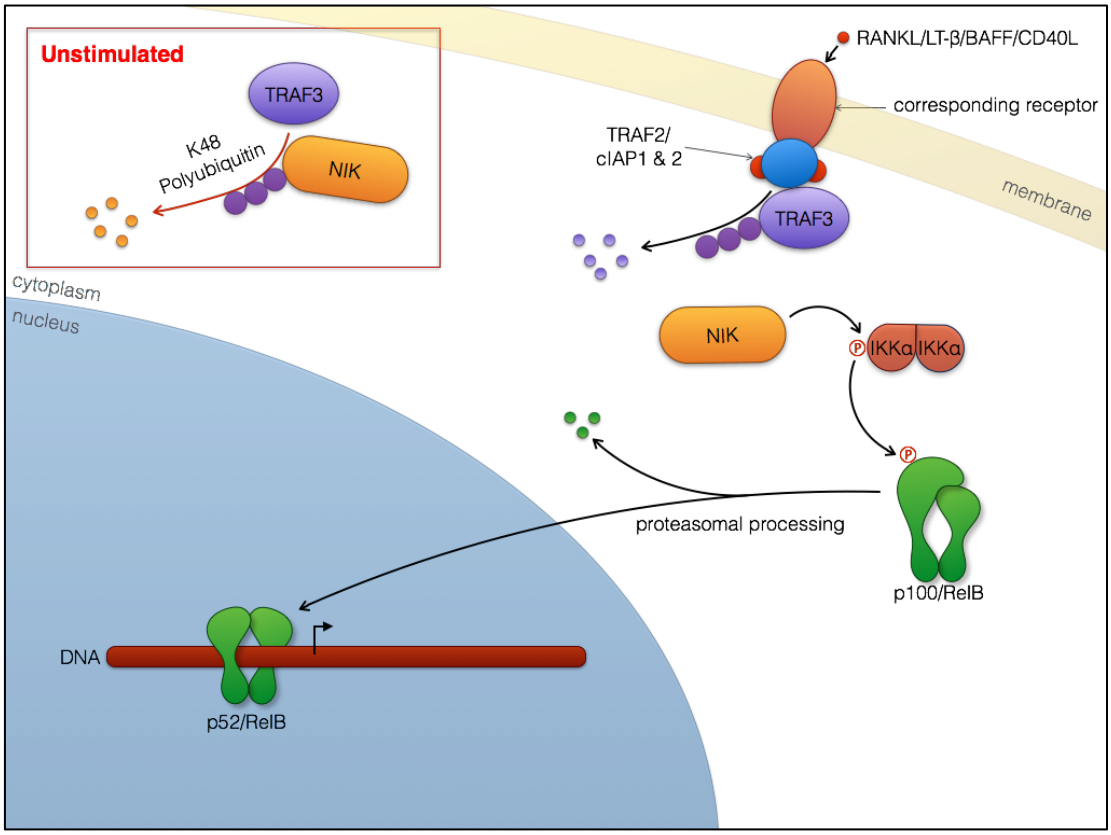

Figure 1.7: The non-canonical pathway of NF-κB activation. This pathway relies on proteasomal processing of p100 to p52 for its activation. Upon stimulation by one of the ligands named in the figure, NIK activates this process by phosphorylating IKKα independent of IKKβ, which in turn phosphorylates p100, complexed with RelB. This phosphorylation recruits a ubiquitin ligase, conjugating lysine-48-linked polyubiquitin to mark p100 for processing. Prior to stimulation (red box) this process is halted by constitutive degradation of NIK by TRAF3 ubiquitin ligase activity. Stimulation causes a shift so the TRAF2/cIAP1/cIAP2 complex marks TRAF3 for degradation instead, allowing NIK accumulation and thus NF-κB activation.

canonical NF-κB activity. Mice with NIK deletions (*Map3k14*$^{-/-}$) were rescued from this phenotype.

Activation of the non-canonical pathway proceeds through a variety of TNFR family receptors, including lymphotoxin-β (LT-β) receptor (LTβR), B-cell-activating factor (BAFF) receptor (BAFFR), CD40, and receptor activator of NF-κB (RANK), which all contain TRAF binding motifs (Sun, 2011). Upon activation of these receptors by their corresponding ligands, the TRAF2/3/cIAP complex relocalises to the cytoplasmic domain of the receptor (Matsuzawa et al., 2008). This causes a functional change in cIAP activity, which instead initiates K48-linked polyubiquitination of TRAF3 and subsequent degradation (Vallabhapurapu et al., 2008). In the absence of TRAF3, the TRAF2/cIAP ubiquitin ligase complex is unable to associate with NIK and thus it is no longer constitutively degraded; translation of NIK continues and cellular abundance increases until it is able to activate p100 processing and thus generate active RelB/p52 dimers.

Non-canonical NF-κB signalling is of utmost importance in the regulation and development of B cells and lymphoid organs. Loss of IKKα or NIK results in a deficiency in B cell maturation (Hahn et al., 2016; Jellusova et al., 2013), and mice deficient in LTβR or NIK display a complete absence of lymph nodes (Fütterer et al., 1998; Yamada et al., 2000). Stimulation of non-canonical NF-κB signalling by ligation of LTβR is required for the development of lymph nodes and lymphangiogenesis (Bénézech et al., 2013; Onder et al., 2013; Vondenhoff et al., 2009). Like the canonical NF-κB pathway, the non-canonical pathway can also be oncogenic. In B cell cancers, aberrant nuclear localisation enhances proliferation, inhibits senescence and represses apoptosis (De Donatis et al., 2015; Park et al., 2006; Vallabhapurapu et al., 2015). Less is known about the target genes of non-canonical compared to canonical NF-κB, however several studies have found proliferative genes such as cyclin D1 (*CCND1*), p21 (*CDKN1A*) and regulated in development and DNA-damage response 1 (*REDD1*) are transcriptional targets of p52 (Ramachandiran et al., 2015; Rocha et al., 2003; Schumm et al., 2006), indicating that regulation of proliferation is a key function of this pathway.

1.4 NF-κB activity regulates the development of atherosclerosis

NF-κB activity is important for regulating vascular health and has been implicated in regulating the development of atherosclerosis, as mice deficient in EC NF-κB display a marked reduction in lesion size (Gareus et al., 2008). Activated NF-κB has been detected in VSMCs, macrophages and ECs of advanced human atherosclerotic lesions in comparison to little or no activation in other regions of the aorta (Brand et al., 1996). Several processes involved in atherogenesis are regulated by NF-κB signalling (de

Winther et al., 2005). Activation of NF-κB in ECs results in the secretion of pro-inflammatory cytokines and the expression of adhesion molecules (Collins et al., 1995; Kaplanski et al., 1993), which collaborate to enhance monocyte infiltration, as well as furthering the inflammatory response in macrophages or VSMCs already present in lesions. Further progression, by monocyte differentiation into macrophages and tissue invasion can also be regulated by NF-κB; expression of the differentiation regulator M-CSF in monocytes has been found to be dependent on NF-κB signalling through TNFα (Kogan et al., 2012). Furthermore, expression of MMP9 is induced by NF-κB activity, and is required to degrade the extracellular matrix (ECM) of the blood vessels to provide optimal macrophage invasion of the tissue (Bond et al., 1998). Indeed, MMP9 deficient mice crossed with mice prone to atherosclerosis showed a reduced level of plaque development throughout the aorta (Luttun et al., 2004).

There is some evidence to suggest that non-canonical NF-κB signalling could be involved in the development of atherosclerosis too. Mice deficient in CD40L are protected from lesion development (Lutgens et al., 1999), potentially implicating downstream non-canonical NF-κB regulation. However, no direct link between non-canonical NF-κB signalling and cardiovascular health has been described.

The activity of NF-κB in ECs at sites prone to atherosclerosis may be as a consequence of stimulation by cytokines such as TNFα and IL-1β (Libby, 2002), or by oxidised LDL (ox-LDL) (Cominacini et al., 2000; Parhami et al., 1993). However, the shear stress experienced by ECs within the vasculature plays an important role in regulating the NF-κB response.

1.5 Endothelial NF-κB is regulated by blood flow patterns.

Corresponding to the observed pattern of atherosclerosis localisation with respect to blood flow patterns within the vasculature, endothelial NF-κB activity is also differentially localised to these particular regions. Examinations of tissue samples from regions of low shear stress in otherwise healthy mice (Hajra et al., 2000) and pigs (Passerini et al., 2004) have shown increased NF-κB abundance without a corresponding increase in activity, indicating cells here enter a 'primed' state where inflammatory signalling molecules can induce a rapid inflammatory response. Novel regions of low shear created in the vasculature of mice with constrictive cuffs have been shown to induce NF-κB expression too (Cuhlmann et al., 2011), supporting the idea that blood flow can control its activation.

There are many *in vitro* data which support these observations. Human ECs grown in culture and subjected to high shear stress (as found in atheroprotective regions *in vivo*)

show a consistent dampening of NF-κB activity and reduced expression of the NF-κB target genes E-selectin, VCAM-1 and IL-8, as well as an induction of anti-inflammatory pathways (Partridge et al., 2007). In addition, these cells showed a dampened response to TNFα induced NF-κB activity. Other studies have shown that cultured cells exposed to oscillatory flow display an increase in inflammatory signalling correlating to that seen at atheroprone regions *in vivo* (Chappell et al., 1998).

Recent experiments have gone further into characterising NF-κB expression in atheroprone haemodynamic conditions, attempting to identify more specifically which aspects of this flow pattern cause an induction of the transcription factor and finding that NF-κB expression is very sensitive to flow dynamics and direction. Feaver et al. (2013) mapped the compound flow pattern experienced at an atheroprone region of the human carotid artery bifurcation into a wave. Calculating the wave equation from this pattern, they split it into its constitutive frequencies and introduced these frequencies to an atheroprotective waveform, finding that certain frequencies were able to specifically induce NF-κB expression. Additionally, Wang et al. (2013a) showed that changing the angle at which the direction of flow intersects the direction of EC alignment can cause an change in NF-κB expression, with perpendicular flow inducing a maximal response in comparison to the minimal response seen with parallel flow. Similar experiments have been carried out *in vivo*, utilising a constrictive cuff placed around the murine carotid artery. The geometry of the cuff generates low shear stress upstream, a gradient of increasing shear stress within the cuff and low oscillating shear stress downstream (Cheng et al., 2005). RelA expression was found to be at its minimum in ECs exposed to high shear stress, with greater expression under low shear stress, and further elevation with the addition of oscillations (Cuhlmann et al., 2011).

The PECAM-1-containing mechanosensor complex has been shown be involved in the NF-κB response to flow. Tzima et al. (2005) showed that low shear stress *in vitro* was no longer able to activate NF-κB in PECAM-1 deficient cells. PECAM-1 may act by inducing MAPK pathway members (Wang and Sheibani, 2006) such as p38 and c-Jun N-terminal kinase (JNK). Proteins in the NF-κB activation pathways are upstream activators of the MAP kinase pathway; TAK2 and NIK are both MAP3K and as such phosphorylation of these can activate the MAPK pathway. The MAPK and NF-κB pathways have been found to be closely linked at sites of low shear stress. RelA expression has been found to be dependent on JNK activity in murine models (Cuhlmann et al., 2011). Furthermore, inhibition of MAPK signalling by MAPK phosphatase-1 (MKP-1) or suppression of upstream activators produces anti-inflammatory effects with a correlated decrease in VCAM-1 expression (Zakkar et al., 2008, 2009).

Given the known risk of hypercholesterolaemia on inducing atherosclerosis (Wilson et al., 1998), as well as the effect of ox-LDL on NF-κB activation (Cominacini et al., 2000), evidence supporting the accumulation and increased transport of LDL into the endothelium at atheroprone regions cannot be ignored as a regulator of atherogenesis. Nevertheless, sensing of shear stress patterns by mechanosensors seems to be ultimately responsible for the priming of cells to begin atherogenesis by inducing expression of NF-κB in response to flow conditions independently from concentrations of LDL. High blood levels of LDL or other inflammatory signalling molecules may accelerate the process of atherogenesis by further stimulating NF-κB.

1.6 The role of ubiquitin in NF-κB regulation

Ubiquitination is of utmost importance to the regulation of NF-κB activation by both canonical and non-canonical pathways. Ubiquitin is a 76 residue, highly stable, 8.5 kDa protein which is well conserved from insects to humans (Vijay-Kumar et al., 1987). Post-translational addition of ubiquitin to proteins is an important step in the regulation of many cellular pathways. Ubiquitin modification tends to occur at lysine residues and can take different forms, with the addition of one ubiquitin molecule (monoubiquitination), or linear or branched linked chains (polyubiquitination). In NF-κB activation, polyubiquitination is key; the function conferred by this modification depends on the conformation of the ubiquitin chain. Polyubiquitin chains can be formed between lysines or the N terminal methionine (M1) of one molecule and the C terminus of the next (Komander and Rape, 2012). There are seven lysines available for polymerisation (Figure 1.8), and chains utilising each of them have been detected *in vivo* (Peng et al., 2003).

Polyubiquitination occurs via a process involving three classes of enzymes, shown in (Figure 1.9). Ubiquitin activating (E1) enzymes prime ubiquitin for polymerisation by conjugating a ubiquitin molecule onto an active-site cysteine residue via an adenylate intermediate in an ATP-dependent reaction (Schulman and Harper, 2009). Ubiquitin-conjugating (E2) enzymes then transfer the activated ubiquitin molecule onto their own active site cysteine residue (Ye and Rape, 2009). A complex between the target molecule, an E2 and a ubiquitin ligase (E3) catalyses the final step in addition, whereby the ubiquitin is transferred from the E2 to a lysine residue on the target or pre-existing ubiquitin, either via transient binding to the E3 or directly from the E2 (Deshaies and Joazeiro, 2009). The E3 component of the complex is responsible for the specificity of target binding, while the type of lysine linkage is regulated by the E2 (David et al., 2010). K48-linked polyubiquitin is perhaps the best studied, it is responsible for inducing proteasomal degradation via the 26S proteasome, which specifically recognises ubiquitinated proteins and degrades them (Baumeister et al., 1998). K63-linked

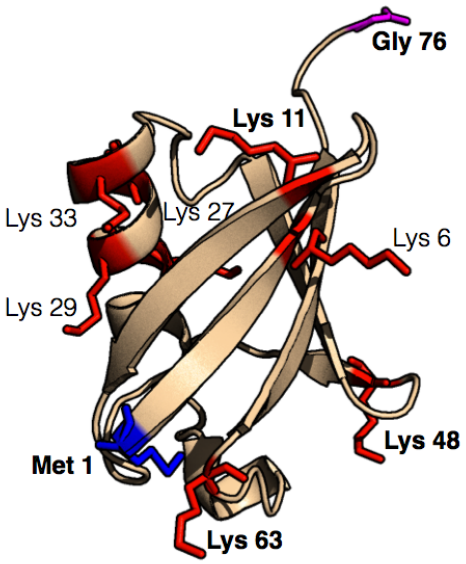

Figure 1.8: The structure of ubiquitin. Ubiquitin is a small molecule, adopting a compact structure through a single α-helix and β-sheet. It is able to form polymers through binding of its C terminal glycine (magenta) to any of the lysines indicated in red, or the N terminal methionine. Shown in bold are those residues which have been shown to be involved in linkages *in vivo*. Binding to different sites causes a change in how open the polyubiquitin chain is.
Structure downloaded from the Protein Data Bank, solved by Vijay-Kumar et al., 1987.

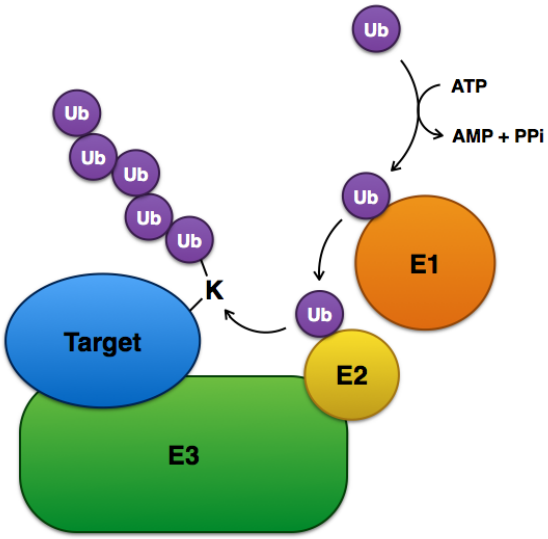

Figure 1.9: The mechanism of polyubiquitination. Ubiquitin monomers become activated by E1 ubiquitin-activating enzymes in an active process requiring ATP. E2 ubiquitin-conjugating enzymes then bind the activated ubiquitin via a cysteine residue, and determine the conformation of the polyubiquitin chain by its lysine-linkage. E3 ubiquitin-ligase enzymes are responsible for targeting the ubiquitin to the correct site; there are many types, which bind to specific sites on target molecules as well as to the E2, creating a bridge for the transfer of the ubiquitin to a lysine on the target molecule or to lengthen a preexisting chain.

polyubiquitin is involved in non-degradative signalling and is widespread in NF-κB activation, as discussed above. Other forms are less well studied, but K11- and M1-linked polyubiquitination are reported to be involved in NF-κB signalling too. K11 chains may promote IKK activation (Dynek et al., 2010) while overexpression of the linear ubiquitin chain assembly complex — responsible for M1-linked chain conjugation — has been shown to induce NF-κB (Tokunaga, 2013).

Constitutive ubiquitination of NF-κB results in pathological dysfunction of NF-κB signalling. Negative feedback mechanisms regulated by several deubiquitinating enzymes (DUBs) are thus in place to remove polyubiquitin and maintain homeostasis. There are five families of DUBs, ubiquitin C-terminal hydrolases (UCHs), ubiquitin-specific proteases (USPs), Josephins, JAB1/MPN/MOV34 metalloenzymes (JAMMs) and ovarian tumour proteases (OTUs), characterised by their functional domains. UCHs, USPs, Josephins and OTUs are cysteine proteases, while JAMMs are zinc metalloproteases (Komander et al., 2009).

Three DUBs have been shown to be of particular importance in NF-κB signalling. The USP cylindromatosis tumour suppressor (CYLD) is able to interact with NEMO and degrade K63 polyubiquitin from TRAF2 and TRAF6, thereby inhibiting IKK activation (Brummelkamp et al., 2003; Kovalenko et al., 2003; Trompouki et al., 2003). CYLD deficiency results in the hereditary disease familial cylindromatosis (Biggs et al., 1995), involving enhanced NF-κB activation as part of its pathogenesis (Zhang and Stirling, 2006). The OTU domain-containing DUB A20 is another inhibitor of NF-κB activity, which forms a negative feedback mechanism due to its induction by NF-κB itself (Evans et al., 2004; Wertz et al., 2004). In humans, single-nucleotide polymorphisms of A20 have been associated with inflammatory diseases including atherosclerosis in diabetic patients (Boonyasrisawat et al., 2007). The catalytically active OTU domain cleaves K63 polyubiquitin from TRAF6 or RIP1 with cysteine protease activity (Komander and Barford, 2008), causing inhibition of IKK activation. Interestingly, A20 also possesses E3 ligase activity through seven zinc finger domains, which polyubiquitinate the deubiquitinated TRAF6 or RIP1 with K48-linked polyubiquitin, inducing their proteasomal degradation and thus further suppressing NF-κB (Wertz et al., 2004). Lastly is the OTU domain 7B (OTUD7B) protein, also known as zinc finger A20 domain-containing protein 1 (ZA20D1) or Cezanne (cellular zinc-finger anti-NF-κB). This DUB was identified due to its similarity to A20, and is similarly able to inhibit NF-κB activation (Evans et al., 2001) of both the canonical (Enesa et al., 2008a) and non-canonical (Hu et al., 2013) pathways.

1.7 Cezanne may be important in regulating the development of atherosclerosis

Cezanne is an 843 residue protein encoded by the OTUD7B gene found at the 1q21.2 locus. It possesses cysteine protease DUB activity through a three residue conserved active site (Cys209, His373 and Asp206) in its OTU domain, and also contains a C terminal zinc finger domain which may be involved in regulating this activity (Evans et al., 2003). The active site cysteine is sensitive to oxidisation, and hydrogen peroxide has been shown to inhibit Cezanne activity through this mechanism (Enesa et al., 2008b).

Cezanne can inhibit canonical NF-κB activation *in vitro* through deubiquitination of K63-linked polyubiquitinated RIP1 (Enesa et al., 2008a) and TRAF6 (Luong et al., 2013), with ECs treated with siRNA and knockout mice both showing elevated expression of target genes such as intracellular adhesion molecule-1 (ICAM-1) and IL-8. Furthermore, in mouse embryonic fibroblasts (MEFs) and B cells, Cezanne has been shown to inhibit non-canonical NF-κB. *Otud7b*$^{-/-}$ cells show a decrease in TRAF3 expression when stimulated with non-canonical pathway activators alongside an increase in K48 polyubiquitination, indicating Cezanne is able to stabilise TRAF3 and thus induce NIK degradation (Hu et al., 2013). Cezanne has been shown to preferentially hydrolyse polyubiquitin *in vitro*, either as K11 chains (Bremm et al., 2010) or as branched chains with K63 or K48 (Evans et al., 2003). There is evidence suggesting that K11 polyubiquitination of RIP1 is important in regulating NF-κB activation (Dynek et al., 2010), however whether this occurs in conjunction with K63 polyubiquitin is not known. Distinct K11 polyubiquitination of RIP1 could indicate that Cezanne plays a novel but as yet uncharacterised role in NF-κB inhibition over and above the previously described roles.

The ability of Cezanne to inhibit both the canonical and non-canonical NF-κB pathways is of great interest. Stimulation of the canonical pathway with TNFα has been shown to increase p100 expression four-fold, leading to cytoplasmic retention of canonical dimers through the inhibitory activity of p100 (Basak et al., 2007). Non-canonical signalling through NIK is thus able to also promote activation of these dimers through p100 degradation (Zarnegar et al., 2008a). Cezanne could be an enzyme involved in control of this balance by inhibiting one or both pathways to stop excessive stimulation. Hu et al. (2013) demonstrated that Cezanne deficiency in mice resulted in an increase of nuclear RelB and p52 in MEFs and B cells upon non-canonical stimulation, however whether or not regulation of the non-canonical NF-κB pathway is relevant in atherosclerosis is not clear. Interestingly, Cezanne has been shown to negatively regulate NF-κB activation in cancer cells, induced by retinoic acid, a known activator of the developmental homeobox

genes (Kanki et al., 2013), which may indicate a further role for Cezanne in linking developmental and inflammatory pathways.

Cezanne has also been shown to increase the stability of hypoxia inducible factor 1α and 2α (HIF-1α, 2α) by separate mechanisms (Bremm et al., 2014; Moniz et al., 2015). It has been shown to remove K11-linked polyubiquitin chains from HIF-1α to rescue it from degradation, while HIF-2α expression is increased by Cezanne stabilising E2F1, which is a transcription factor upstream of HIF-2α.

Cezanne's regulation by different flow patterns is key in the understanding of its physiological function. Using ECs isolated from atheroprone and atheroprotected regions from porcine aortic arches, a microarray identified Cezanne upregulation in the atheroprotected area (Passerini et al., 2004). Endothelial Cezanne expression *in vitro* has been found to be induced by TNFα stimulation, exposure to high shear stress relative to static cells (Enesa et al., 2008a) and hypoxia (Luong et al., 2013). All of these have been found to be differentially regulated between atheroprone and protected sites of the vasculature. As such, the mechanism for Cezanne's regulation by flow is not understood, and given the multifunctional role of Cezanne in inhibition of both pathways of NF-κB activation it warrants further investigation to determine whether Cezanne is responsible for changes in endothelial gene expression observed between regions of low and high shear stress.

1.8 Summary

Atherosclerosis is a chronic disease of the vasculature whereby fatty plaques occlude arterial blood flow and in severe cases leads to myocardial infarction or stroke, which can be fatal. The development of atherosclerosis is a complex series of events which occur over many years, involving monocyte infiltration into the arterial wall and uptake of circulating lipids. Localisation of lesion development is regulated by blood flow; the frictional force (shear stress) at bends and branches within the vasculature is locally decreased and exhibits oscillations. Endothelial cells which line the lumen can sense these differences in shear stress and display a large shift in gene expression, from a quiescent phenotype to an activated one, displaying enhanced apoptosis, proliferation and inflammation.

A central regulator of these changes is the transcription factor NF-κB, a dimeric family split into two pathways – canonical and non-canonical – that can induce gene expression of many molecules which promote lesion development. Canonical NF-κB expression and activity in ECs is dynamically regulated by shear stress, elevated by low shear stress both *in vitro* and *in vivo* and thus contributes in transducing shear stress into biochemical

signals which promote atherosclerosis. Low shear stress has also been observed to increase non-canonical NF-κB expression in a microarray study, but has not been investigated further. Its activity in ECs and potential role in atherosclerosis is unknown.

The deubiquitinase Cezanne is a negative regulator of both canonical and non-canonical NF-κB through removal of ubiquitin chains from upstream signalling pathways. Cezanne expression has also been found to be regulated by factors altered between atheroprone and protected areas, including shear stress, inflammatory cytokine stimulation and hypoxia, however its regulation by physiological flow conditions has not been studied. Given its ability to inhibit both pathways of NF-κB as well as promote hypoxic signalling, understanding how the expression and function of Cezanne is controlled in the context of atherosclerosis may help understand how these pathways are regulated, and potentially aid in controlling them to limit lesion development.

1.9 Hypotheses

1. Cezanne expression is differentially regulated in ECs in areas prone to or protected from atherosclerosis, due to differences in shear stress in combination with inflammatory signalling or hypoxia.

2. Cezanne functions to inhibit NF-κB and promote hypoxic signalling, and thus protect arteries from the development of atherosclerosis.

3. The non-canonical NF-κB pathway is regulated by shear stress, and functions to control EC proliferation.

1.10 Aims of this study

The preceding hypotheses will be tested as follows:

1. Utilising *in vivo* and *in vitro* models of shear stress to investigate Cezanne expression under different shear patterns, combined with the addition of inflammatory cytokines or culture under hypoxic conditions.

2a. Employing siRNA to deplete cells of Cezanne expression in conjunction with the application of shear stress *in vitro* and investigating the effect on canonical NF-κB, non-canonical NF-κB and HIF stability.

2b. Investigating the development of atherosclerosis in a novel *Otud7b*$^{-/-}$*Ldlr*$^{-/-}$ mouse model.

3a. Utilising *in vivo* and *in vitro* models of shear stress to investigate flow effects on non-canonical NF-κB expression and activity.

3b. Using siRNA to deplete cells of non-canonical NF-κB subunits and test the effect on proliferation and inflammation.

3c. Testing proliferation in the aortic arches of *Nfkb2*$^{-/-}$ mice.

2. Materials and Methods

2.1 Isolation of human umbilical vein endothelial cells (HUVECs)

Human umbilical cords were obtained anonymously from the Royal Hallamshire Hospital with ethical approval (Sheffield REC 10/H1308/25). At the time of birth, umbilical cords were placed into pots containing collection media (Eagle's minimum essential medium (EMEM; Life Technologies) with 1% 100X penicillin/streptomycin (Life Technologies), 1% 250 µg/ml amphotericin B (Fisher Scientific), 2% 1 M HEPES (Lonza) and 0.9 mg/ml sodium bicarbonate (Sigma). Cords were stored at 4 °C until further use.

A 75 cm^2 growth area flask (T75; Corning) was prepared for each cord by incubating for 30 minutes at 37 °C with 5 ml of 1% (w/v) gelatin from bovine skin (Sigma) in phosphate buffered saline (PBS; Oxoid) coating the growth surface. Each cord was cleaned and the vein cannulated with a 14G cannula and flushed with 20 ml of incomplete M199 medium (Appendix 7.1). The free end was then clamped and the vein inflated with sterile filtered 1 mg/ml collagenase A from *Clostridium histolyticum* (Sigma) in incomplete M199. The cord was incubated with the collagenase for 20 minutes before flushing into a 50 ml tube with a further 20 ml of incomplete M199. The resulting cell suspension was centrifuged for 5 minutes at 1200 rpm, the supernatant discarded and the cell pellet resuspended in complete M199 (Appendix 7.2), then transferred to gelatin-coated T75 flasks and incubated at 37 °C with 5% CO_2. After 24 hours, the media was refreshed.

2.2 Passaging HUVECs

Confluency was assessed regularly and cells passaged upon reaching confluence. The growth media was aspirated and replaced with 5 ml sterile PBS; gentle rocking washed the cells before the PBS was discarded. Another wash was carried out and then 1 ml of 0.25% trypsin-EDTA (Life Technologies) added to the cells, ensuring full coverage. The HUVECs were incubated with the trypsin for 2-5 minutes, until cells were visibly dislodged. The trypsin was neutralised by the addition of complete M199. The resulting cell suspension was centrifuged at 1200 rpm for 5 minutes in a bench top centrifuge, the supernatant discarded and the cell pellet resuspended in fresh media and split into 3 new gelatin-coated T75 flasks.

2.3 Gene knockdown using Lipofectamine RNAiMAX

HUVECs were seeded onto gelatinised six well plates the day before transfection, at a density of 2×10^5 cells per well in 2 ml complete M199. A 1.25 µl volume of each 20 µM stock of siRNA to be used (Appendix 7.3) was diluted to a final volume of 150 µl in Opti-MEM® I Reduced Serum Media (Life Technologies). In separate tubes, 7.5 µl Lipofectamine® RNAiMAX was diluted to a final volume of 150 µl in Opti-MEM®. After gentle mixing, the siRNA dilutions were combined with the Lipofectamine® dilutions, mixed and incubated for 20 minutes at room temperature to allow complex formation. Pre-warmed antibiotic-free complete M199 was added to the tubes to a final volume of 1000 µl and this media used to replace that of the plated HUVECs, resulting in a final siRNA concentration of 25 nM. The cells were incubated with this mixture for 5 hours before being washed and replaced with 3 ml complete M199.

2.4 Gene knockdown using the Neon™ electroporation system

Flasks of confluent HUVECs were washed twice with PBS, then incubated with 1 ml trypsin at 37 °C for 2-5 minutes to dislodge the cells. Trypsin activity was then neutralised with 4 ml per flask of complete M199 lacking antibiotics and amphotericin B, with aggravation to resuspend the cells. The cell suspension was centrifuged at 1200 rpm for 5 minutes before removing the supernatant and washing twice with Ca^{2+}/Mg^{2+} free PBS (Life Technologies). Depending on the number of cells being transfected, two different protocols were followed.

2.4.1 Small transfection (10 µl)

For one to five wells per condition, 2.5×10^6 cells were resuspended in 66 µl of resuspension buffer (R buffer, Life Technologies). This suspension was then divided into 0.6 ml tubes along with a 50 µM siRNA solution to a total volume of 12 µl and siRNA concentration of 5-10 µM. The Neon™ pipette with 10 µl tip was used to take up the suspension and the pipette and tip placed into the electroporation apparatus (Neon™ Transfection System model MPK5000; Life Technologies) so the tip containing the cells was dipped into a tube containing 3 ml E buffer. Electroporation was carried out using a single pulse for 30 ms at a voltage of 1350 V. The pipette was then removed and cells dispensed directly into 2 ml of pre-warmed M199 without antibiotics or amphotericin B in a gelatinised six-well plate (Greiner bio-one). This process was repeated for each well, the plate gently rocked to disperse the cells and the plate left in the incubator for at least four hours to allow the cells to adhere. The media was then removed and replaced with 3 ml complete media and the cells used for further experiments.

2.4.2 Large transfection (100 µl)

For six wells per transfection, 2.5×10^6 cells were resuspended in a total of 120 µl of R buffer containing 50 µM siRNA solution at a concentration of 3-6 µM. A 100 µl tip was fitted to the Neon™ pipette and the suspension taken up. Electroporation was carried out using a single pulse for 40 ms at 1200 V. The pipette was removed and the cells dispensed into 9 ml pre-warmed M199 without antibiotics or amphotericin B. This was thoroughly mixed and then 1.5 ml added to each well of a gelatinised six-well plate containing 0.5 ml of the same media. The cells were left to adhere in the incubator for at least four hours before the media being replaced with 3 ml complete media and the cells used for further experiments.

2.5 Culturing HUVECs under shear stress

Flasks of confluent HUVECs at passage 3 were washed twice with PBS, then incubated with 1 ml trypsin for 2-5 minutes. The trypsin was neutralised with 4 ml complete M199 with aggravation to resuspend cells. The suspension was centrifuged at 1200 rpm for 5 minutes and the cell pellets resuspended in fresh media. A haemocytometer was used to count cells.

2.5.1 Using the orbital shaker apparatus

Six-well cell culture plates were coated with 1 ml 1% (w/v) gelatin in PBS for 30 minutes at 37 °C, then were seeded with $2\text{-}5 \times 10^5$ cells per well in 2 ml of complete M199 and placed in the incubator for at least 4 hours until the cells had adhered. The media was changed and 3 ml fresh media added. The plates were placed onto an orbital shaker (model PSU-10i; Grant-Bio) set at 210 rpm in a 37 °C incubator with 5% CO_2. CFD models have previously calculated that the centre and periphery of each well experience different time-averaged wall shear stress magnitudes, with the centre experiencing complex multidirectional flow with a shear stress of 5 dyn/cm², and the periphery a pulsatile unidirectional flow with shear stress of 13 dyn/cm² (Warboys et al., 2014).

2.5.2 Using the ibidi parallel plate flow apparatus

Each µ-Slide $I^{0.4}$ Luer (ibidi) was coated with 150 µl 1% gelatin for 30 minutes. After this, 2.5×10^5 cells in 150 µl of complete M199 were carefully seeded onto the slide, adding the suspension to the inlet and removing gelatin from the outlet to pull the cells into the chamber by capillary action. The cells were allowed to adhere for one hour then the slides washed twice with fresh media. Media reservoirs were sterilised by spraying with 70% ethanol (Sigma) and left to fully air dry in a laminar flow cabinet. The reservoirs were then inserted into a fluidic unit (v1.1; ibidi) and connected to 15 cm tubing (ibidi) before being loaded with 13.6 ml complete M199 media, ensuring there were no air bubbles.

Filters were placed on top of the media reservoirs and connected to the air tubing. Using a clamp to prevent leakage, the central connector on the tubing was removed and the free ends connected to each end of the slide. The clamp was then removed and the tubing connected to the appropriate channels on the fluidic unit. Lastly, the fluidic unit was placed into an incubator at 37 °C with 5% CO_2 and the air tubing and data cables connected to the main pump (ibiPump 2; ibidi). The air inlet was placed into the incubator and attached to a flask containing silica beads in order to remove moisture before entering the pump. On the software the shear stress values were selected, using one of two different profiles. The unidirectional high shear stress profile was the same for the master and all slaves, increasing from 4 dyn/cm^2 to 13 dyn/cm^2 over ten minutes. The low shear stress profile was 4 dyn/cm^2 unidirectional for the master unit and 4 dyn/cm^2 oscillating every 0.5 seconds for the slaves.

2.6 Exposing HUVECs to shear stress and hypoxia.

HUVECs were exposed to hypoxia using the GenBOX apparatus (bioMérieux). This utilises an oxygen scavenging pouch to alter the atmospheric composition of a sealed container. HUVECs were seeded onto six-well plates and exposed to shear stress with the orbital shaker system as normal for 48 hours. Then, plates were placed into the GenBOX and secured in place with tape. The provided indicator was placed into the container to ensure the appropriate environment was created. The GenBOX was then placed onto the orbital shaker for 24 hours. Samples were collected from these cells as quickly as possible to minimise time spent in a normoxic environment.

2.7 RNA isolation from HUVECs

At least three wells (orbital shaker) or a single slide (ibidi) were required for sufficient RNA for further analysis.

2.7.1 Sample collection from the orbital shaker

Plates were removed from the orbital shaker after 72 hours and placed directly onto ice. Media was removed by aspiration and the cells washed twice with 0.5 ml cold PBS. A further 0.5 ml cold PBS was added to each well and cells from the periphery scraped with the plunger from a 1 ml syringe. The cell suspension was recovered and pooled from replicate wells. Each well was washed a further two times with cold PBS and the scraping process repeated for the centre of the well. Cell suspensions were centrifuged in a refrigerated centrifuge at 12000 rpm for 1 minute. The supernatants were removed and cell pellets resuspended in 350 µl lysis buffer (RLT buffer; Qiagen) containing 1% (v/v) β-mercaptoethanol (Sigma).

2.7.2 Sample collection from ibidi slides

Slides were removed from the flow apparatus and placed directly onto ice. Media was removed from one inlet, then cold PBS was passed through twice and the chamber left as dry as possible. 150 µl RLT buffer was then added to the slide and left for 20 minutes on ice, rocking periodically, before removing to a fresh tube.

2.7.3 QIAGEN RNEasy spin column

Each sample was passed through a 21G needle (BD Bioscience) five times to homogenise the lysate before being diluted in an equal volume of 70% ethanol and mixed well. This was added to an RNEasy spin column (QIAGEN), the lid closed gently and centrifuged for 15 s at 10000g in a microcentrifuge. The flow-through was discarded and 350 µl Buffer RW1 (QIAGEN) added to the spin column which was then centrifuged for 15 s at 10000g and the flow-through discarded. 10 µl DNase I stock solution (QIAGEN) was added to 70 µl Buffer RDD (QIAGEN) for each sample and this added directly to the membrane of each spin column and incubated at room temperature for 15 minutes. Next, 350 µl RW1 was added to the column and centrifuged for 15 s at 10000g and the flow-through discarded. 500 µl Buffer RPE (QIAGEN) was added to each column and centrifuged for 15 s at 10000g, then the flow-through discarded, a further 500 µl Buffer RPE added to the column and centrifuged for another 2 min at 10000g. The spin column was removed from the collection tube and placed into a fresh tube and centrifuged at full speed for a further minute to dry the membrane. Lastly, the column was placed into a final 1.5 ml collection tube, 30 µl RNase free water (QIAGEN) was added directly to the membrane and centrifuged for 1 min at 10000g to elute the RNA.

2.7.4 Measuring RNA concentration and complementary DNA (cDNA) synthesis

RNA concentrations were measured using a Nanodrop 1000 spectrophotometer. Blank measurements were obtained using a water sample, then absorbances measured for each sample. Quality control was carried out by ensuring each sample had a 260/230 and 260/280 ratio between 1.9 and 2.1. Reverse transcription was carried out using 200 ng RNA. The total reaction consisted of 76% sample (diluted to a total mass of 200 ng with RNase free water), 20% 5X iScript Supermix (BioRad) and 4% iScript reverse transcriptase (BioRad). Samples were placed into a thermal cycler which heated the samples to 25 °C for 5 minutes, 42 °C for 30 minutes then 85 °C for 5 minutes. The cDNA was then placed on ice and diluted to 0.4 ng/µl with RNase free water.

2.8 Quantitative real-time PCR

For each gene to be analysed, a master mix was first created, combining SYBR Green Supermix (BioRad) with 0.5 µM forward primer and 0.5 µM reverse primer (Appendix 7.4), loading each reaction in triplicate. A 384-well plate was loaded first with the master mix, then with 1.76 ng cDNA per reaction to a total reaction volume of 10 µl. A plastic seal was placed on top of the plate, and the plate centrifuged at 1000 rpm for 1 minute to ensure the liquid was collected at the bottom of each well. The plate was then loaded into a BioRad CFX384 qPCR machine and the thermal profile set to 95 °C for 30 s to start, then 40 cycles of 95 °C for 5 s, 60 °C for 30 s, taking a fluorescence reading after each cycle. Finally, a melt curve was generated by raising the temperature from 60 to 95 °C in 0.5 °C increments, taking a reading at each stage. Data was exported as CT values and analysed using the $2^{-\Delta\Delta CT}$ method, normalising to the housekeeping gene HPRT.

2.9 Western blotting

2.9.1 Cell lysis

For cells grown on six-well plates, two static wells or six orbited wells were used to obtain enough material for further analysis. Plates were removed from the incubator and placed immediately onto ice. Each well was washed twice with cold PBS then cells from the periphery and centre were scraped separately into 500 µl cold PBS, with two PBS washes between each isolation. The resulting cell suspensions were then centrifuged at 10000 rpm for 5 minutes at 4 °C in order to pellet the cells. To lyse the cells, 50 µl of RIPA buffer (Sigma) containing 1% 100× Halt™ protease inhibitor cocktail (Thermo Scientific) and 1% 100× phosphatase inhibitor cocktail (Cell Signaling) was used to resuspend the pellet and incubated on ice for 20 minutes with periodic vortexing.

For cells grown using the ibidi® system, slides were removed from the incubator and placed immediately onto ice. Media was removed from the chamber using an aspirator, and each slide washed twice with cold PBS, ensuring complete removal of the PBS once completed. Next, 150 µl of RIPA buffer containing protease and phosphatase inhibitors was added directly to the chamber and the slides incubated on ice for 20 minutes with rocking. After lysis was complete, the samples were centrifuged at 12000 rpm for 15 minutes at 4 °C and the supernatants transferred to fresh tubes for further use.

2.9.2 Protein quantification and normalisation

Before loading onto a Western blot, the protein content of each sample was quantified and normalised to ensure equal loading. A bicinchoninic acid (BCA) assay kit (Thermo Scientific) was used for this according to the manufacturer's instructions. Albumin standards were made by diluting the stock (2000 µg/ml) in RIPA buffer containing

protease and phosphatase inhibitors. In a 96 well plate, 10 µl of each standard and 2 µl of each sample to be tested were loaded in triplicate and 200 µl working solution (50:1 ratio of Reagent A to Reagent B) was added to the wells. The plate was incubated at 37 °C for 30 minutes to allow the reaction to progress. The plates were then taken out of the incubator and incubated at room temperature for 5 minutes before the absorbance at 562 nm was measured for each well. Concentrations of each sample were calculated using the standard curve, and normalisation of the samples achieved by diluting to the concentration of the least concentrated sample.

Each sample was prepared for loading by adding dithiothreitol (DTT; Sigma) to a concentration of 92 mM and 25% 4× Loading Dye (Life Technologies). The tubes were vortexed briefly to mix and incubated at 100 °C for 10 minutes followed by 5 minutes on ice.

2.9.3 SDS-PAGE and transfer to PVDF

Samples were loaded into pre-cast 3-8% or 4-12% Bis-Tris gradient gels (Novex®, Life Technologies) depending on the molecular weight of the protein of interest, along with a protein ladder to identify band sizes (Spectra™ Multicolor Broad Range Protein Ladder; Thermo Scientific). Electrophoresis was carried out according to the manufacturer's instruction; gel tanks (XCell SureLock™; Thermo Scientific) were filled with 1X MES-SDS running buffer (Life Technologies) and run at 200 V for 35 minutes to allow the samples to migrate through the gel. Next, the samples were transferred to polyvinylidene fluoride (PVDF) membrane (Immobilon-P, Millipore). Gels were removed from the apparatus and assembled into a transfer stack pre-soaked in 1X transfer buffer (Life Technologies) containing 10% (v/v) methanol (VWR chemicals) and 0.1% NuPAGE® Antioxidant (Life Technologies), this stack was loaded into the transfer apparatus and run at 35 V for 65 minutes. After completion of the transfer, the PVDF membrane containing the separated proteins was removed and used for further immunoblotting.

2.9.4 Immunoblotting

Membranes were blocked in 5% skimmed milk powder (Premier Foods Group) in Tris buffered saline (TBS) containing 0.1% (v/v) Tween-20 (Sigma) (TBST) for 1 hour, then incubated with the appropriate primary antibody (Appendix 7.5) in a 100 ml tube with rotation overnight at 4 °C. For initial experiments, full membranes were used for each antibody. For repeat experiments, when detecting multiple targets from the same membrane, the membrane was carefully cut using the protein ladder as a marker before incubation with antibody.

Following primary antibody incubation, the membranes were washed 3 times for 5 minutes each in TBST at room temperature then incubated with the appropriate secondary antibody for 1 hour at room temperature with rotation. Membranes were washed again as previously then placed protein side up onto a sheet of cling film and incubated with 1.5 ml enhanced chemiluminescent solution (ECL Select™ Western blotting detection reagent; GE Healthcare) for 5 minutes.

Images were collected using a LI-COR C-DiGit® Blot Scanner (Model 3600; LI-COR) on the high sensitivity setting and quantification analysis carried out using the tools provided in the Image Studio Digits software (LI-COR).

2.10 Immunofluorescence staining of HUVECs

The day before beginning the protocol, 34 mm^2 round cover clips were cleaned with 70% ethanol, left to dry in a laminar flow cabinet then autoclaved to ensure sterility. Three drops of di-N-butylphthalate polystyrene xylene (DPX; VWR) were added to each well of a six-well plate and a cover slip placed into the well using forceps. The lid was placed onto the plate and the DPX left to dry overnight. The following day, HUVECs were seeded into the six-well plates according to the particular protocol for the experiment to be carried out.

Following the experiment, plates were placed directly onto ice. The media was removed from each well and the cells washed three times with ice-cold PBS. The cells were then fixed with 4% formaldehyde at room temperature without rocking for 12 minutes, then washed a further three times with 1 ml ice-cold PBS. Cells were then permeabilised with 700 µl 0.1% Triton-X100 (Sigma) in PBS at room temperature for 15 minutes with rocking, then blocked with 500 µl 20% goat serum (Sigma) in PBS for one hour at room temperature. The primary antibodies to be used for staining were diluted to the appropriate concentration (Appendix 7.5) in 5% goat serum in PBS and a 120 µl drop placed onto a sheet of parafilm (Bemis) in a humid staining tray. Using curved forceps, the cover slips were then gently lifted from the wells and placed face-down onto the

droplet of antibody solution. The lid was then placed on the staining tray and it was incubated overnight at 4 °C.

Following incubation with the primary antibody, cover slips were placed face-up into a fresh six-well plate and washed three times with 1 ml PBS. Secondary antibody was then diluted in 5% goat serum in PBS and a 120 µl drop placed onto a new sheet of parafilm. Coverslips were placed face-down onto the secondary antibody and incubated for 1 hour at room temperature protected from light, then washed as before. Cover slips were kept in the wells for the next step; 2 µg/ml 4,6-Diamidino-2-phenylindole (DAPI) (Life Technologies) in PBS was added to each well and rocked for 15 minutes at room temperature protected from light. Cover slips were washed a final time then removed from the wells and placed face-down onto a drop of ProLong® Gold mounting medium (Life Technologies) on a glass slide. Nail varnish (Clinique) was placed around the edge of the cover slip and allowed to dry protected from light before imaging.

2.11 Isolation of RNA from the porcine aortic arch.

Porcine hearts and attached major vessels were obtained from a local abattoir (N Bramall & Sons) shortly following the death of the animal. Tissue was placed immediately into cold transport medium consisting of Dulbecco's modified Eagle's medium (DMEM; Life Technologies) containing 1% penicillin/streptomycin, 1% amphotericin B and 100 µg/ml gentamycin (Sigma) and brought to the laboratory. The aortic arches were dissected and cleaned, ensuring they were kept cold throughout. Then using a scalpel, 1 cm^2 sections were cut from regions of the inner and outer curvatures corresponding to low and high shear stress respectively, as calculated by computational fluid dynamics (Serbanovic-Canic et al., 2016). These sections were then incubated endothelial side down on a 1 ml drop of M199 containing 1 mg/ml collagenase for 15 minutes, then the solution was collected to a 1.5 ml tube, and the edge of a clean scalpel used to gently scrape remaining ECs into the corresponding solution. Cell suspensions were centrifuged for 6 minutes at 1000 rpm and supernatants carefully removed using a pipette. RNA was then isolated from each sample as described in Section 2.7.3.

2.12 Genotyping from mouse ear-clips

Ear-clips were lysed in ear-clip lysis buffer (Appendix 7.6) containing 3% Proteinase K (Thermo Scientific). To each sample, 150 µl of this solution was added and incubated at 55 °C overnight. Following a brief vortex to disrupt the tissue, the clips were heated to 100 °C for 12 minutes before being placed on ice and diluted with 600 µl nuclease-free H_2O. A genotyping PCR was then carried out, with reaction volumes outlined in Appendix 7.7. The samples were placed in a thermal cycler and run on a thermal profile consisting of melting at 95 °C for 30 s, followed by an annealing stage for 30 s at 63 °C (Cezanne wild-type reaction), 65 °C (*Ldlr* reaction) or 67 °C (Cezanne gene-trap reaction), then an extension stage at 72 °C for 45 s; this cycled 40 times. Following the PCR, 6× DNA loading dye (Thermo Scientific) was added to each sample (diluting by 1:6). A DNA ladder mixture was made by combining 8.33% 100 bp ladder (New England Biolabs) with 16.67% 6× DNA loading dye in water. A 1.5% agarose gel was cast by dissolving agarose (Bioline) in Tris-acetate EDTA (TAE) buffer (diluted from 50× stock, Geneflow) by heating in a microwave until completely dissolved. After allowing to cool slightly, 0.05% ethidium bromide (Sigma) was added and mixed well. The agarose solution was poured into a gel tray with the ends covered with tape and a comb inserted and left to set for approximately 30 min. The gel was then placed into an electrophoresis tank and covered with TAE buffer; the ladder and DNA samples were loaded onto the gel then the apparatus connected to a power supply. Electrophoresis was carried out at 100 V for 25 min, then the gel removed and placed in a transilluminator attached to a PC running GeneSnap software (SynGene). Images were acquired and printed then genotypes evaluated.

2.13 Mouse strains and breeding strategy

2.13.1 *Otud7b*$^{-/-}$

Mice were obtained from the Toronto Centre for Phenogenomics (Toronto, Canada) heterozygous for an allele of *Cezanne* containing an insertion of a NorCOMM (North American Conditional Mouse Mutagenesis) cassette (Figure 2.1), *Otud7b*$^{tm1(NCOM)Cmhd}$ on a C57BL/6N background. This causes a deletion of 5397 bp, removing exons 4-7. For brevity, this allele will be referred to as a knockout allele. *Otud7b*$^{+/+}$ and *Otud7b*$^{-/-}$ mice were generated as littermates by breeding the heterozygotes. Figure 2.1b and c show the genotyping results from the progeny of a heterozygous cross.

a

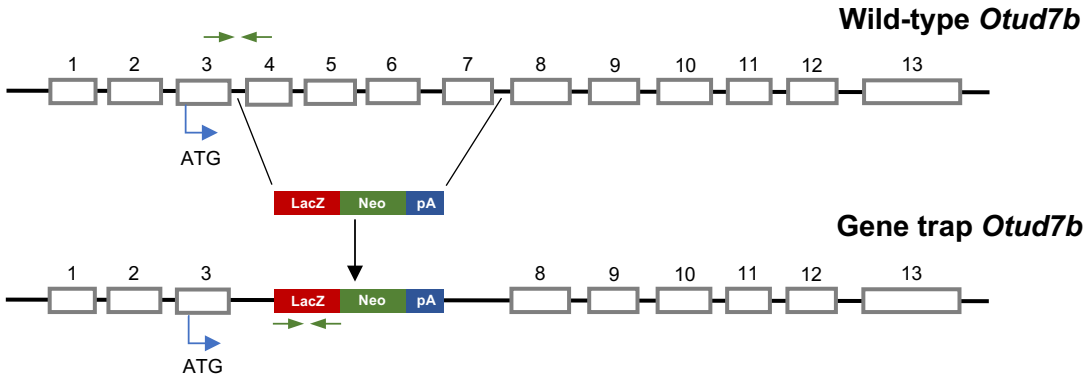

b

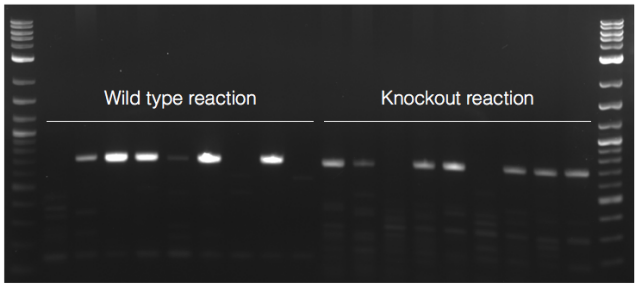

Mouse #	Sex	WT band	KO band	Genotype
74426	M		✓	–/–
74427	M	✓	✓	+/–
74428	M	✓		+/+
74429	M	✓	✓	+/–
74430	F	✓	✓	+/–
74431	F	✓		+/+
74432	F		✓	–/–
74433	F	✓	✓	+/–
74434	F		✓	–/–

c

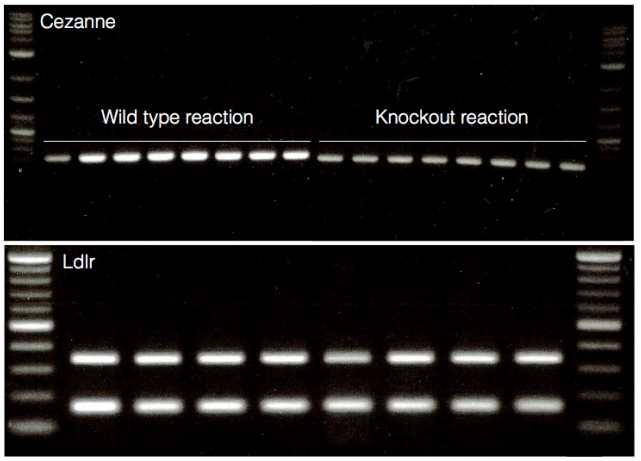

Mouse #	Sex	Cezanne		Genotype	LDLR		Genotype
		WT band	KO band		WT band	KO band	
80782	M	✓	✓	+/–	✓	✓	+/–
80783	M	✓	✓	+/–	✓	✓	+/–
80784	M	✓	✓	+/–	✓	✓	+/–
80785	M	✓	✓	+/–	✓	✓	+/–
80786	M	✓	✓	+/–	✓	✓	+/–
80787	M	✓	✓	+/–	✓	✓	+/–
80788	M	✓	✓	+/–	✓	✓	+/–
80789	F	✓	✓	+/–	✓	✓	+/–

Figure 2.1: Genotyping mice for *Otud7b* and *Ldlr* alleles. (a) A schematic showing the structure of the wild-type and gene trapped knockout Cezanne alleles. A LacZ cassette inserted in place of exons 4-7 disrupts expression of functional protein. Green arrows indicate the approximate position of primers used in the genotyping reactions. **(b)** The offspring of a cross between *Otud7b* heterozygotes were genotyped. Genomic DNA was isolated from ear clip tissue and amplified by PCR in two reactions using primers specific to the wild-type and gene-trap alleles respectively. Reaction products were run on an agarose gel with ethidium bromide and bands imaged using a UV transilluminator. Genotypes are noted in a table. **(c)** Cezanne knockouts were bred with *Ldlr* knockouts. Wild-type and knockout alleles of each gene were assessed using PCR and subsequent electrophoresis. Results are summarised in the table

2.13.2 *Ldlr*$^{-/-}$

Homozygous *Ldlr*^{tm1her} mice were obtained from the Jackson Laboratory and bred on site, maintained as a homozygous colony. The *Ldlr*^{tm1her} allele contains a neomycin resistance cassette insert into exon 4 of the *Ldlr* gene, resulting in a truncation within the ligand binding domain, and loss of the membrane spanning region (Ishibashi et al., 1993).

2.13.3 *Otud7b*$^{-/-}$*Ldlr*$^{-/-}$

Otud7b$^{-/-}$ mice were bred with *Ldlr*$^{-/-}$ mice to obtain *Otud7b*$^{+/-}$*Ldlr*$^{+/-}$ animals. These were intercrossed, and *Otud7b*$^{+/-}$*Ldlr*$^{-/-}$ progeny selected for further breeding to fix the *Ldlr* alleles. A further round of intercrossing generated *Otud7b*$^{-/-}$*Ldlr*$^{-/-}$ animals, which were incrossed to generate experimental animals.

2.13.4 *Nfkb2*$^{-/-}$

Nfkb2$^{-/-}$ mice were obtained from the laboratory of Prof Mark Pritchard and Dr Carrie Duckworth (University of Liverpool), in collaboration with Dr Jorge Camaaño (University of Birmingham). The mutant allele contains a phosphoglycerin kinase neomycin cassette inserted into exon 4, resulting in a loss of protein expression (Caamaño et al., 1998). All animals were housed at the University of Liverpool and tissue taken offsite.

2.14 Intraperitoneal injection of bacterial lipopolysaccharide

Lipopolysaccharides (LPS) from *Escherichia coli* 0111:B4 (LPS; Sigma) were dissolved in sterile PBS to a concentration of 1 mg/ml. Mice were weighed and injected intraperitoneally with a volume of LPS to deliver 4 mg/kg. The animals were continually monitored and sacrificed after 6 hours.

2.15 Administration of a high-fat Western diet

Animals were fed Western RD diet (Special Diets Services), the composition of which is described in Appendix 7.8. Multiple mice were housed in each cage and normal chow replaced with the Western diet at 5 g per mouse per day. Mice were monitored daily throughout feeding.

2.16 Isolation and *en face* staining of the murine aorta

Each mouse was sacrificed by intraperitoneal injection of 100 µl pentobarbitone to induce anaesthetic overdose; once the pedal reflex was lost, blood was taken by cardiac puncture. The ribcage was then opened and the vasculature cleaned by clipping the right atrium and perfusion of 10 ml PBS through the left ventricle. Following this, 10 ml of 4% formaldehyde was perfused to fix the endothelial cells *in situ*. The ribcage was then removed and placed in 2% formaldehyde for one hour before being placed in PBS and stored at 4 °C. The aorta was dissected from the ribcage using fine forceps and a dissection microscope and cleaned thoroughly. Each aorta was cut into three sections; the aortic arch, and two pieces of the descending aorta, which were cut additionally lengthways to open the endothelial surface (Figure 2.2). Aortic sections were placed in individual wells of a 96-well plate, then blocked and permeabilised in 100 µl of 20% goat serum in 0.5% Triton-X100 PBS at 4 °C overnight. Antibody against the endothelial marker PECAM-1, conjugated to Alexa Fluor® 488 (BioLegend) was then diluted in 5% bovine serum albumin (BSA; Sigma) in PBS and the sections incubated in 100 µl for 5 days. Following this, the sections were washed by flushing several times with PBS before being incubated at 4 °C overnight with primary antibodies to the gene of interest (Appendix 7.5), diluted to 5 µg/ml in 100 µl of 5% BSA in PBS. The sections were washed with PBS again and incubated at room temperature for 5 hours with 100 µl secondary antibody diluted in 5% BSA in PBS. Next, the sections were washed again before being incubated with the nuclear stain TO-PRO-3 (Life Technologies) diluted 1/300 in PBS. Finally, the sections were mounted endothelial side down on coverslips in a droplet of ProLong® Gold, a slide was placed on top of this and the slides placed under weights overnight to flatten the sections. Nail varnish was applied to the edge of the coverslip to prevent the slides drying out.

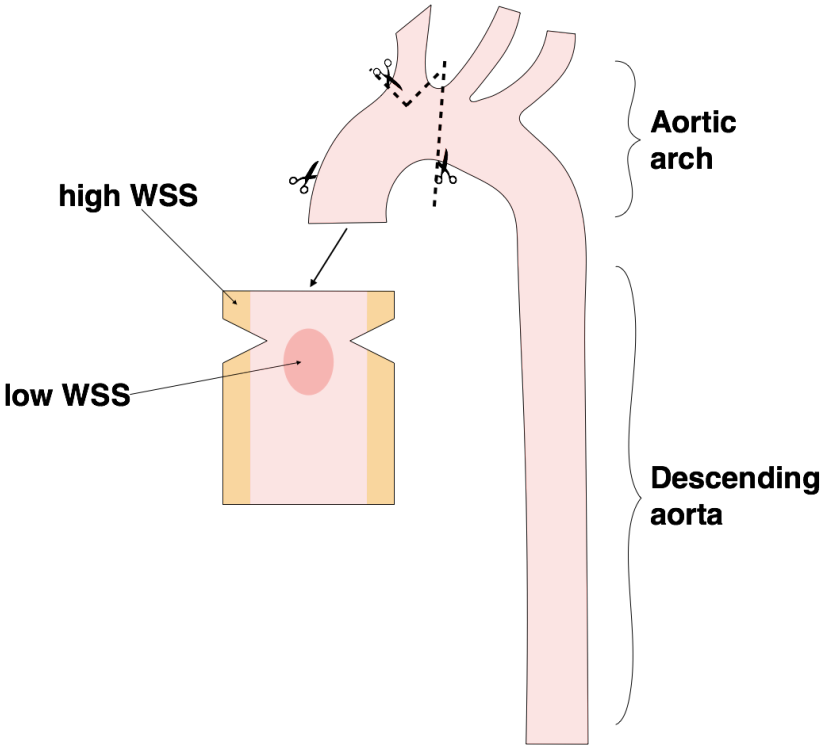

Figure 2.2: Sectioning of the murine aorta. Aortae were perfusion fixed with formaldehyde and dissected before being cut into sections for further immunostaining. The descending aorta was cut into two sections which were both used. The aortic arch was cut following the brachiocephalic artery allowing a single flattened section with both disturbed and undisturbed flow, shown by pink and yellow shading respectively.

2.17 Oil Red O staining of the murine aorta.

To make the Oil Red O staining solution, 1% H_2O was added to 99% isopropanol (VWR Chemicals), the Oil Red O powder (Sigma) added to the solution until saturation. The slurry was then filtered using Whatman filter paper to remove undissolved Oil Red O. On the day of staining, this solution was diluted to 60% in H_2O.

Aortas were perfusion fixed, removed from the animals and cleaned as in Section 2.16, then opened longitudinally. Each aorta was rinsed in H_2O followed by 60% isopropanol for 2 minutes each, then immersed in Oil Red O solution for 15 minutes. Following staining, aortas were washed in 60% isopropanol, then H_2O for a further 2 minutes each. To image the stained tissue, molten wax was poured into a petri dish and allowed to partially solidify. While the wax was still warm, the aortas were pinned flat using insect pins (Fine Science Tools) and immersed in PBS. Aortas were imaged using a dissection microscope, including an image of a ruler for software calibration. Analysis was carried out using ImageJ; total aortic area and lesion area were outlined and the area calculated using the software.

3. Regulation of Cezanne expression by shear stress

3.1 Introduction

The development of atherosclerotic lesions within the vasculature is not uniform; ECs at sites of predilection such as at bends and branch points are activated, leading to enhanced inflammation, proliferation and apoptosis. Haemodynamic conditions at these sites lead to an alteration in the cellular environment. Notably, the low oscillating shear stress exerted on the vessel wall at these regions promotes an induction of NF-κB (Hajra et al., 2000) via a JNK-ATF2 (activating transcription factor 2) pathway (Cuhlmann et al., 2011). Furthermore, local oxygen tension is reduced at these sites (Santilli et al., 1995), suggesting that cells here may possess differences in oxygen mediated pathways such as hypoxia or ROS signalling.

The deubiquitinase Cezanne has been linked to the regulation of several pathways involved in the pathogenicity of atherosclerosis, but it is unknown whether Cezanne is differentially expressed in ECs exposed to physiological levels of shear stress found at atheroprotected and atheroprone sites *in vivo*. Previous research has revealed that the application of unidirectional shear stress to HUVECs was able to cause induction of Cezanne mRNA expression, as was stimulation of several NF-κB inducing ligands, including TNFα (Enesa et al., 2008a), CD40L and LT-β (Hu et al., 2013). Exposure to hypoxia has also been found to significantly induce Cezanne expression in human ECs from a variety of vascular beds. Moreover, surgically induced kidney ischaemia followed by reperfusion was sufficient to induce Cezanne expression in whole kidney samples from both rats and mice (Luong et al., 2013).

Of particular note, a microarray study identified an enrichment in Cezanne expression at an atheroprotected site, although expression of Cezanne at the protein level was not studied (Passerini et al., 2004). It is important to discover whether cells at these regions possess an elevated level of Cezanne expression and the mechanisms governing its activation, as Cezanne has been implicated in regulating NF-κB and hypoxic signalling and thus may be responsible for focal atherosclerosis.

3.2 Hypothesis and aims

Hypothesis: Cezanne expression is differentially regulated at sites of predisposition to atherosclerosis in ECs, due to either differences in shear stress, inflammatory signalling or hypoxia.

Aim 1: Characterise Cezanne expression at sites prone to and protected from atherosclerosis *in vivo*.

Aim 2: Characterise Cezanne expression in ECs exposed to different shear stress patterns.

Aim 3: Characterise Cezanne expression upon stimulation with NF-κB-activing molecules in ECs exposed to different shear stress patterns.

Aim 4: Characterise Cezanne expression in ECs exposed to hypoxia in addition to different shear stress patterns.

3.3 Cezanne expression was elevated at regions predisposed to atherosclerosis.

The localisation of atherosclerotic lesions within the murine vasculature has been well described (VanderLaan et al., 2004), with a major site of development being at the inner curvature of the aortic arch in genetically modified disease models. To determine whether Cezanne expression was differentially regulated in ECs at regions prone to or protected from the development of atherosclerosis, aortas from 8-week-old mice were dissected and Cezanne expression analysed using immunofluorescence staining (Figure 3.1). Staining of PECAM-1 to mark endothelial junctions showed a marked difference in EC morphology between the regions investigated, with cells from the inner curvature of the aortic arch displaying the 'cobblestone' appearance typical of low shear stress (Davies et al., 1986), in comparison to the elongated, aligned conformation seen in cells and nuclei from both the outer curvature and descending aorta. Staining of Cezanne revealed a cytoplasmic localisation, with heterogeneity in the signal between different cells. Total expression was found to be significantly elevated in ECs at the inner curvature of the aortic arch compared to the outer curvature. Expression in the descending aorta was greater than in the outer curvature of the aortic arch, but this was not statistically significant. This suggests that Cezanne expression is upregulated at sites prone to atherosclerosis, but the pathway governing this expression change is not clear.

3.4 Cezanne expression is elevated under low shear stress *in vitro*.

Differences in expression between the inner and outer curvatures of the murine aorta can be due to a variety of mechanisms. Due to the curving geometry of the aortic arch, shear stress exerted by flowing blood is not distributed evenly (Figure 1.2). At the outer curvature, shear stress is unidirectional and high magnitude, while at the inner curvature it is oscillating and lower magnitude. A range of mechanosensitive molecules and structures can sense these differences in shear stress and lead to modulation of EC gene expression, causing profound changes to cellular phenotype (reviewed by Chiu and Chien, 2011). Cezanne expression at the inner curvature could be directly stimulated as a downstream target of one or more mechanosensors, alternatively its expression could be regulated by the activity of another signalling pathway – such as HIF or NF-κB signalling – that are known to be differentially expressed under different shear stress conditions (Akhtar et al., 2015; Hajra et al., 2000).

To test the effect of different shear stress patterns on the expression of Cezanne, primary HUVECs were exposed to physiologically relevant shear stress patterns *in vitro* using two complimentary systems – the ibidi® and orbital shaker systems. Using the ibidi®

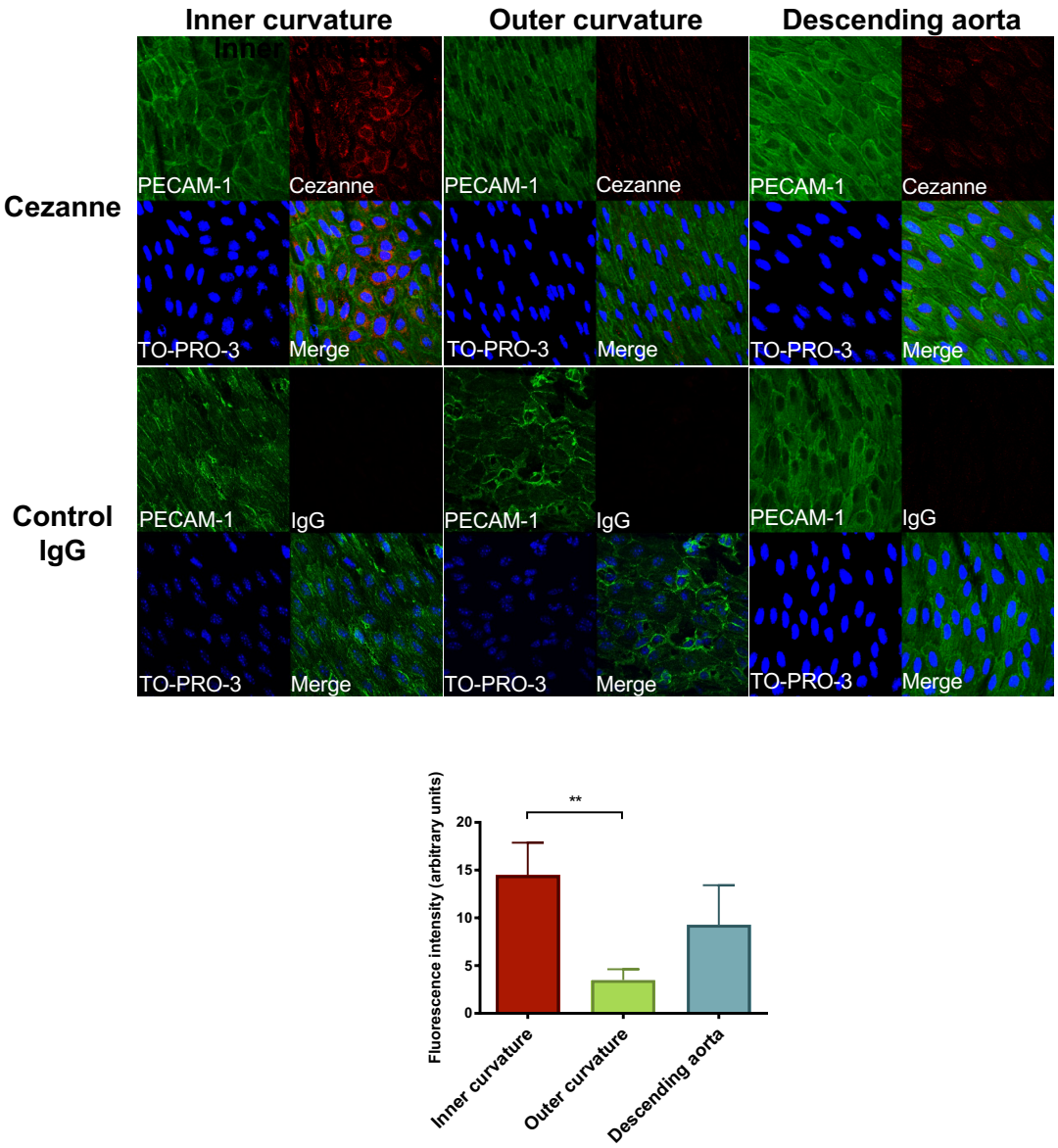

Figure 3.1: Cezanne expression is elevated under low shear stress *in vivo*. Aortas from 8 week old wild-type C57BL/6 mice were perfusion fixed, dissected and stained using antibodies against Cezanne or an isotype control rabbit IgG. In addition, each tissue section was stained using an antibody against the endothelial cell marker PECAM-1 conjugated to Alexa Fluor 488, and the nuclear marker TO-PRO-3 Iodide. Sections were mounted *en face* onto glass coverslips and cells from the inner and outer curvatures of the aortic arch, as well as the descending aorta were imaged using confocal microscopy. The mean fluorescence intensity was determined for each region using ImageJ software. Data are presented as mean ± SD.
n=4; $p<0.01$; One-way ANOVA with Tukey's multiple comparisons.

pump system, HUVECs were exposed to either unidirectional 13 dyn/cm² (high) or oscillating (1 Hz) 4 dyn/cm² (low) shear stress, conditions which approximate the shear stress environment experienced by human aortic ECs (Doriot et al., 2000; Milner et al., 1998; Samady et al., 2011). While the ibidi® system applies a precise magnitude of shear stress to cells within a chamber slide, it applies only a unidirectional flow or bidirectional oscillations to cells. In contrast, ECs *in vivo* are subject to complex shear stress patterns, with pulsatility and multidirectionality varying across the endothelial surface. The orbital shaker system allows a single population of ECs to be exposed to both high and low shear stress within a single well, and cells in the centre are exposed to multidirectional shear. It also allows for higher throughput experiments. Following the application of shear stress in these systems, the alignment of the ECs was assessed to confirm a differential response (Figure 3.2). In both the ibidi® and orbital shaker systems, ECs aligned with the direction of flow when exposed to high shear stress, but adopted the polygonal "cobblestone" appearance under low shear stress, indicating that the cells were behaving as *in vivo*.

Next, mRNA expression in cells exposed to both low and high shear stress was analysed in samples from each of the flow systems. The expression of control genes MCP-1 and endothelial nitric oxide synthase (eNOS) were tested, as these are known to be upregulated in low and high shear stress conditions respectively, as well as expression of Cezanne (Figure 3.3). MCP-1 and eNOS expression was enriched under low and high shear stress respectively in both systems. Expression of Cezanne was significantly higher in ECs isolated from the low shear stress condition of each of the systems in comparison to cells exposed to high shear stress. To test whether this difference in mRNA expression coincided with an elevation in protein expression, lysates were also generated from cells exposed to both low and high shear stress using each of the flow systems and Cezanne expression measured by Western blotting. Cezanne protein was more highly expressed under low shear stress compared to high shear stress (Figure 3.4). Interestingly, while Cezanne is predicted to have a molecular weight of 100 kDa, two bands were found on the Western blots, at 90 and 110 kDa. To determine which band corresponded to Cezanne, a second antibody targeting the carboxy terminus of Cezanne was used to probe the samples, finding bands at 90 and 110 kDa which matched those seen with the first antibody and suggesting that both bands correspond to Cezanne. These results suggest that the induction of Cezanne expression observed *in vivo* at the inner curvature of the aortic arch is as a result of low shear stress acting on ECs, rather than due to the effects of neighbouring cells or mass transport mechanisms.

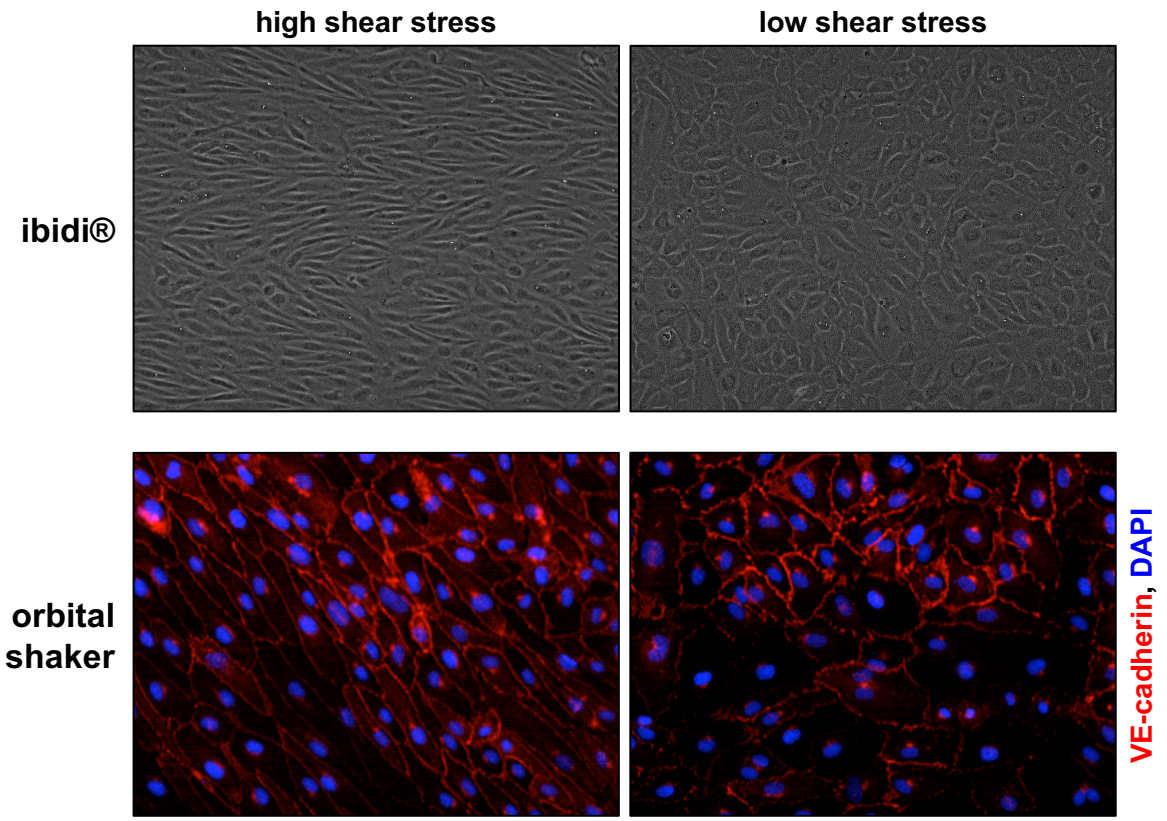

Figure 3.2: HUVEC alignment is altered when exposed to high or low shear stress *in vitro*. (top panels) HUVECs at passage 3 were seeded onto gelatinised ibidi® µ-Slide $I^{0.4}$ chamber slides and allowed to adhere. The slides were then connected to the pump systems and exposed to either ±4 dyn/cm2 at 1 Hz (low shear stress) or 13 dyn/cm2 (high shear stress) for 72 hours. Following the application of flow, images were taken of each slide using phase contrast microscopy. **(bottom panels)** HUVECs at passage 3 were seeded onto gelatinised six-well plates and allowed to adhere. The media was changed to 3 ml of fresh media and plates placed on an orbital shaker at 210 rpm for 72 hours to generate a defined shear stress pattern across the well, with low shear stress of approximately 4 dyn/cm2 in the centre and high shear stress of approximately 13 dyn/cm2 in the periphery. Following exposure to shear stress, cells were washed with PBS then fixed with 4% formaldehyde and stained for VE-cadherin using immunofluorescence techniques, DAPI staining was also included as a nuclear marker. Images were then taken using fluorescence microscopy.

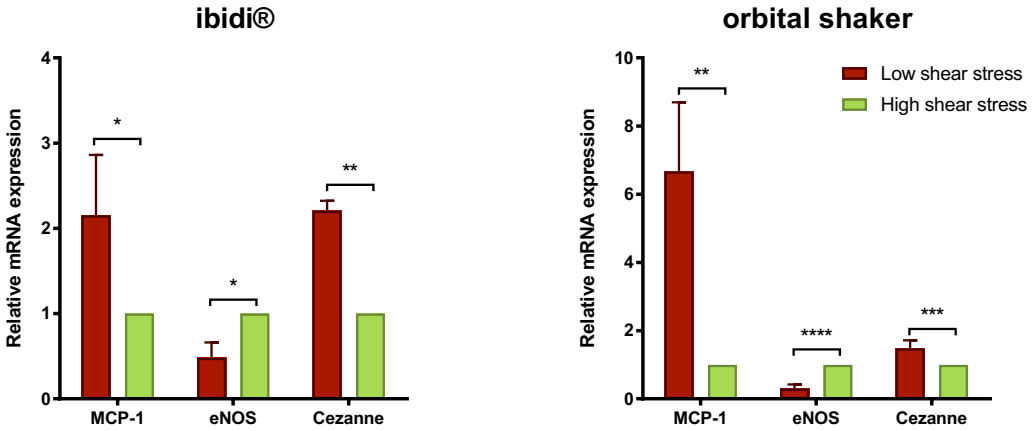

Figure 3.3: Cezanne mRNA expression is elevated under low shear stress *in vitro*. HUVECs were exposed to low or high shear stress for 72 hours using the ibidi® (left) and orbital shaker (right) systems. Following the application of flow, cells were lysed directly and RNA isolated using a commercially available kit. Next, cDNA was generated and mRNA expression of control genes MCP-1 and eNOS, as well as Cezanne quantified by qPCR, normalising to expression of the housekeeping gene HPRT. Fold change was calculated using the $2^{-\Delta\Delta CT}$ method. Data are presented as mean ± SD.
n=3; *p<0.05; **p<0.01; ***p<0.005; ****p<0.001; Two-tailed paired t test. Statistical tests were carried out on ΔCT values.

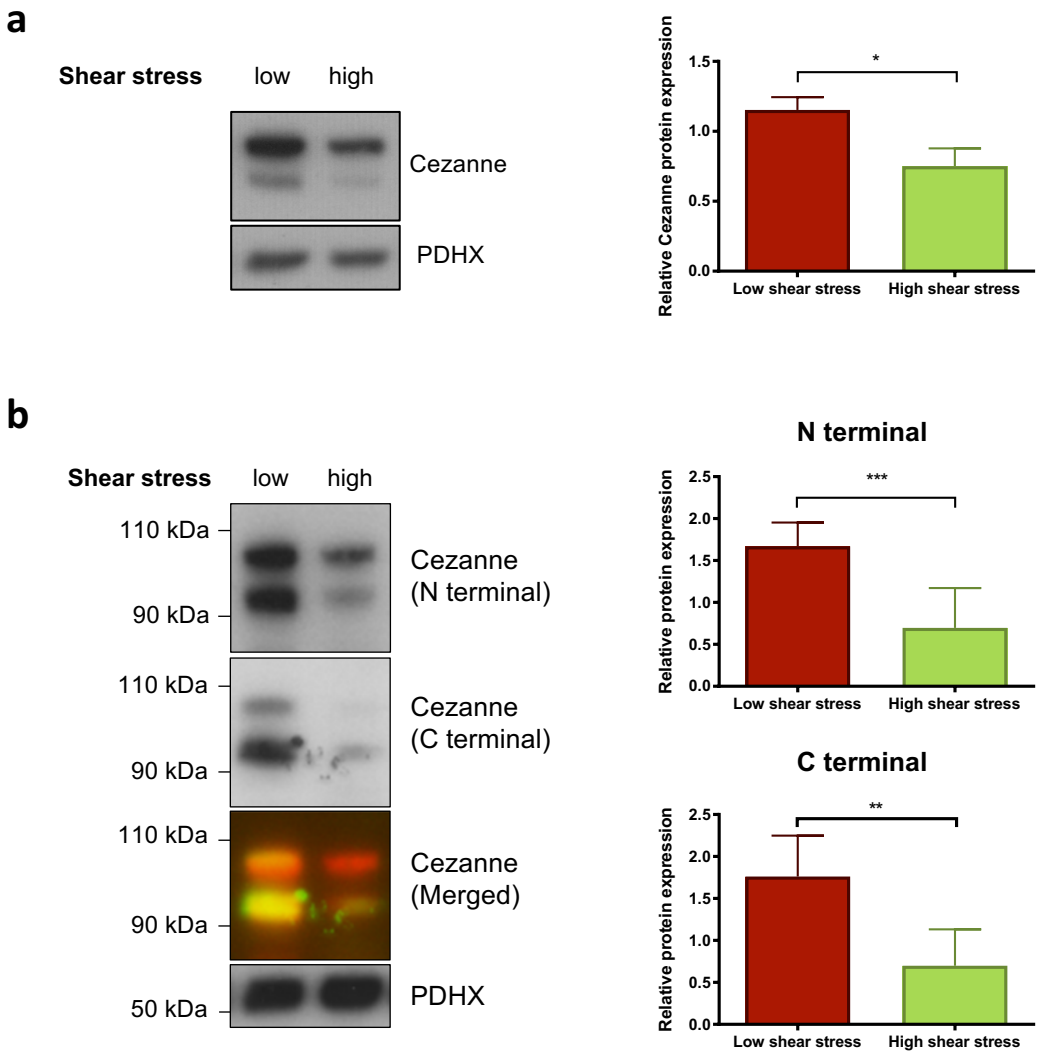

Figure 3.4: Cezanne protein expression is elevated under low shear stress *in vitro*. HUVECs were exposed to low and high shear stress using the ibidi **(a)** and orbital shaker **(b)** systems for 72 hours. Following the application of flow, cells were lysed separately from each condition. Protein concentration was determined using a BCA assay, and samples normalised accordingly. The expression of Cezanne was determined by Western blotting, normalising to the housekeeper PDHX. For orbital shaker samples, a second C terminal antibody was used following stripping of the membrane and images of each overlaid using ImageJ. Densitometry was carried out using ImageJ software, on the combined intensity of both Cezanne bands. Data are presented as mean ± SD.
n=3 (ibidi) n=10 (orbital shaker); *p<0.05; **p<0.01; ***p<0.005; Two-tailed paired t test.

3.5 TNFα does not further induce Cezanne expression under low shear stress.

Previous studies have shown that Cezanne expression in ECs can be induced by the addition of inflammatory stimuli such as TNFα and reoxygenation following hypoxia (Enesa et al., 2008a; Luong et al., 2013). As Cezanne has also been shown to be a negative regulator of the inflammatory NF-κB pathway, this is of relevance to its potential role in atherosclerosis as inflammatory signalling is enhanced at atheroprone sites *in vivo* (Cuhlmann et al., 2011; Hajra et al., 2000) due to differences in both haemodynamic conditions (Mohan et al., 1997; Nagel et al., 1999; Wang et al., 2013a) and the release of proinflammatory cytokines from adherent leukocytes (Libby, 2002). Thus, the presence of exogenous cytokines may be a regulatory factor in the expression levels of Cezanne, causing its expression to increase during atherogenesis.

To test whether Cezanne expression is upregulated by inflammatory cytokine exposure in ECs exposed to flow, HUVECs were cultured under shear stress using the orbital shaker system, then treated with TNFα to activate NF-κB. Immunofluorescence staining of the NF-κB subunit RelA was carried out in cells exposed to low shear stress in the presence or absence of TNFα. The degree of nuclear localisation of RelA was used to control for endothelial responses to TNFα. As expected, the addition of TNFα strongly induced nuclear localisation of RelA, verifying that the HUVECs responded to TNFα (Figure 3.5a). Furthermore, mRNA expression of the NF-κB target gene and positive control MCP-1 was strongly induced by TNFα (Figure 3.5b). By contrast, Cezanne transcript expression was not found to be significantly altered by stimulation with TNFα, although there was a trend towards an increase particularly in cells from the high shear stress site (Figure 3.5c). These data indicate that activation of the TNFR pathway is not sufficient to further induce Cezanne expression in cells exposed to low shear stress, thus the mechanism underlying elevated Cezanne expression at atheroprone regions *in vivo* may not be as a result of the presence of exogenous TNFα and potentially other cytokines, but instead due to low shear stress acting through another pathway.

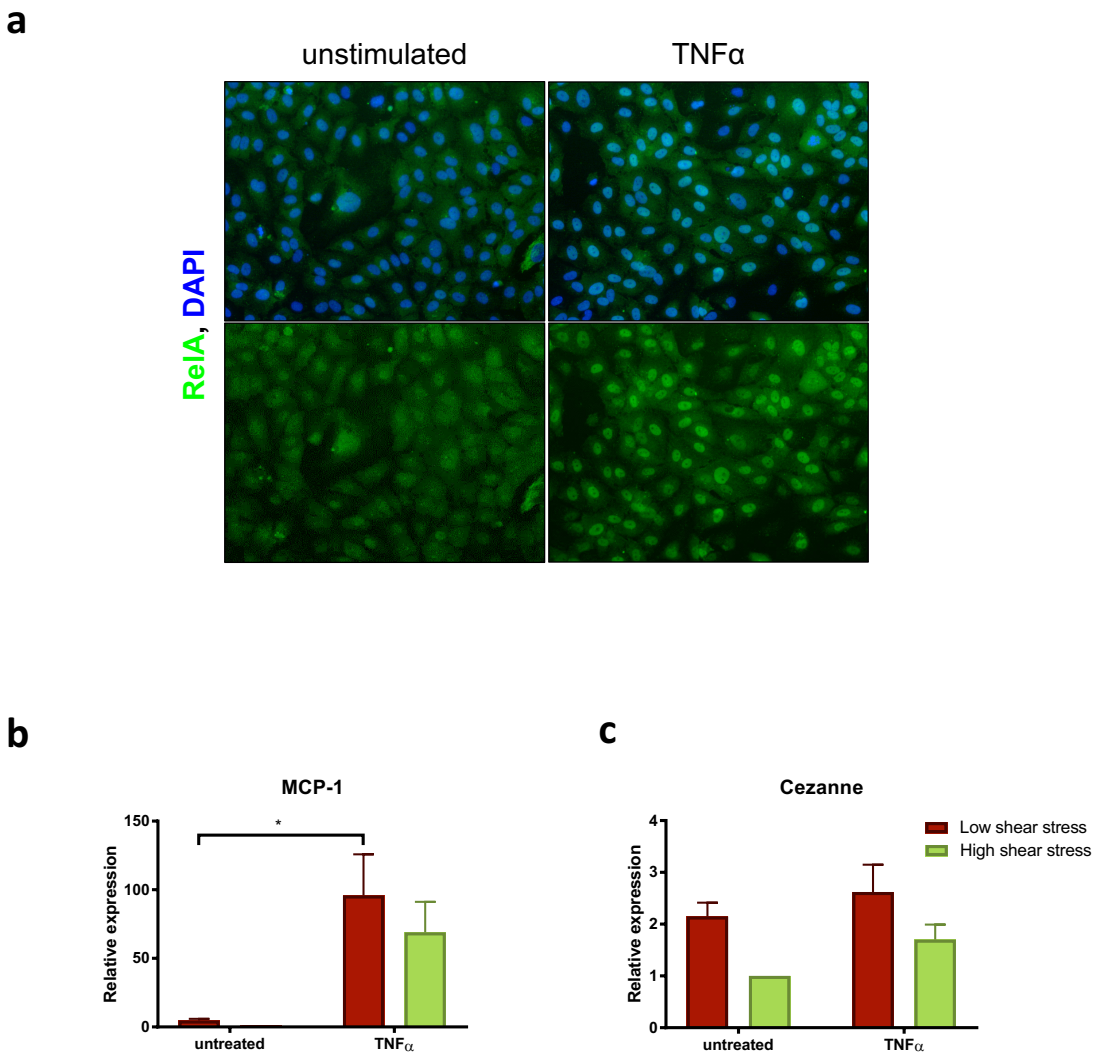

Figure 3.5: Cezanne expression is not regulated by TNFα in cells exposed to shear stress. HUVECs were exposed to low and high shear stress using the orbital shaker system for 72 hours. The same populations of cells were exposed to both conditions depending on their location within the well. TNFα (10 ng/ml) was added to half the wells for the last 4 hours of shear stress, with the remainder left untreated. **(a)** Following treatment, cells were fixed with 4% formaldehyde and stained for the NF-κB subunit RelA (green) as well as the nuclear marker DAPI (blue). Cells were visualised by wide-field fluorescence microscopy and images captured using the Leica LAS AF software. **(b & c)** After treatment, cells were scraped from each condition. RNA was obtained using a commercially available kit and cDNA generated. The expression of both MCP-1 **(b)** and Cezanne **(c)** were quantified by qPCR, normalising to the housekeeping gene HPRT. Data are presented as mean ± SD.
n=3; $p<0.05$; Two-tailed paired t test. Statistical tests for qPCR results were carried out on ΔCT values.

3.6 Non-canonical NF-κB signalling does not regulate Cezanne expression in endothelial cells exposed to shear stress.

There is published evidence that Cezanne expression is under the regulation of the non-canonical branch of the NF-κB pathway in B cells, with stimulation by CD40L and LT-β causing enhanced Cezanne expression (Hu et al., 2013). These cytokines are expressed by various cell types present in the blood such as B cells, T cells and platelets (Henn et al., 1998; Sun, 2011) and thus could influence the expression of Cezanne in ECs. In order to investigate whether Cezanne expression is under the control of this molecular pathway in ECs exposed to shear stress, HUVECs were cultured using the orbital shaker system to generate shear stress and then stimulated with CD40L to activate the non-canonical NF-κB pathway. Confirmation of activity was obtained by Western blotting for p100/p52; these blots showed that stimulation consistently induced cleavage of p100 to p52, indicated by a reduction in p100 levels and a concomitant increase in p52 (Figure 3.6). Interestingly, the expression of these proteins was also found to be strongly regulated by shear stress (see Chapter 5). The expression of Cezanne was not altered by CD40L in cells from either the low or high shear stress regions of the plate. These data indicate that the induction of Cezanne expression at atheroprone sites *in vivo* is not due to the presence of ligands which activate the non-canonical NF-κB pathway.

3.7 Hypoxia does not alter Cezanne expression in endothelial cells exposed to shear stress.

The expression of Cezanne in ECs has previously been reported to be enhanced following exposure to hypoxia (Luong et al., 2013), however this was not investigated in cells exposed to shear stress. There is evidence to suggest that atheroprone sites have lower oxygen availability than protected sites (Santilli et al., 1995), and ECs overlying lesions display enhanced expression of HIF-1α (Akhtar et al., 2015), a transcription factor central to promoting cellular responses to hypoxia. The expression of Cezanne in ECs exposed to shear stress may therefore also be regulated by exposure to hypoxia. To test whether changes in Cezanne expression generated by differential shear stress can be modified by hypoxic signalling, HUVECs were exposed to shear stress for 72 hours using the orbital shaker system and placed into a hypoxic chamber for the last 4 or 24 hours. Cells were isolated and the expression of Cezanne was tested by Western blotting (Figure 3.7). Cezanne expression was elevated by low shear stress, but did not appear to be altered by either 4 or 24 hours of hypoxia. These results indicate that the presence of hypoxia does not regulate Cezanne expression in ECs exposed to shear stress.

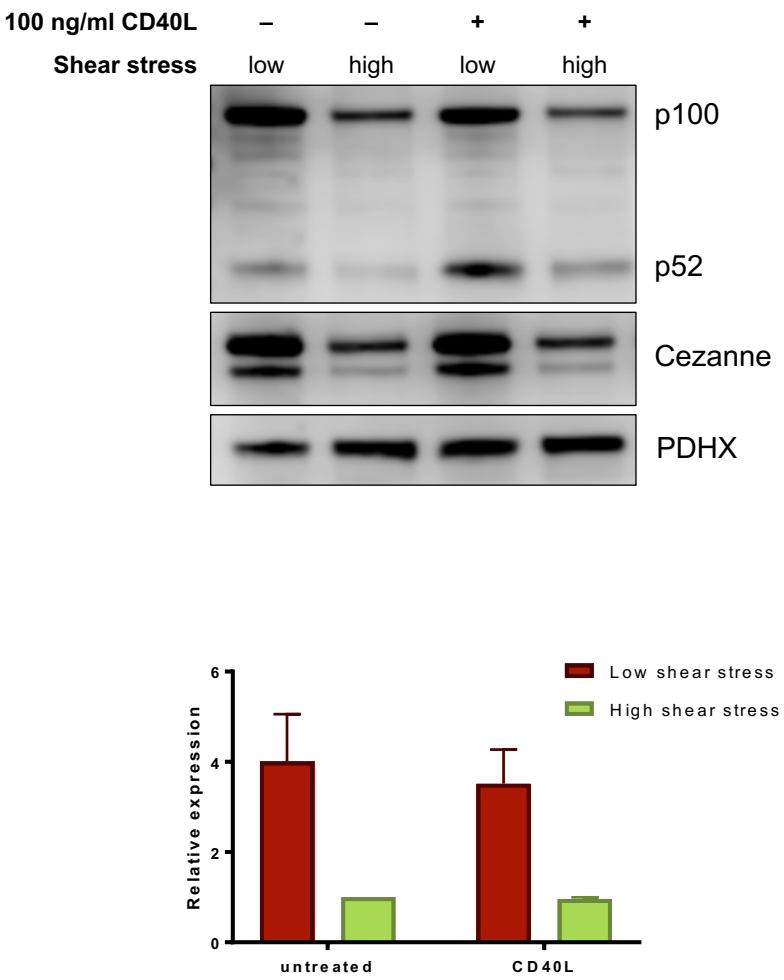

Figure 3.6: Cezanne expression is not regulated by CD40L in cells exposed to shear stress. HUVECs were exposed to low and high shear stress using the orbital shaker system for 72 hours. The same populations of cells were exposed to both conditions depending on their location within the well. CD40L (100 ng/ml) was added to a proportion of the wells for the last 2 hours of shear stress, with the remainder left untreated. Following the application of flow, cells were scraped from each condition and lysed. Protein concentration was determined by BCA assay and samples normalised accordingly. The expression of p100/p52 and Cezanne was quantified by Western blotting, normalising to the housekeeper PDHX. Densitometry was carried out using ImageJ software. Data are presented as mean ± SD.
n=3; Two-tailed paired t test. Statistical tests were carried out on raw data.

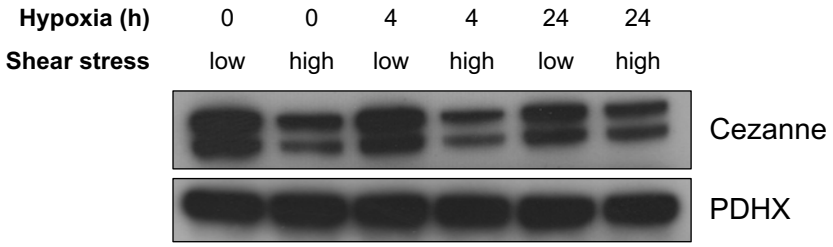

Figure 3.7: Cezanne expression is not regulated by hypoxia in cells exposed to shear stress. HUVECs were exposed to low and high shear stress using the orbital shaker system for 72 hours. The same populations of cells were exposed to both conditions depending on their location within the well. For the final 4 or 24 hours of shear stress, plates were placed into the GENbox apparatus, generating a hypoxic environment, one plate was left in normoxic conditions as a control. Following treatment, cells were scraped from each condition and lysed. Protein concentration was assessed by BCA assay and samples normalised accordingly. Expression of Cezanne was analysed by Western blotting.
Data is from a single experiment.

3.8 Conclusions

Cezanne expression has been found to be induced *in vivo* at a site of predilection to atherosclerosis. The driving factor for this induction is the presence of low shear stress at this site, as *in vitro* studies show elevated Cezanne expression under low shear stress. This induction is dominant over stimulation with TNFα, CD40L or hypoxia, as addition of these factors conferred no further increase in Cezanne expression in cells exposed to low shear stress.

3.9 Discussion

The ovarian tumour deubiquitinase Cezanne has been previously shown to be a negative regulator of EC inflammation through inhibition of NF-κB (Enesa et al., 2008a; Evans et al., 2001; Luong et al., 2013). In addition, these and other studies have identified factors which can induce expression of Cezanne, including shear stress, inflammatory cytokines and hypoxia. These conditions are all altered in ECs at sites of atherosclerosis, and as NF-κB signalling is known to be critical in the development of lesions (Gareus et al., 2008), Cezanne may be important in regulating this process. The role of Cezanne has not been previously studied in the context of atherosclerosis, but analysis of its contribution may shed light on a mechanism by which it can be controlled.

3.9.1 Cezanne expression was elevated by low shear stress *in vivo* and *in vitro*.

The experiments described demonstrate that Cezanne is consistently more highly expressed in ECs which have been exposed to shear stress patterns associated with regions of the vasculature which are prone to the development of atherosclerotic lesions. This induction of Cezanne expression is seen *in vivo* in the aortas of wild-type mice. Immunofluorescence staining of ECs from the inner and outer curvatures of the aortic arch revealed cytoplasmic localisation of Cezanne, as previously reported (Evans et al., 2001). Expression was found to be significantly higher in ECs from the inner curvature of the aortic arch, in comparison to the outer curvature, with ECs in the descending aorta possessing intermediate levels. The inner curvature is documented to be a site prone to the development of inflammation and atherosclerosis (VanderLaan et al., 2004) so this suggests that Cezanne induction may act as a negative feedback mechanism for NF-κB signalling, thereby dampening inflammation. There are several notable differences in the cellular environment of cells from the inner and outer curvatures which may result in alterations in Cezanne expression – differences in shear stress as a result of the geometry of the vessel, enhanced inflammatory signalling, and a decrease in oxygen tensions. To test whether haemodynamic forces were responsible for regulation of Cezanne expression, shear stress was exposed to ECs *in vitro* using two complimentary systems.

These experiments recapitulated the expression changes seen *in vivo*. In both the ibidi® and orbital shaker systems, Cezanne mRNA and protein was more highly expressed under low compared to high shear stress. However, the relative differences in expression between the two shear stress conditions in each system was notably different. The levels of mRNA were over two-fold greater in the low compared to high shear stress in the ibidi® system, while in the orbital shaker system there was less than a 1.5-fold difference. By contrast, protein expression showed the opposite. Increases of 1.5-fold and 2.5-fold were seen in the ibidi® and orbital shaker systems, respectively. The differences between

these results may reflect the sensitivity of Cezanne expression to directionality of shear stress. The ibidi® system exposes cells to shear stress along a single axis, whereas the orbital shaker system is multiaxial and pseudopulsatile. The expression of other shear-sensitive molecules have been shown to be profoundly regulated by the application of shear at different angles relative to cellular alignment (Wang et al., 2013a), and Cezanne expression could be governed by a similar mechanism. Alternatively, the separation of both shear stress conditions in the ibidi® system may be a causative factor in these differences. Molecules such as nitric oxide – produced as a result of eNOS activity – and MCP-1 are secreted by cells under high and low shear stress respectively (Figure 3.3a), and have opposing functions on EC inflammation (Kuchan and Frangos, 1994; Passerini et al., 2004; Shyy et al., 1994). Therefore, ECs in the orbital shaker and ibidi® systems are exposed to different secretory milieus which could potentially influence Cezanne expression.

Further research could focus on identifying whether alterations in expression due to shear stress are due to transcription, translation, or post-translational mechanisms. An observation which may be of relevance to this was the presence of two bands corresponding to Cezanne on Western blots. This could be as a result of alterations in splicing, in the addition of post-translational modifications such as ubiquitination, or cleavage of the protein. Interestingly, the related protein A20 can be cleaved, causing a subsequent reduction in function (Malinverni et al., 2010); potentially Cezanne could be regulated by a similar mechanism. Further work utilising actinomycin D or cyclohexamide experiments should be carried out on cells exposed to shear stress, in order to test whether the alterations in Cezanne expression were as a result of altered transcription or translation.

The expression of Cezanne was previously reported as being induced at an atheroprotected site in the porcine aorta, based on a microarray study (Passerini et al., 2004). Surprisingly, the results described here show the opposite expression pattern, however there are several explanations for this disagreement. Firstly, the haemodynamic conditions vary between the studies. The regions that were studied in the porcine aortic arch by Passerini et al. were directly opposite the brachiocephalic and subclavian branches for the atheroprone site, and approximately 2 cm distal for the atheroprotected site. We have recently used CFD to precisely model the shear stress within the porcine aorta, finding that the atheroprotected site used in the aforementioned work possesses a high degree of oscillatory shear stress (Serbanovic-Canic et al., 2016). Given that Cezanne expression was found to be induced by oscillating shear stress in the ibidi® system, this may be a factor in the heightened expression of Cezanne mRNA observed at

this site. The *in vivo* Cezanne expression data included in this thesis was carried out using murine aortas, compared to the porcine vessels used by Passerini et al. The average shear stress experienced within the murine vasculature is an order of magnitude higher than in pigs (Feintuch et al., 2007; Suo et al., 2007), and the geometry is different due to a much smaller size and the presence of three major branching arteries. These differences may also contribute to the difference in the pattern of Cezanne expression seen between this research and the previous work. Further study of Cezanne expression in the porcine aortic arch at a variety of sites with known shear stress levels may shed light on the sensitivity of Cezanne expression to small changes in flow magnitude and direction.

3.9.2 Low shear stress confers an insensitivity to Cezanne induction by cytokines or hypoxia.

While the previous experiments show that low shear stress was able to elevate the expression of Cezanne, other studies have shown that its expression can also be enhanced by TNFα (Enesa et al., 2008a), CD40L (Hu et al., 2013) and hypoxia (Luong et al., 2013). These factors have all been previously associated with atherosclerotic lesions; infiltrating leukocytes release TNFα and CD40L, amongst other cytokines (Libby, 2002), while HIF-1α expression was found to be increased in ECs overlying lesions (Akhtar et al., 2015). Cezanne expression at sites of predilection may be driven further by exposure to these factors and thus have a significant effect on the inflammatory response of ECs and thus on atherosclerosis.

Thus, Cezanne expression was tested in ECs exposed to shear stress using the orbital shaker system in the presence of these cytokines, or hypoxia. Surprisingly, Cezanne expression under low shear stress was found to be unaffected by the addition of TNFα, CD40L or culturing in hypoxia. The lack of elevated expression following exposure to these stimuli is contradictory to the previously published studies, however there are several important differences in the methodology which may explain the differences.

In one paper, Cezanne expression was modestly induced by unidirectional shear stress and this was further elevated by treatment with TNFα (Enesa et al., 2008a). However, those experiments were comparing expression between static cultures and 12 dyn/cm^2 unidirectional shear stress. In contrast, the results described here compare the expression differences between two shear stress conditions. It is plausible that the stimulus of low shear stress may be sufficient to provide maximal Cezanne expression, thus further stimulation with TNFα has no effect. Indeed, while not statistically significant, a trend towards an induction in Cezanne mRNA expression was seen in cells exposed to high shear stress and TNFα, consistent with this idea.

The discrepancy between induction of Cezanne expression by CD40 ligation in B cells and MEFs (Hu et al., 2013) and the data presented here may be simply due to differences in cell type. The authors do not describe a mechanism for the induction of Cezanne by CD40L stimulation, but suggest that it requires non-canonical NF-κB. While the results in this chapter show that there is an appreciable level of p100/p52 expression in ECs, they are less than those expressed in B cells (biogps.org) and may not be sufficient for Cezanne induction.

Previously, Cezanne expression was seen to be induced by exposure to hypoxia in static ECs in a p38/ATF2 dependent mechanism (Luong et al., 2013). Interestingly, the upregulation was sensitive to oxygen concentration. Induction was found to occur at 1% O_2, but not 2% or 5%. In this chapter, the results showed that hypoxia did not cause an induction of Cezanne expression in ECs exposed to shear stress. However, it is plausible that oxygen levels were not reduced sufficiently for Cezanne induction. Alternatively, it is possible that the p38/ATF2 mechanism described is also sensitive to shear stress. The activity of p38 has found to be higher at sites prone to atherosclerosis, due to inhibition under high shear stress (Zakkar et al., 2008). Cezanne expression under low shear stress may be driven by this signalling pathway and as such, the addition of hypoxia may not further enhance p38/ATF2 signalling, resulting in no change in Cezanne expression.

In order to fully explore the contribution that NF-κB and hypoxic signalling make to the expression of Cezanne, it would be necessary to perform detailed experiments with RNA silencing or chemical inhibition of the pathways. The results presented in this chapter show that additional activation of these pathways do not confer a change in Cezanne expression, however it may be possible that exposure to low shear stress causes sufficient activation of the pathways to promote Cezanne upregulation. Silencing or inhibition of NF-κB or HIF pathways in HUVECs exposed to shear stress followed by assessment of Cezanne expression would allow the testing of whether these pathways promote Cezanne transcription or translation without excess stimulation.

3.9.3 Localisation of Cezanne expression may determine its function in atherosclerosis.

Research from several groups has previously implicated Cezanne in the regulation of pathways related to atherosclerosis. It has been shown to inhibit canonical and non-canonical NF-κB signalling, and promote hypoxic signalling (Bremm et al., 2014; Enesa et al., 2008a; Hu et al., 2013; Luong et al., 2013). The results in this chapter may give an insight into the potential role of Cezanne in carrying out these functions to regulate endothelial activation. The induction of Cezanne by low shear stress, thus at sites prone to atherosclerosis, suggests that it is able to negatively regulate NF-κB signalling, which

is also upregulated under these conditions and is critical to the development of atherosclerosis (Gareus et al., 2008). Thus, Cezanne may act as a protective factor by limiting the expression of adhesion molecules and cytokines which drive lesion development. As stimulation with activating cytokines does not appear to further increase its expression under low shear stress this may mean that Cezanne is responsible for maintaining homeostasis by inhibiting aberrant NF-κB in vessels which are not exposed to an inflammatory stimulus, but will allow a response by cells to signalling which may also be caused by injury or infection, thus not compromising the ability of ECs to respond when they are required to for survival.

Cezanne has been shown to increase levels of both HIF-1α (Bremm et al., 2014) and HIF-2α (Moniz et al., 2015) via independent mechanisms and thus may promote the expression of hypoxia target genes which can regulate proliferation and apoptosis (Carmeliet et al., 1998). Hypoxic signalling is another pathway of interest in atherosclerosis. Nuclear HIF-1α has been found to be present in ECs covering human and murine atherosclerotic lesions. In addition, mice with an inducible endothelial knockout of *Hif1a* have been shown to be protected from the development of atherosclerosis (Akhtar et al., 2015). Although hypoxia did not increase Cezanne expression under low shear stress, it may still function at these sites to maintain an enhanced level of HIF expression and lead to lesion progression.

Understanding the function of Cezanne at sites of low shear stress is crucial to understanding its potential role in atherosclerosis. Testing these pathways in cells with Cezanne levels depleted will allow the functional consequence of Cezanne's elevated expression in low shear stress to be analysed.

3.9.4 Summary

Increased expression of Cezanne at the inner curvature of the murine aortic arch is likely due to the curving geometry of this site causing blood flow to exert low magnitude, oscillating shear stress on ECs. This is supported by *in vitro* studies in two systems to apply shear stress to cultured ECs, both showing that Cezanne mRNA and protein expression was elevated under these conditions. Contrary to previous work, exposure of ECs cultured under shear stress to hypoxia or NF-κB activating cytokines did not further elevate expression of Cezanne. This may reflect phenotypic differences in ECs exposed to shear stress and gives further information about the potential role of Cezanne in regulating the development of atherosclerosis. Cezanne may regulate NF-κB or hypoxic signalling and thereby alter vascular physiology, but further experiments are required to test this hypothesis.

4. Functional studies of Cezanne

4.1 Introduction

The findings presented in chapter 3 show that the expression of Cezanne in ECs is strongly and consistently regulated by shear stress, with its expression being the highest in cells exposed to low shear stress with oscillations in direction. These conditions approximate the haemodynamic environment which cells at regions prone to atherosclerosis experience in the human vasculature (Doriot et al., 2000; Milner et al., 1998; Samady et al., 2011), suggesting that Cezanne may be involved in cellular signalling events which lead to the initiation or progression of atherosclerotic lesion development. There are several mechanisms by which Cezanne could be acting to alter EC phenotype at these sites.

As a deubiquitinase, the previously studied functions of Cezanne are in the removal of ubiquitin from several key molecules involved in important cellular pathways which may be involved in regulating endothelial activation at sites of low shear stress. Cezanne has been implicated in the regulation of canonical NF-κB signalling via disassembly of the polyubiquitin chain linking either RIP1 (Enesa et al., 2008a) or TRAF6 (Luong et al., 2013) to NEMO. Ubiquitin in this context acts as a scaffold to allow recruitment of TAK1 and TAB2, which initiate a kinase cascade resulting in IκBα degradation and subsequent release of NF-κB complexes from the cytoplasm. Cezanne's deubiquitinase activity therefore inhibits release of NF-κB from the cytoplasm and thus dampens canonical NF-κB signalling. Active NF-κB signalling in ECs is known to be critical for the development of early lesions (Gareus et al., 2008), so Cezanne may be playing a role in limiting canonical NF-κB signalling at sites of low shear stress, potentially protecting these regions from lesion development.

A role for Cezanne in non-canonical NF-κB signalling has also been described. In a recent paper, Hu et al. posit that Cezanne can remove lysine 48-linked polyubiquitin chains from TRAF3, thereby stabilising the protein by blocking proteasomal degradation (Hu et al., 2013). TRAF3 is responsible for targeting the NIK for degradation and as such, enhancement of TRAF3 levels lead to a downregulation of NIK and consequently a downregulation of non-canonical NF-κB signalling. While non-canonical NF-κB has not been directly implicated in the pathogenesis of atherosclerosis, expression of the subunits p52 and RelB is increased at sites of low shear stress (see Chapter 5), as are cellular processes which the pathway regulates – such as proliferation (Ishikawa et al., 1997; Schumm et al., 2006) and apoptosis (Burkitt et al., 2015; Saxon et al., 2016). I

therefore hypothesised a potential role for Cezanne may be to limit non-canonical NF-κB signalling at sites of low shear stress, to reduce cell turnover at these sites.

Finally, the activity of Cezanne has been implicated in the regulation of hypoxic signalling via HIF-1α and HIF-2α. Classically, HIF protein levels are thought to be tightly controlled within cells by an oxygen-sensitive upstream mechanism involving the von Hippel-Lindau tumour suppressor (VHL) which leads to degradation of HIF under normoxic conditions. Loss of Cezanne, however, has been associated with a decrease in both HIF-1α and HIF-2α stability, via separate mechanisms independent of proteasomal degradation (Bremm et al., 2014; Moniz et al., 2015). In ECs exposed to low shear stress, Cezanne may act to maintain a pool of HIF and promote hypoxic signalling, potentially leading to aberrant proliferation at these sites.

The function of Cezanne in ECs at sites of low shear stress is unclear, however the pathways that it has been reported to regulate in other cell types or contexts may be extremely important in altering EC phenotype to the classical activated state present in early atherogenesis. Understanding which pathways Cezanne may regulate in the context of atherosclerosis may be key in prevention or treatment of the disease.

4.2 Hypothesis and aims

Hypothesis: Cezanne functions to negatively regulate NF-κB signalling and/or positively regulate HIF signalling in ECs exposed to low shear stress.

Aim 1: Use siRNA technology to deplete Cezanne from ECs exposed to shear stress and test the resulting effect on:

a) Canonical NF-κB signalling (via phosphorylation of RelA and target gene analysis),
b) Non-canonical NF-κB signalling (via processing of p100 to p52),
c) HIF signalling (via assessing the stability of HIF-1α).

Aim 2: Use aortic tissue from mice lacking Cezanne and determine the consequential effect on:

a) Endothelial inflammation,
b) Endothelial proliferation,
c) Atherosclerotic lesion development.

4.3 Optimisation of Cezanne gene silencing

A powerful tool to probe the function of a gene of interest in a particular biological context is to utilise RNA interference technology to deplete levels of endogenous mRNA and thus the expressed protein. Analysis of putative target pathways can reveal differences between cell populations transfected with specific siRNA compared to the non-targeting "scrambled" control siRNA, thus suggesting that the gene of interest is involved in the particular cellular event. In order to probe the function of Cezanne in ECs exposed to shear stress, siRNA specific to the *OTUD7B* gene was transfected into HUVECs via liposomal delivery (Lipofectamine RNAiMAX) and electroporation to determine the optimal method for delivery (Figure 4.1). The percentage knockdown of Cezanne mRNA and protein was determined for each delivery method; electroporation was found to be effective at reducing Cezanne expression, providing a 77% reduction in mRNA expression (Figure 4.1d) and an 87% reduction in protein (Figure 4.1b) in low shear stress as analysed by qPCR and Western blotting respectively. In comparison, with Lipofectamine, mRNA expression was reduced by only 37% (Figure 4.1c) and protein 47% (Figure 4.1a). Furthermore, Cezanne expression with the control siRNA was more similar to untransfected cells in electroporated samples as compared to those transfected with Lipofectamine, indicating that there may be less off-target effects. Electroporation was thus chosen as the method of transfection for use in the following experiments.

4.4 Cezanne limits phosphorylation of NF-κB RelA under low shear stress.

The NF-κB subunit RelA has been previously found to exhibit differential expression regulated by shear stress patterns *in vivo*, with expression being induced at sites of low shear stress (Cuhlmann et al., 2011). A reported function of Cezanne is in the regulation of the upstream signalling cascade leading to NF-κB activation (Enesa et al., 2008a) or phosphorylation (Luong et al., 2013), so to test whether Cezanne was carrying out this function in ECs exposed to low shear stress, siRNA targeting Cezanne was delivered to HUVECs by electroporation prior to exposure to shear stress using the orbital shaker system. RelA activity was then assessed by Western blotting for phosphorylated RelA (at serine 536) as well as total levels (Figure 4.2). Analysis of total RelA expression showed an increase in both control and Cezanne knockdown cells under low shear stress in comparison to high shear stress, no difference was seen in total RelA levels between control and knockdown samples (Figure 4.2 – upper panels). Western blotting with the antibody specifically targeting RelA phosphorylated at serine 536 showed that although there was a trend towards an increase in expression in low compared to high shear stress, this was not statistically significant (Figure 4.2 – lower right panel). There was, however,

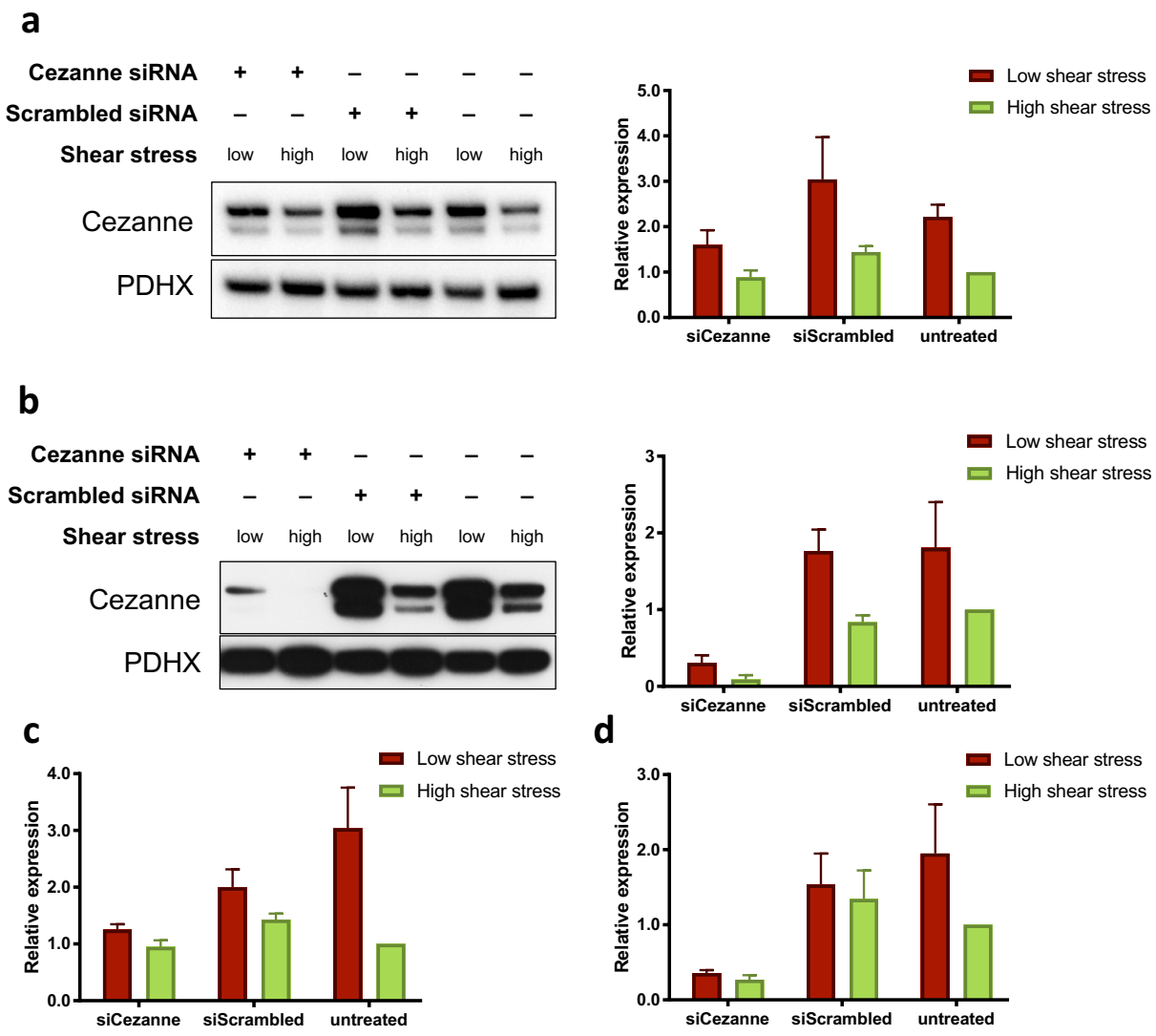

Figure 4.1: Electroporation is more effective than liposomal delivery at delivering siRNA to silence Cezanne expression. At passage 3, HUVECs were transfected with siRNA targeting Cezanne or scrambled control siRNA with two methods to test the efficiency of knockdown. **(a)** HUVECs were seeded onto gelatinised six well plates and allowed to adhere overnight. Lipofectamine RNAiMAX and siRNA solutions were then prepared in Opti-MEM media before being combined and added to wells. Five hours later, the transfection media was replaced with M199 and the plates placed on the orbital shaker for 72 hours. Cezanne expression was quantified by Western blotting, normalising to the housekeeper PDHX. **(b)** HUVECs were trypsinised and washed in PBS before being resuspended in R buffer containing siRNA. The cells were then electroporated using the Neon system and plated onto gelatinised six well plates containing warm antibiotic free M199. After six hours, when the cells were adherent, plates were placed on the orbital shaker for 72 hours. Cezanne expression was quantified by Western blotting, normalising to the housekeeper PDHX. In addition, cDNA was generated and mRNA expression of Cezanne in cells transfected by **(c)** Lipofectamine RNAiMAX and **(d)** electroporation quantified by qPCR, normalising to the housekeeper HPRT.
n=3.

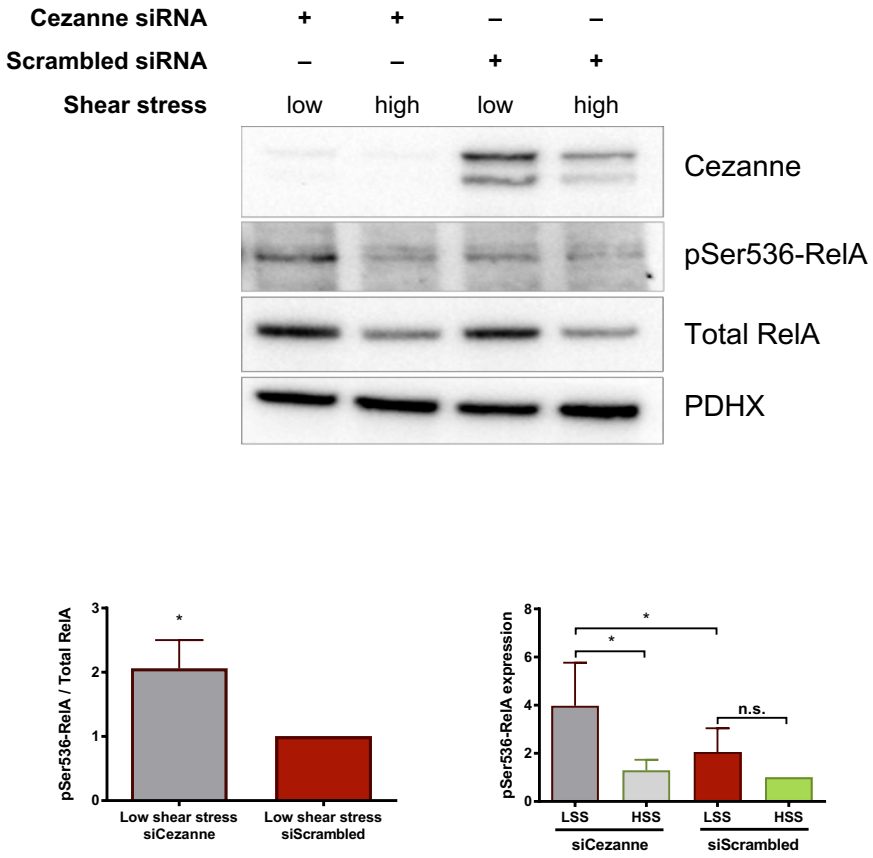

Figure 4.2: Depletion of Cezanne results in an increase in RelA phosphorylation in cells exposed to low shear stress. HUVECs were transfected with siRNA targeting Cezanne or a scrambled control siRNA using electroporation. The cells were then seeded onto six-well plates. Once adherent, cells were exposed to shear stress for 72 hours using the orbital shaker system, then scraped from each condition separately. Samples were lysed, protein concentration determined using a BCA assay and normalised accordingly. The expression of Cezanne, total RelA and RelA phosphorylated at serine 536 were analysed by Western blotting, normalising to the housekeeper PDHX. Densitometry was carried out using ImageJ.
n=3; $p<0.05$; Two-way ANOVA.

a significant increase in phosphorylated RelA in the Cezanne knockdown samples under low shear stress in comparison to all other conditions (Figure 4.2 – lower left panel). This could suggest that Cezanne functions in ECs exposed to low shear stress to inhibit the phosphorylation of RelA, without affecting its overall expression levels. This may be indicative of regulation of NF-κB activity and so this was explored further by studying NF-κB target genes.

4.5 Expression of NF-κB target genes is not affected by Cezanne knockdown.

Several target genes of canonical NF-κB signalling are upregulated at sites of low shear stress *in vivo*. Some important examples are adhesion molecules such as ICAM-1, VCAM-1 and E-selectin, which are involved in the attachment of circulating monocytes to sites of low shear stress in early plaque development (Van der Heiden et al., 2010). The RelA subunit is the NF-κB subunit which possesses the transactivation domain responsible for inducing gene expression in the canonical NF-κB pathway (Huxford and Ghosh, 2009), and as Cezanne is capable of regulating its shear stress-dependent phosphorylation this may result in an alteration in target gene expression. To investigate whether the role of Cezanne dependent inhibition of RelA phosphorylation is to repress the expression of NF-κB target genes, HUVECs were transfected with either Cezanne or scrambled siRNA and exposed to shear stress in combination with TNFα as a known activator of NF-κB activity. Following treatment, cDNA was collected and the relative expression levels of a panel of known NF-κB target genes measured by qPCR (Figure 4.3). Many of the genes were regulated by shear stress in the untreated samples, with upregulation in low shear stress where RelA expression is also elevated. In addition, stimulation with TNFα caused the expression of many the genes to be strikingly enhanced, with fold changes in excess of one thousand in some cases. Notably, expression of the anti-apoptotic genes Bcl-2 and growth arrest and DNA-damage-inducible β (GADD45β) were unaffected by TNFα treatment, despite having been previously found to be regulated by this pathway (Catz and Johnson, 2001; De Smaele et al., 2001). Silencing of Cezanne, however, conferred no effect on the expression level of any of the NF-κB target genes studied, suggesting that modulation of RelA phosphorylation by Cezanne does not alter target gene expression in this context.

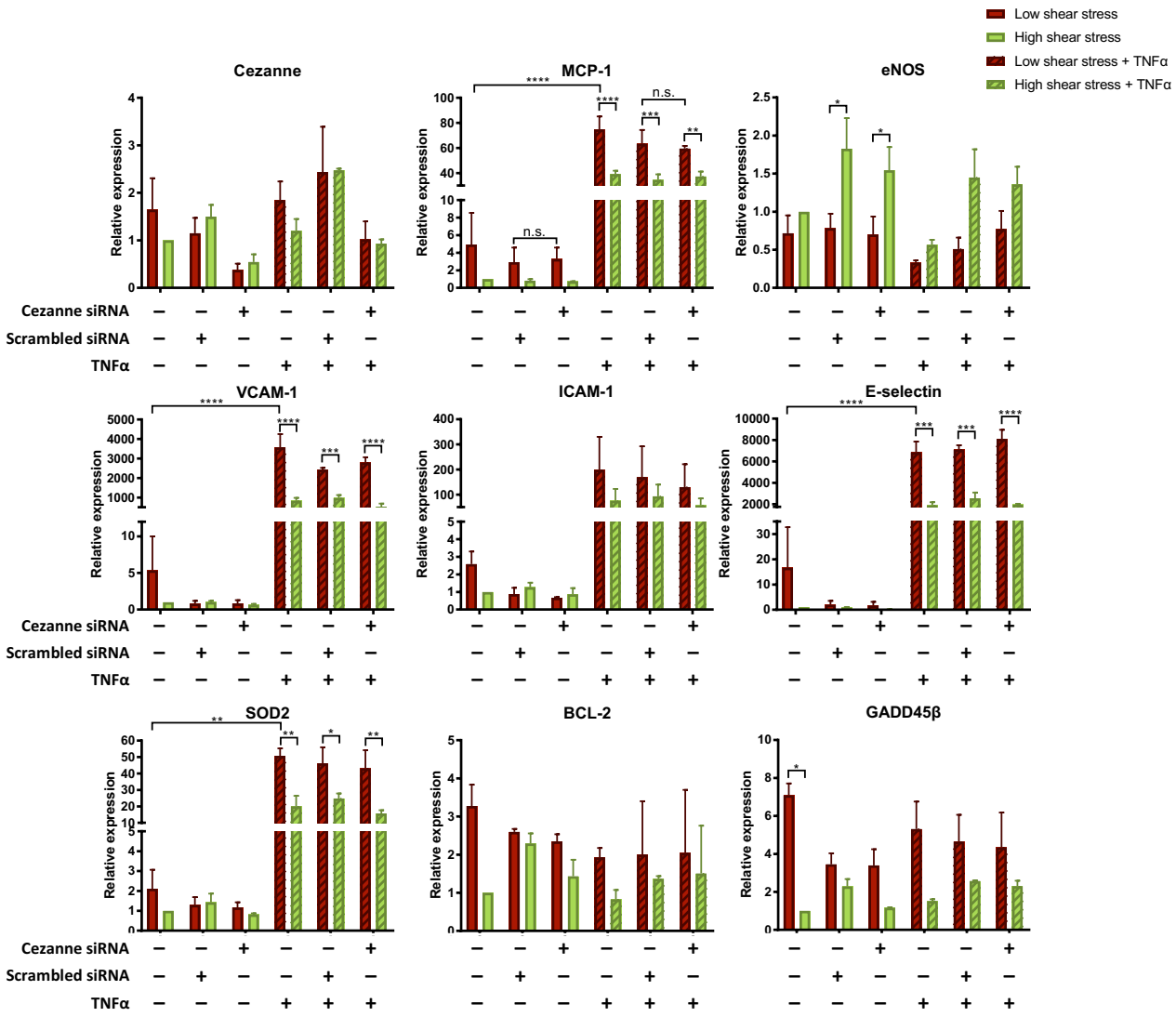

Figure 4.3: Depletion of Cezanne does not alter the expression of NF-κB target genes. HUVECs were transfected with siRNA targeting Cezanne or a scrambled control siRNA using electroporation. The cells were then seeded onto six-well plates. Once adherent, cells were exposed to shear stress for 72 hours using the orbital shaker system, then scraped from each condition separately. RNA was collected from the samples and converted to cDNA. The expression level of the various genes were tested using qPCR, normalising to the housekeeping gene HPRT.
n=3; *p<0.05; **p<0.01; ***p<0.005; ****p<0.001; Two-way ANOVA with Tukey's post test analysis.

4.6 Cezanne does not regulate non-canonical NF-κB signalling in endothelial cells under shear stress.

Recent evidence from experiments in B cells has indicated that Cezanne may play a role in the regulation of non-canonical NF-κB signalling via deubiquitination of TRAF3 leading to repression of the pathway (Hu et al., 2013). The canonical and non-canonical branches of NF-κB also exhibit a degree of cross-talk (Oeckinghaus et al., 2011) so to test whether non-canonical NF-κB signalling was regulated by Cezanne in ECs, siRNA was used to deplete Cezanne expression and the processing of p100 to p52 investigated using Western blotting (Figure 4.4). HUVECs were transfected with either non-targeting control siRNA or siRNA specifically targeting Cezanne using electroporation. Transfected cells were then seeded on six-well plates and once adherent placed on the orbital shaker for 72 hours of shear stress. Cells were scraped from the high and low shear stress regions from each condition and lysed for Western blotting. Samples were probed with an antibody which detects both p100 and p52 so cleavage could be assessed. The blots show that expression of p100 and p52 was significantly higher under low shear stress than high shear stress, however there were no significant differences in either p100 or p52 levels between control or Cezanne knockdown samples. These results indicate that Cezanne is not responsible for regulating non-canonical NF-κB signalling in ECs exposed to shear stress.

4.7 Cezanne does not alter HIF-1α stability or transcriptional activity in endothelial cells exposed to shear stress.

There is some published evidence to suggest that Cezanne may be involved in the regulation of hypoxic signalling, utilising a mechanism of HIF-1α deubiquitination which increases stability of the hypoxia-driven transcription factor and leads to a prolonged transcriptional response (Bremm et al., 2014). In order to test whether Cezanne is responsible for regulating HIF-1α expression in ECs exposed to shear stress, Cezanne expression was depleted using a specific siRNA with and without the presence of dimethyloxaloglycine (DMOG), a potent upstream activator of HIF. Western blotting was used to assess the expression of HIF-1α (Figure 4.5). The results show that HIF-1α expression is increased under low shear stress conditions both in the absence and presence of DMOG, but there is no difference in expression between cells transfected with Cezanne siRNA compared to the scrambled siRNA control. In addition, the expression of the HIF-1α transcriptional targets enolase 2 (ENO2) and 6-phosphofructo-2-kinase/fructose-2,6-biphosphatase 3 (PFKFB3) were analysed by Western blotting in the samples treated with DMOG (Figure 4.6). Consistent with the results for HIF-1α stability, depletion of Cezanne did not alter levels of these HIF-1α target genes in low

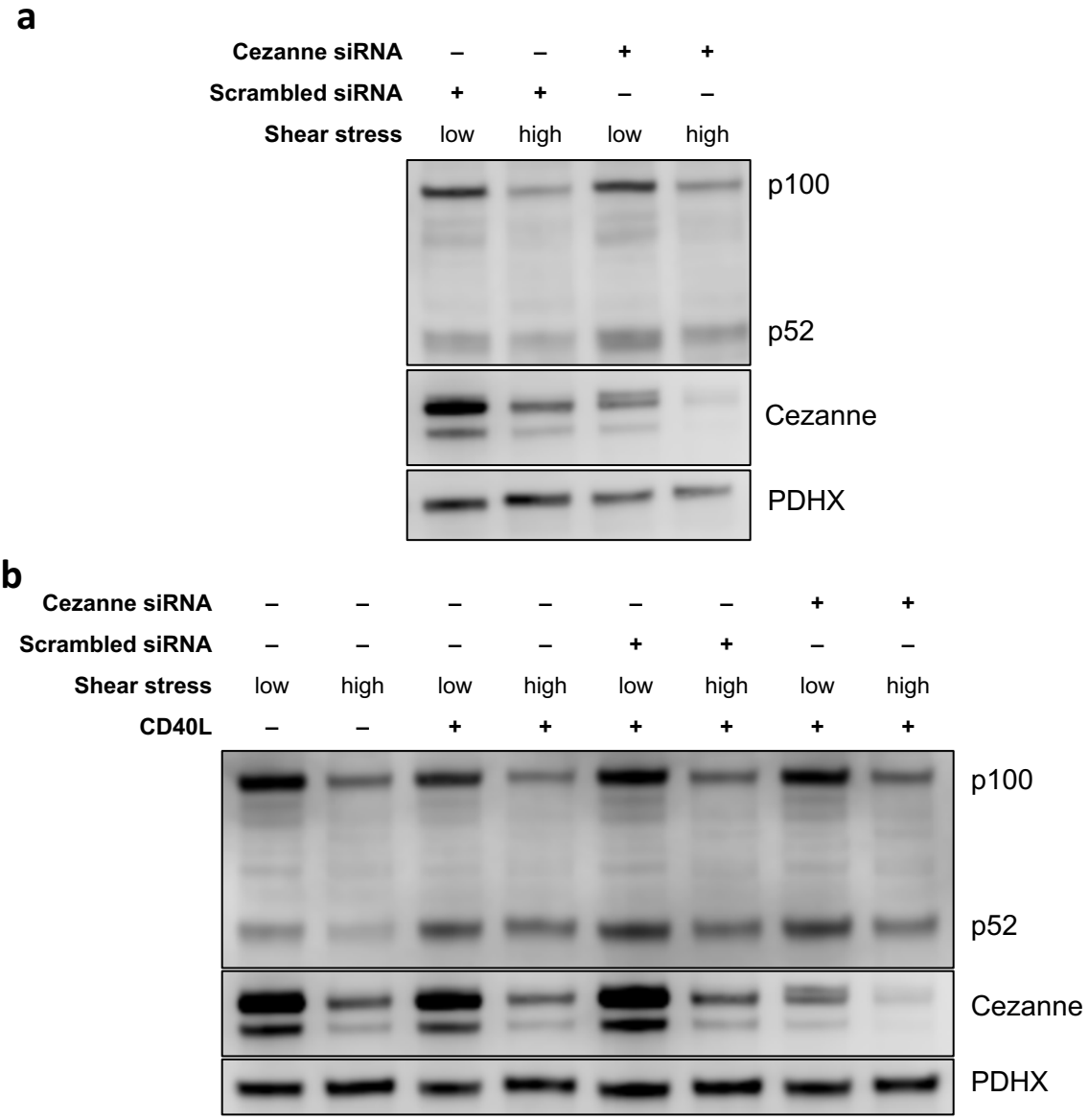

Figure 4.4: Depletion of Cezanne does not alter processing of p100 to p52. HUVECs were transfected with siRNA targeting Cezanne or a scrambled control siRNA using electroporation. The cells were then seeded onto six-well plates. Once adherent, cells were exposed to shear stress for 72 hours using the orbital shaker system. **(a)** Cells from each condition were lysed and protein content normalised. The expression of p100, p52 and Cezanne were determined by Western blotting, normalising to the housekeeper PDHX. **(b)** For the final 2 hours of orbiting, 100 ng/ml CD40L was added to the indicated samples to induce p100 processing to p52. Samples were then lysed and the expression of p100, p52 and Cezanne determined by Western blotting, normalising to the housekeeper PDHX.
n=3

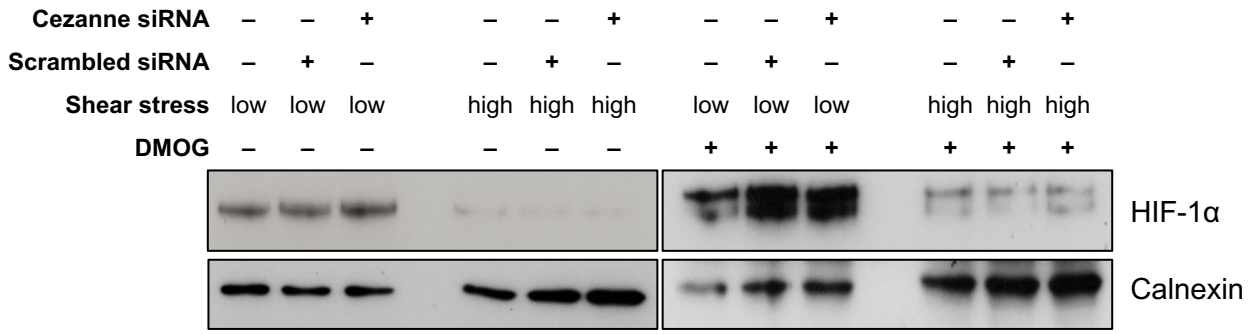

Figure 4.5: Depletion of Cezanne does not alter stability of HIF-1α. HUVECs were transfected with siRNA targeting Cezanne or a scrambled control siRNA using electroporation. The cells were then seeded onto six-well plates. Once adherent, cells were exposed to shear stress for 72 hours using the orbital shaker system. Half of the wells were stimulated with 0.5 mM DMOG for the final 4 hours of shear stress, while the other half were unstimulated. Cells from each condition were lysed and protein content normalised. The expression of HIF-1α was determined by Western blotting, normalising to the housekeeper calnexin.
n=4. Western blot performed by Dr Shuang Feng.

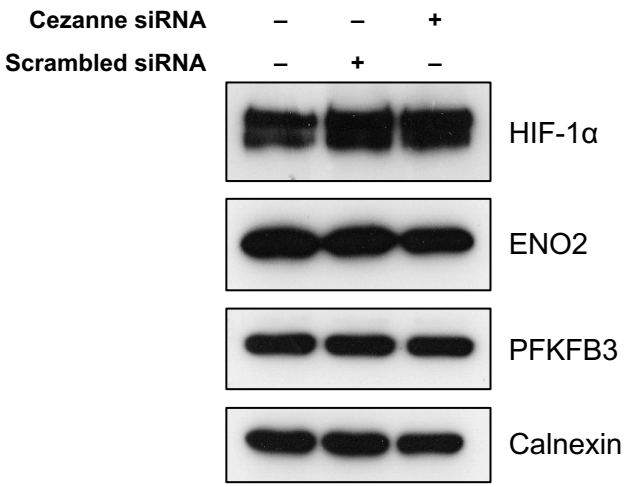

Figure 4.6: Depletion of Cezanne does not alter HIF-1α target gene expression in low shear stress. HUVECs were transfected with siRNA targeting Cezanne or a scrambled control siRNA using electroporation. The cells were then seeded onto six-well plates. Once adherent, cells were exposed to shear stress for 72 hours using the orbital shaker system. The wells were stimulated with 0.5 mM DMOG for the final 4 hours of shear stress, then cells exposed to low shear stress from each knockdown were lysed and protein content normalised. The expression of HIF-1α, ENO2 and PFKFB3 were determined by Western blotting, normalising to the housekeeper calnexin.
n=4. Western blot performed by Dr Shuang Feng.

shear stress. Taken together, these data suggest that while expression of HIF-1α is elevated under the same shear stress conditions as Cezanne, the mechanism for this differential expression or subsequent transcriptional activity does not require Cezanne.

4.8 VCAM-1 expression in the endothelium of *Otud7b*$^{-/-}$ mice is unchanged from wild-type

There are several reasons that could account for depletion of Cezanne *in vitro* not conferring an effect on the expression of inflammatory target genes, despite the elevation in RelA phosphorylation at serine 536. Depletion with siRNA leaves a small pool of functional protein which may possess enough activity to mask changes that are occurring. Looking *in vivo* at endothelial cells from *Otud7b*$^{-/-}$ mice may give more information about the true function of Cezanne, avoiding residual expression. In this system, ECs are exposed to not only shear stress of different magnitudes but also an array of low level inflammatory stimuli from circulating sources. In order to test whether NF-κB signalling is influenced by removal of Cezanne, inflammatory signalling was induced by intraperitoneal injection of bacterial LPS before expression of VCAM-1 was analysed by *en face* staining of the aortic arches of both wild-type and *Otud7b*$^{-/-}$ mice (Figure 4.7). Expression of VCAM-1 was found to co-localise with PECAM-1, indicating surface expression as expected. The results showed that was no significant difference in the expression levels of VCAM-1 between wild-type and knockout mice. These data recapitulate the *in vitro* results by demonstrating that Cezanne did not regulate NF-κB target gene expression under low shear stress.

4.9 Endothelial proliferation in the murine aortic arch is not regulated by Cezanne.

The other putative targets of Cezanne were in the non-canonical NF-κB and HIF pathways. These pathways are both known to regulate cellular proliferation by divergent mechanisms. Non-canonical NF-κB signalling has been shown to alter the expression of cell cycle genes, inhibiting expression of the antiproliferative p21 while also enhancing expression of Cyclin D1, which drives cell cycle progress (Schumm et al., 2006). HIF signalling, on the other hand, has been shown to drive expression of vascular endothelial growth factor (VEGF), leading to enhanced cell proliferation (Carmeliet et al., 1998; Semenza, 1996). Endothelial turnover is thought to play a crucial role in the development of atherosclerosis through elevation of proliferation at sites of low shear stress, where lesions develop (Akimoto et al., 2000; Choy et al., 2001; Davies et al., 1986). In order to determine whether Cezanne may be affecting either of these pathways *in vivo*, wild-type and *Otud7b*$^{-/-}$ mice were culled and aortic arches stained for the proliferation marker

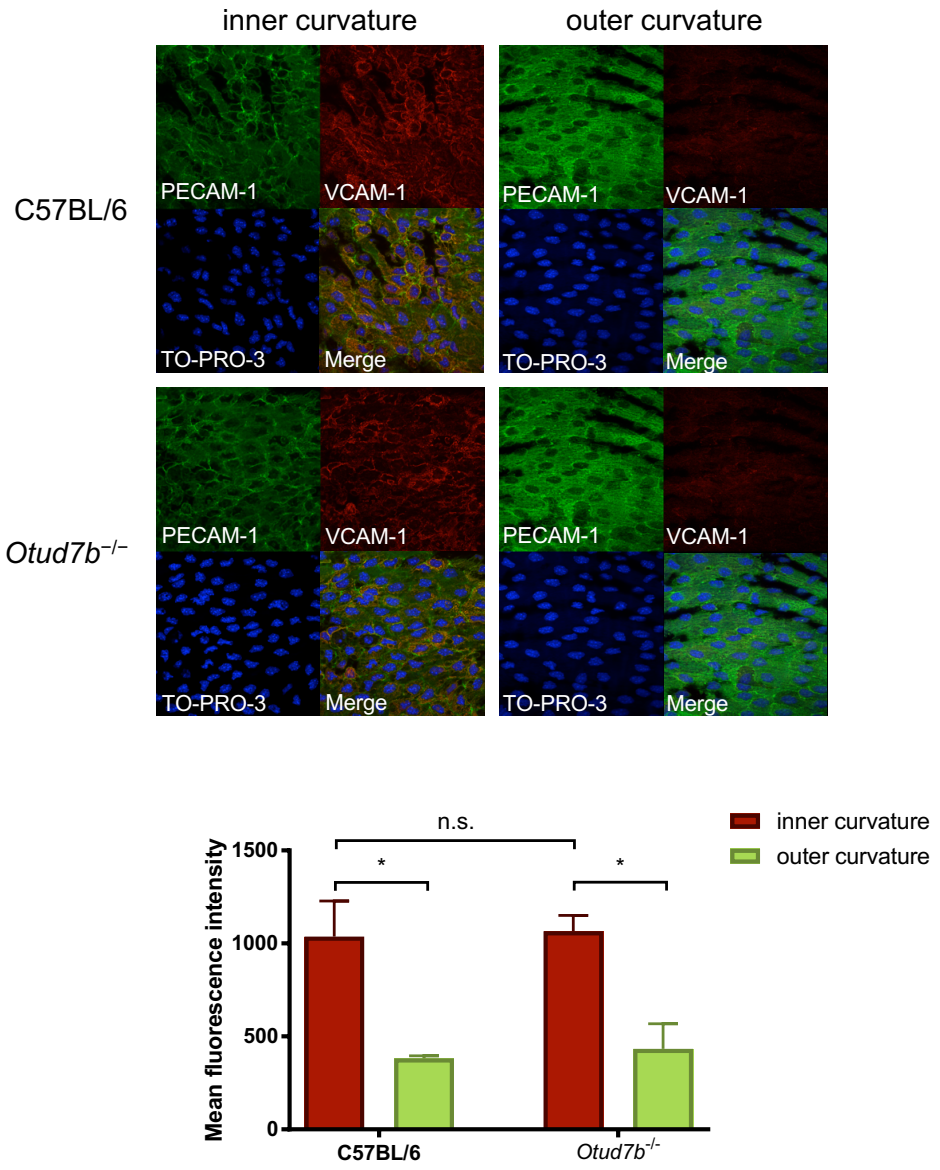

Figure 4.7: Cezanne gene trap mutant mice do not have altered VCAM-1 expression in response to LPS challenge. Ten week old *Otud7b*$^{-/-}$ or C57BL/6 mice were weighed and administered an intraperitoneal injection of bacterial lipopolysaccharide at a dose of 4 mg/kg to induce systemic inflammation. The animals were monitored for six hours before being culled. The vasculature of each animal was fixed by perfusion with 4% formaldehyde and then aortic arches dissected and opened longitudinally. This tissue was then stained with antibodies targeting VCAM-1, as well as PECAM-1 to label endothelial junctions and TO-PRO-3 iodide as a nuclear counterstain. Aortic arches were then mounted *en face* on cover slips and imaging carried out using confocal microscopy. Quantification of VCAM-1 fluorescence was performed using ImageJ software, measuring the fluorescent signal at junctions.
n=4; $p<0.05$, Two-way ANOVA with Tukey's post test analysis.

Ki-67 by *en face* staining (Figure 4.8). Ki-67 localisation was found to be strongly nuclear, and the cells expressing this staining were counted as positive. All other nuclei labelled with TO-PRO-3 iodide were counted as negative. Analysis of the images by counting the percentage of positive nuclei showed that there were significantly more proliferating cells in the inner curvature in comparison to the outer curvature of the aortic arch. However, no difference in proliferation was detected between wild-type and *Otud7b*$^{-/-}$ samples. This lack of effect on proliferation suggests that non-canonical NF-κB and HIF signalling are unlikely to be regulated by Cezanne in this context.

4.10 Cezanne does not regulate the development of atherosclerotic lesions.

The development of atherosclerosis in ECs exposed to low shear stress is a multifactorial process, and the outcome of a complex network of biochemical signalling (Hopkins, 2013). To investigate whether Cezanne is responsible for the regulation of lesion development, an *in vivo* model of atherosclerosis was employed. A commonly used model is that of *Ldlr*$^{-/-}$ mice, these animals lack the low-density lipoprotein receptor which is normally responsible for uptake of LDL from the bloodstream into the liver. As a consequence, when these animals are fed a diet high in cholesterol, plasma cholesterol levels are enhanced due to lack of clearance and they develop atherosclerotic lesions in the major arteries (Ishibashi et al., 1994). To test the function of Cezanne in the development of atherosclerosis, *Otud7b*$^{-/-}$ mice were bred with *Ldlr*$^{-/-}$ mice to generate a double mutant *Otud7b*$^{-/-}$*Ldlr*$^{-/-}$ strain. These mice were fed a high-fat Western diet and the size of atherosclerotic plaques measured compared to *Ldlr*$^{-/-}$ controls by staining for lipids with Oil Red O (Figure 4.9). The mean lesion area in *Ldlr*$^{-/-}$ animals was found to be approximately 0.55 mm^2, or 1.9% of the total aortic area. Lesions were found to be localised predominantly to the inner curvature of the aortic arch, and at the major branches from the aorta. Some smaller regions of lipid were also detected in the descending aorta, likely localised to the intercostal artery branches, corresponding to haemodynamic changes. Analysis of *Otud7b*$^{-/-}$*Ldlr*$^{-/-}$ animals showed no significant difference in either lesion size or percentage coverage of the lesions within the aorta. These data indicate that Cezanne does not regulate the development of atherosclerosis at sites of low shear stress.

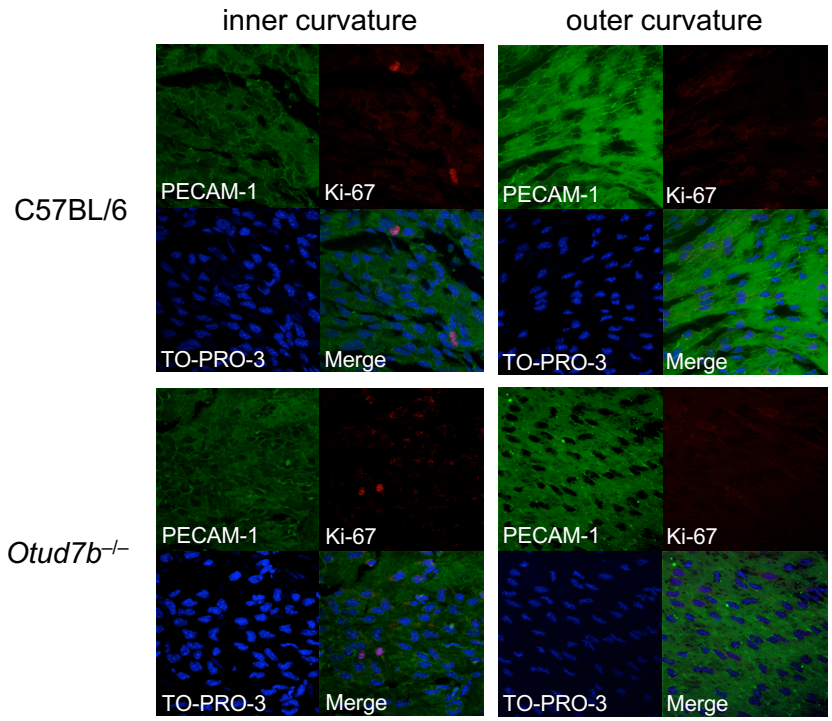

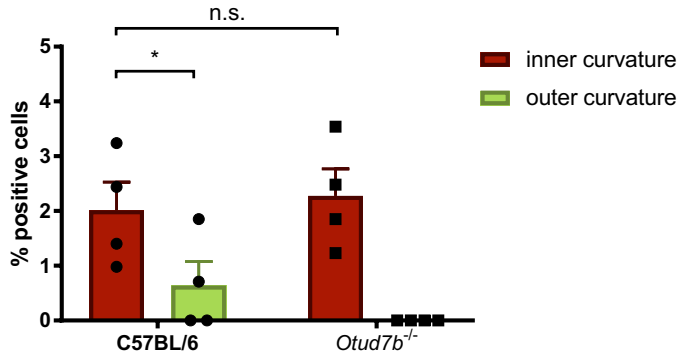

Figure 4.8: Cezanne gene trap mutant mice do not have altered endothelial proliferation. Ten week old *Otud7b*$^{-/-}$ or C57BL/6 mice were culled by pentobarbitone overdose. The vasculature of each animal was fixed by perfusion with 4% formaldehyde and then aortic arches dissected and opened longitudinally. This tissue was then stained with antibodies targeting the proliferation marker Ki-67, as well as PECAM-1 to label endothelial junctions and TO-PRO-3 iodide as a nuclear counterstain. Aortic arches were then mounted *en face* on cover slips and imaging carried out using confocal microscopy. Quantification of Ki-67 was performed using ImageJ software, counting positive nuclei labelled with Ki-67 and total nuclei labelled with TO-PRO-3 iodide to calculate the percentage of positive cells.
n=4; $p<0.05$, Two-way ANOVA with Tukey's post test analysis.

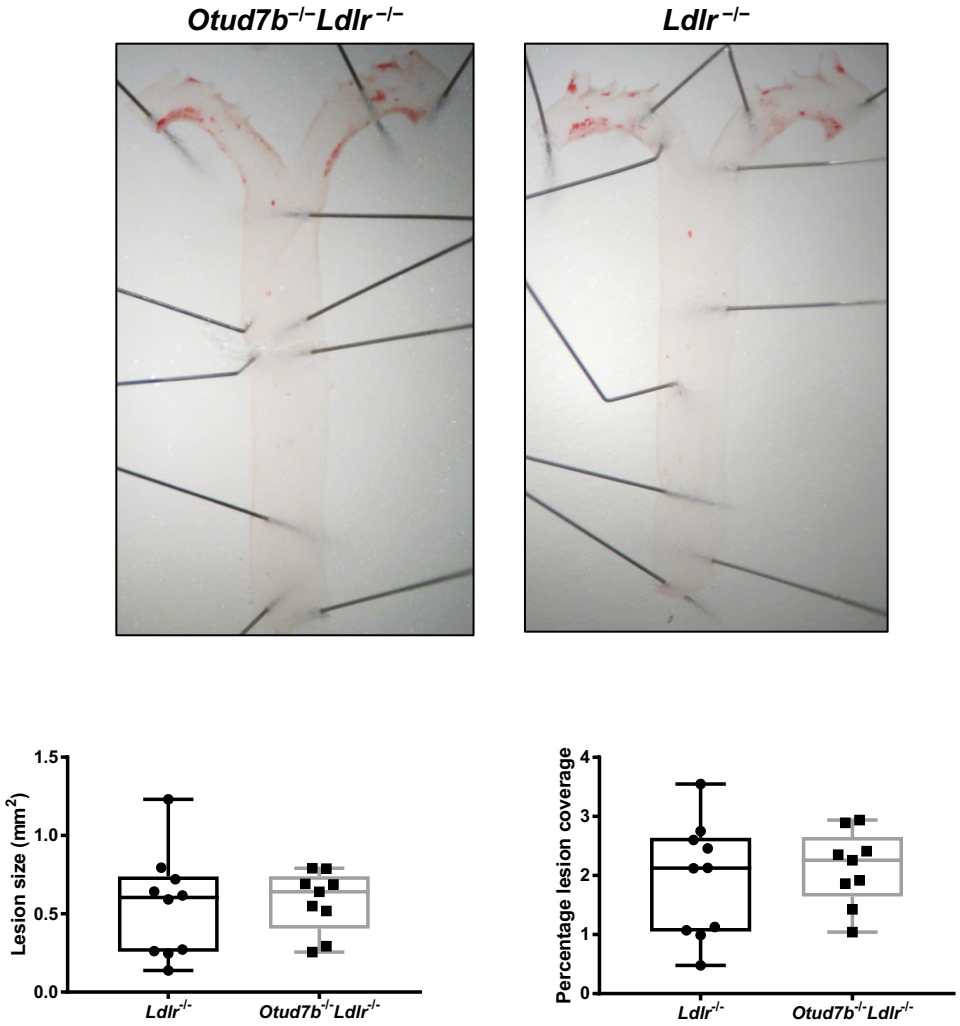

Figure 4.9: Cezanne gene trap mutant mice do not display altered atherosclerotic lesion size. Eight week old female *Ldlr*$^{-/-}$ and *Otud7b*$^{-/-}$*Ldlr*$^{-/-}$ mice were fed a Western diet for six weeks in order to allow development of atherosclerotic lesions. Following the diet, mice were sacrificed and perfusion fixed with 4% formaldehyde. The aortas were then dissected and cleaned, ensuring the removal of any external fat. Each aorta was then fixed for a further 24 hours before being stained with Oil Red O to identify lipids. Following staining, each aorta was cut longitudinally and pinned *en face* in paraffin wax for imaging, using a digital camera attached to a dissection microscope. The percentage of lesion coverage was quantified by measuring the area of lesion coverage and the total aortic area with ImageJ.
n=9; unpaired t-test.

4.11 Conclusions

Cezanne activity is responsible for inhibiting RelA phosphorylation specifically in ECs under low, but not high shear stress *in vitro*. This modification does not appear to affect expression of canonical NF-κB target genes, as no difference in expression was detected between silenced or control samples, with or without TNFα stimulation. The expression of the non-canonical NF-κB subunit p100/p52 and HIF-1α were both elevated under low shear stress, however depletion of Cezanne had no effect on processing of p100 to p52 or stability of HIF-1α. Further studies *in vivo* confirmed these observations. No difference in the canonical NF-κB target gene VCAM-1 was seen between wild-type and *Otud7b*$^{-/-}$ mice, indicating that NF-κB activity was unchanged. In addition, analysis of endothelial proliferation by Ki-67 immunofluorescence staining revealed similar levels of proliferation between both groups, suggesting that non-canonical NF-κB and HIF signalling were not affected by loss of Cezanne. Furthermore, a comparison between *Otud7b*$^{-/-}$*Ldlr*$^{-/-}$ and *Ldlr*$^{-/-}$ mice fed a Western diet for six weeks revealed no difference between the two groups in atherosclerotic lesion size as determined by Oil Red O staining, indicating that pathways regulating the development of atherosclerosis were not affected by loss of Cezanne. Thus, although Cezanne regulated RelA phosphorylation in ECs exposed to low shear stress, the physiological significance of this is uncertain.

4.12 Discussion

Several studies to date have been primarily concerned with identifying the function of Cezanne in regulating downstream cellular events. However, these studies have involved a variety of techniques, cell types and signalling pathways, summarised in Table 4.1, which complicates the interpretation of the findings as a whole. The experiments in the previous chapter have shown Cezanne expression to be significantly elevated in ECs exposed to low shear stress in comparison to high shear stress. In addition, NF-κB and hypoxic signalling pathways are known to be important in the regulation of cardiovascular health and the development of atherosclerosis (Gao et al., 2012; Van der Heiden et al., 2010). Therefore, the aim of this chapter was to investigate whether NF-κB or HIF-1α was regulated by Cezanne in ECs exposed to low shear stress.

4.12.1 Cezanne function in canonical NF-κB signalling

The most striking difference observed in Cezanne depleted cells was the effect on the canonical NF-κB pathway. In ECs exposed to shear stress *in vitro*, loss of Cezanne by siRNA was sufficient to significantly induce phosphorylation of the NF-κB subunit RelA at the serine 536 residue specifically in cells exposed to low shear stress, while cells under high shear stress did not show any effect of knockdown on this pathway. However, given the lack of a significant difference in phosphorylated RelA between cells exposed to high and low shear stress (where Cezanne expression is also significantly different) this conclusion is not certain. It is plausible that the effects of Cezanne depletion on phosphorylated RelA under low shear stress are more pronounced than in high shear stress. Further experiments utilising a Cezanne knockout mouse model are justified in order to understand whether Cezanne plays a significant role in limiting RelA phosphorylation *in vivo*.

Intriguingly, further experiments which tested mRNA expression of a variety of RelA target genes with divergent functions did not detect any alteration in gene expression in cells which were exposed to the same conditions or following additional exposure to the NF-κB stimulating cytokine TNFα. These data suggest that Cezanne is capable of negatively regulating activity of the canonical NF-κB pathway through inhibition of RelA phosphorylation, but this does not result in an alteration in gene expression resulting from the pathway.

Previous research has identified an induction of inflammatory gene expression upon Cezanne depletion in ECs. Stimulation with TNFα following transfection with Cezanne siRNA showed an increase in IL-8 expression compared to scrambled control siRNA (Enesa et al., 2008a). Additionally, silencing of Cezanne was sufficient to enhance expression of VCAM-1, ICAM-1 and E-selectin in ECs exposed to a period of hypoxia

Publication	Method of Cezanne alteration	Cell type	Signalling pathway	Effect
Hu et al. (2013)	*Otud7b*$^{-/-}$ mice	B lymphocytes	Non-canonical NF-κB	Elevated DNA binding activity in response to CD40, BAFF ligation.
		Embryonic fibroblasts		
Hu et al. (2016)	*Otud7b*$^{-/-}$ mice	T lymphocytes	Canonical NF-κB	Elevated IκBα with reduced phosphorylation
			T cell receptor pathway	Impaired signalling.
Luong et al. (2013)	*Otud7b*$^{-/-}$ mice	Kidney	Canonical NF-κB	Enhanced renal injury and adhesion molecule expression in response to ischaemia/reperfusion
				Enhancement of adhesion molecule expression in response to hypoxia/reoxygenation
	siRNA	Endothelial cells (HUVEC)		
Enesa et al. (2008)	siRNA	Endothelial cells (HUVEC)	Canonical NF-κB	Enhancement of IL-8 expression in response to TNFα.
	Overexpression	HEK293 cells		Dose-dependent inhibition of DNA binding activity.
Bremm et al. (2014)	siRNA	HeLa cells	HIF-1α	Reduction in stability in response to hypoxia.
	Overexpression	U2OS cells		Dose-dependent increase in expression.
	Otud7b$^{-/-}$ mice	Embryonic fibroblasts		Reduction in stability in response to hypoxia
Moniz et al. (2015)	siRNA	HeLa cells	HIF-2α	Reduction in HIF-2α expression following hypoxia.
		Renal cancer cells (786-O)		Reduction in HIF-2α expression.

Table 4.1: Previously identified functions of Cezanne.

followed by reoxygenation – a stimulus which can activate NF-κB (Natarajan et al., 2002). Notably, increased phosphorylation of RelA at serine 536 was also detected in these experiments (Luong et al., 2013). Importantly, however, in each of these studies Cezanne function was observed in activated cells, where its expression was elevated in comparison to unstimulated controls. There was no reported effect on inflammatory gene expression in the absence of TNFα or hypoxia and reoxygenation. In the experiments presented in this chapter, Cezanne expression under flow may be lower than in the other studies with stimulated cells. This could mean that Cezanne expression under shear is insufficient to provide an inhibitory effect on NF-κB target genes. A comparison of Cezanne expression between the conditions studied here and in previous research may shed light on the discrepancy in Cezanne function seen between the studies.

Additionally, low shear stress activates NF-κB via a different mechanism compared to TNFR and this may not be responsive to Cezanne activity. Indeed, there is some evidence to suggest that Ras-GTPase signalling can induce NF-κB nuclear localisation independent of IκBα degradation in ECs exposed to shear stress (Ganguli et al., 2005). As the reported function of Cezanne in the canonical NF-κB pathway is to deubiquitinate RIP1 or TRAF6 linked polyubiquitin chains in TNFR mediated signalling, Cezanne may not be capable of inhibiting NF-κB signalling resulting from changes in shear stress, and explain why silencing of its expression did not have any effect in this context. Further experiments could focus on using different stimuli which may be more similar to an atherogenic environment, for example a lower dose of TNFα may be sensitive to Cezanne inhibition in ECs exposed to shear stress. Alternatively, other inflammatory molecules found in atherosclerotic plaques could be used, such as IL-1 or ox-LDL. Utilisation of a less overwhelming stimulating factor may reveal more subtle regulation of the NF-κB pathway by Cezanne, while also being relevant to atherosclerosis.

4.12.2 Does RelA phosphorylation influence transcriptional activity?

An important question is what is the significance of limiting RelA phosphorylation at serine 536 if Cezanne does not regulate the expression of NF-κB target genes. Phosphorylation at this residue is controlled by several upstream kinases, including IKKα (Sakurai et al., 2003), IKKβ (Jeong et al., 2005) and ribosomal S6 kinase 1 (RSK1) (Bohuslav et al., 2004). Several studies have investigated the function of serine 536 phosphorylation on RelA and NF-κB activity, however there is some disagreement within the literature as to its role. Depending on the method used to modify phosphorylation of this residue and in which cell type, there are very different conclusions. In general, two broad theories for the function of this phosphorylation have been suggested. The first is

that it alters the kinetics of nuclear NF-κB; serine 536 phosphorylation in the Saos-2 osteosarcoma cell line has been shown to reduce the affinity of the RelA protein for IκB, thereby allowing nuclear import independent of classical IκB degradation (Bohuslav et al., 2004). In addition, a study published in Nature in 2005 utilised overexpression of a mutated version of RelA with serine 536 replaced with an alanine residue to block phosphorylation at this site, finding that this greatly reduced LPS induced turnover of the protein in human macrophages, maintaining nuclear RelA expression and DNA binding activity at later time points (Lawrence et al., 2005).

The second theory is that the serine 536 phosphorylation event is responsible for altering the target gene specificity of the RelA protein. For example, transcription of ICAM-1, but not IL-8, was blocked by a phosphomimetic RelA via a mechanism involving altered heterodimer association and thus promoter specificity (Sasaki et al., 2005). Further research using a competitive peptide for IKKα *in vivo* to limit serine 536 phosphorylation in mouse livers once again found that the modification only affected transcriptional activation of certain genes, for instance TNFα and IL-1β but not MCP-1 (Moles et al., 2013). Taken together, these studies suggest that phosphorylation of RelA at serine 536 may result in an alteration of the consensus sequence for RelA potentially via a shift to homodimerisation.

Either of these mechanisms may explain why Cezanne was found to alter phosphorylation of RelA, but have no discernible effect on NF-κB target genes. Due to the design of the experiments presented in this chapter, the expression of the target genes was only analysed at a single time point. If phosphorylation alters RelA nuclear translocation kinetics, it is conceivable that Cezanne controls nuclear entry or transcriptional activity of RelA at different time points, which were not studied. Moreover, the genes that were tested following Cezanne silencing were only a subset of all the genes known to be regulated by NF-κB signalling, and did not include certain genes which have been found to be altered by phosphorylation, including TNFα and IL-1β. If RelA phosphorylation in this context resulted in an alteration of gene specificity, perhaps the genes that are regulated were not studied. A broader approach such as RNA sequencing, chromatin immunoprecipitation (ChIP)-sequencing or microarray analysis may reveal unstudied genes which are specifically targeted by serine 536 phosphorylated RelA and thus Cezanne.

4.12.3 Cezanne function in non-canonical NF-κB signalling

Processing of p100 to p52 in the non-canonical NF-κB pathway was also investigated following depletion of Cezanne in ECs exposed to shear stress. Non-canonical NF-κB signalling is not well studied in the context of atherosclerosis (see Chapter 5), however

the role of the pathway in regulating proliferation (Ishikawa et al., 1997; Schumm et al., 2006) and apoptosis (Burkitt et al., 2015; Saxon et al., 2016) is of interest as these pathways are known to be dysregulated in ECs at sites of atherosclerosis (Akimoto et al., 2000; Choy et al., 2001). Western blot analysis revealed that although both p100 and p52 expression was elevated under low shear stress, there was no difference in processing in cells transfected with Cezanne siRNA compared to controls, both with and without stimulation of the pathway.

The function of Cezanne reported by Hu et al. is to inhibit p100 processing to p52 through inhibition of TRAF3 degradation by removal of lysine-48 linked polyubiquitin chains. However, there are several important differences in methodology which may explain the discrepancy in the results. The first major difference is in the cell types chosen to study; the published work utilised primary B cells and embryonic fibroblasts isolated from both wild-type and *Otud7b*$^{-/-}$ mice. B cells in particular have very high levels of non-canonical NF-κB gene expression (biogps.org), and the pathway is intimately linked to the development and maturation of this cell type (Cildir et al., 2016). In ECs, while appreciable expression of p100 and p52 were detected, levels of these and other molecules in the pathway are lower than in B cells. Thus, it is possible that TRAF3 stability is being reduced as a result of Cezanne silencing but levels of NIK are insufficient to increase in processing to p52. Analysis of these molecules may allow a greater understanding of Cezanne function in this context. In addition, the most striking differences seen in the work by Hu et al. are in the nuclear expression of p52 and RelB in *Otud7b*$^{-/-}$ cells, perhaps Cezanne regulates p52 nuclear localisation, an event that was not studied during this PhD. Alternatively, it could be a cell-type specific effect; Cezanne function in B cells and MEFs could differ from that in ECs, or exposure to shear stress could alter the function of either Cezanne or non-canonical NF-κB pathway components. Another important distinction between the two studies is the difference between using primary cells from knockout mice in comparison to siRNA mediated knockdown. While the efficiency of knockdown was very good, there was still a proportion of residual Cezanne expression which may have been sufficient to still carry out its function.

4.12.4 Cezanne function in HIF signalling

The final *in vitro* experiments to investigate Cezanne function involved testing the expression of HIF-1α. Cezanne has been shown to stabilise both HIF-1α (Bremm et al., 2014) and HIF-2α (Moniz et al., 2015) levels via direct and indirect mechanisms respectively. As endothelial HIF-1α has been shown to be upregulated in low shear stress and promote the development of atherosclerosis (Akhtar et al., 2015), determining whether Cezanne was involved in its expression was of great interest. Upon analysis,

HIF-1α expression was elevated in ECs exposed to low shear stress both in the presence and absence of DMOG, however levels were not found to differ significantly between Cezanne knockdown and control samples.

There are some key points which may explain the lack of functional effect in comparison to the observations of Bremm et. al. Firstly, the authors suggest a mechanism whereby Cezanne removes lysine-11 linked polyubiquitin from HIF-1α, resulting in the inhibition of a non-proteasomal degradation pathway. A role for chaperone mediated autophagy was suggested but not studied in depth. It is feasible that the mechanism by which Cezanne regulates HIF-1α stability is cell-type specific. Indeed, in contrast to the HeLa and MEF cell lines which displayed a decrease of HIF-1α following Cezanne silencing, two renal cell carcinoma cell lines did not show an effect. Analysis of the ubiquitination state of HIF-1α in ECs exposed to shear stress may explain why Cezanne did not alter HIF-1α stability in this cell type. Secondly, HIF-1α expression in ECs has previously been shown to be regulated in an oxygen-independent fashion, enhanced in cells overlying atherosclerotic lesions, in partially ligated carotid arteries (Akhtar et al., 2015) and as a result of NF-κB activity (Tirziu et al., 2012). Our data shows that HIF-1α is expressed more highly in ECs exposed to low shear stress in normoxic conditions, indicating a novel mechanism of HIF-1α induction. It is feasible that Cezanne regulates HIF-1α specifically in hypoxia and not in the context of low shear stress under normoxia.

A potential pathway which was not investigated here was the role that Cezanne may play in regulation of HIF-2α. Cezanne promotes HIF-2α expression via binding to and stabilising the transcription factor E2F1, which targets HIF-2α (Moniz et al., 2015). Interestingly, this effect was observed in the 786-O renal cell line which lacks VHL and so expresses HIF-2α in normoxia, indicating that the mechanism is not dependent on hypoxia. It would be interesting to test the expression of HIF-2α and E2F1 in ECs exposed to low shear stress with depletion of Cezanne expression to see whether in this context their expression levels are reduced.

4.12.5 Cezanne function *in vivo*

The experiments carried out using the Cezanne gene trap mutation on either normal C57BL/6 or atheroprone *Ldlr*$^{-/-}$ backgrounds aimed to investigate the same pathways as the *in vitro* experiments, however technical limitations resulting from analysis of ECs from a small area within the aortic arch meant that analyses were limited to quantification of expression by *en face* staining. Firstly, VCAM-1 expression was used as a surrogate for NF-κB activity. Following LPS challenge, there was no difference in levels of the adhesion molecule between wild-type or knockout samples, mimicking the observations *in vitro*. Similar to exposure to TNFα in cell culture, it is possible that the

LPS challenge was a harsh inflammatory stimulus and therefore any increase in inflammatory activity generated from loss of Cezanne would be masked. Expression of VCAM-1 in unstimulated aortas was not studied as pilot experiments revealed that VCAM-1 was not detected by *en face* staining without the addition of LPS.

Assessment of proliferation was undertaken as both HIF and non-canonical NF-κB signalling have been linked to regulation of the cell cycle. Staining of the proliferative protein Ki-67 showed that while there was significantly more proliferation in cells from the inner curvature of the aortic arch compared the outer curvature, no difference in proliferation was seen between the wild-type and knockout mice. A limitation in using Ki-67 is its expression across the cell cycle; maximal activation of the Ki-67 promoter occurs in G_2 and M phase (Zambon, 2011). Quantification relying on Ki-67 excludes actively proliferating cells in G_1 phase which may potentially be regulated by Cezanne. Furthermore, if Cezanne does affect the cell cycle in these mice, it may cause an alteration in checkpoint progression and thus accurate measurement of each phase of the cell cycle may reveal more information about any changes.

The final *in vivo* experiment utilised a cross of the atheroprone *Ldlr*$^{-/-}$ line with the *Otud7b*$^{-/-}$ line to generate double knockout *Otud7b*$^{-/-}$*Ldlr*$^{-/-}$ mice. Mice on this background develop atherosclerotic lesions when fed a Western diet. Analysis of lesion size between *Otud7b*$^{-/-}$*Ldlr*$^{-/-}$ and *Ldlr*$^{-/-}$ mice following six weeks of atherogenic diet revealed that there was no significant difference between the two groups. Given that *Otud7b*$^{-/-}$ mice had no discernible difference in inflammation or proliferation at the atheroprone inner curvature of the aortic arch, it stands to reason that there would also be no effect on lesion development, however there are some limitations in the study which mean that a role for Cezanne in regulating atherosclerosis cannot be ruled out. Firstly, lesion size was assessed after only six weeks of Western diet. However, lesions in *Ldlr*$^{-/-}$ animals fed this diet continue to grow for at least twelve months (Ma et al., 2012) and so potentially at a later time point some effect of Cezanne deletion would be seen. Lesion size is not the sole factor in determining the severity of atherosclerosis; in human disease, a major cause of mortality associated with atherosclerosis is the occurrence of myocardial infarction or stroke as a result of plaque rupture. Several factors regarding the composition of a plaque – including collagen content, macrophage and smooth muscle infiltration, lipid core size and calcification – have been shown to be predictors of cardiovascular events (Hellings et al., 2010). Many of these features become present at later stages in plaque progression, and determining whether Cezanne plays a role in these events is necessary to fully understand its role in the pathogenicity of atherosclerosis.

Linking this work to previous *in vivo* studies of Cezanne function is complicated both by the scarcity of data and the pathways investigated. Three published papers have investigated the functional consequence of Cezanne mutation, but none have looked at the regulation of atherogenic signalling in ECs from low shear stress atheroprone sites. Luong et al. (2013) identified a role for Cezanne in inhibiting renal inflammation and injury in response to ischaemia reperfusion. The *in vivo* part of the work used whole kidney lysates to investigate expression of VCAM-1 and E-selectin in both wild-type and mutant mice. While expression of both adhesion molecules was elevated in Cezanne mutant mice following ischaemia/reperfusion injury, interestingly the expression in uninjured kidneys was unaffected. This may have also been the case in the experiments presented here; perhaps with an appropriate stimulus a function of Cezanne would have become apparent. The other two studies were both carried out in the lab of Shao-Cong Sun, and look at the function of Cezanne in B and T lymphocytes. In B lymphocytes isolated from *Otud7b*$^{-/-}$ mice, no difference in canonical NF-κB signalling was seen in response to TNFα, LPS or IL-1β. However, an increase in non-canonical NF-κB DNA binding activity as well as elevated proliferation was seen in splenic B cells from the Cezanne mutants when stimulated with CD40 or BAFF (Hu et al., 2013). Intriguingly, their later work showed that *Otud7b*$^{-/-}$ T cells had increased expression of IκBα with less phosphorylation in response to ligation of CD3 and CD28, indicating lower canonical NF-κB activity (Hu et al., 2016). The discrepancy between these two studies further lends weight to the idea that the function of Cezanne could be cell-type or context specific.

Recent unpublished data has suggested that complete removal of the *Otud7b* gene in mice results in embryonic lethality; which may mean that the gene trap mutants utilised in this and other studies are not true representations of Cezanne loss. Perhaps a small amount of functional protein is sufficient for activity, generated via a cryptic splice site or other mechanism. To combat this, future experiments using these animals could use tissue specific or inducible knockouts to reduce lethality. Tissue specificity could also help to dissect the function of Cezanne in the endothelium further. It is possible that loss of Cezanne in other cell types involved in atherosclerosis (monocytes, macrophages, VSMCs) may mask any EC specific effects. Using either bone marrow transplants to ensure leukocyte genotype does not affect vascular cells, or a EC specific knockout model may help clarify these factors.

There are several other explanations for the lack of downstream functional effect seen with depletion of Cezanne *in vitro* or *in vivo*. For example, other genes or proteins may be able to compensate for the loss of Cezanne. Several other deubiquitinases are known to be involved in the negative regulation of NF-κB, notably A20 (Wertz et al., 2004) and

CYLD (Trompouki et al., 2003). Perhaps these or other NF-κB inhibitors become more active following Cezanne depletion and result in no net change in NF-κB activity. In addition, Cezanne-2 (*OTUD7A*) may play a role in compensating for loss of Cezanne. Cezanne-2 is another ovarian tumour domain deubiquitinase with close sequence similarity to Cezanne in the OTU domain. It has been shown to also interact with TRAF6 and inhibit ICAM-1 expression (Xu et al., 2014). Further research is required to identify if these other genes are compensating for loss of Cezanne, as the prospect of a family of genes coordinating to inhibit NF-κB signalling would provide great mechanistic insight into the function of the pathway.

4.12.6 Summary

In summary, the primary function of Cezanne which was identified in these experiments appeared to be in the negative regulation of RelA phosphorylation at the serine 536 residue. This modification has been previously identified as controlling NF-κB activity, but the exact mechanism is still unclear. Surprisingly, in these experiments, additional phosphorylation of RelA in Cezanne knockdown samples did not appear to affect mRNA expression of several NF-κB target genes tested, which may reflect the complexity of NF-κB regulation. Further research should employ a broader approach, utilising microarray or RNA sequencing technology to elucidate if specific target genes are being regulated by a change in DNA binding specificity of the NF-κB complex.

Two other molecular events were also measured *in vitro*; processing of p100 to p52 in the non-canonical NF-κB pathway and stability of HIF-1α. Each of these events have been previously reported to be regulated by Cezanne, but not in ECs. Neither were found to be affected by Cezanne silencing in the context of ECs exposed to shear stress. This may have been due to cell-type specific differences in Cezanne function.

The *in vivo* experiments utilising Cezanne gene-trap mutant mice gave similar results to the *in vitro* experiments. Published work has identified Cezanne's function *in vivo* as regulating canonical and non-canonical NF-κB signalling. However, no difference in these pathways were detected in ECs. The size of atherosclerotic lesions was also not significantly altered by the absence of Cezanne in these animals, although the composition of plaques was not analysed. It is plausible that Cezanne deletion led to activation of compensatory mechanisms, for example induction of other OTU deubiquitinases.

Cellular signalling events tend to form complex networks with multiple levels of regulation. Cezanne was not responsible for regulating canonical NF-κB gene expression, p100 processing or HIF signalling in the experiments carried out as part of this PhD. However, a role in regulating RelA phosphorylation under shear stress was discovered and further research is required to discover the importance of this modification in the vascular endothelium.

5. Non-canonical NF-κB drives EC proliferation under low shear stress

5.1 Introduction

The NF-κB pathway is a key regulator of cellular inflammation, and plays a critical role in the progression of many inflammatory diseases, including atherosclerosis. NF-κB signalling can be broadly split into two pathways, defined by the subunit combinations and upstream signalling pathways leading to nuclear localisation. The canonical NF-κB pathway has been predominantly studied in vascular disease, finding that RelA (Gareus et al., 2008) and c-Rel (Djuric et al., 2012) subunits promote the development of atherosclerotic lesions. In contrast, very little is known about the role that the non-canonical NF-κB pathway may play in controlling atherosclerosis.

Non-canonical NF-κB signalling results in the processing of the precursor p100 subunit to p52 and subsequent nuclear localisation of the p52:RelB heterodimer. While there is some degree of cross-talk between canonical and non-canonical NF-κB (Oeckinghaus et al., 2011), activation of p100 processing is primarily potentiated by a distinct pathway involving post-translational control of NIK. This kinase is constitutively expressed, and is responsible for phosphorylating p100 via IKKα, allowing processing. Prior to stimulation, NIK is marked for proteasomal degradation by the addition of ubiquitin by TRAF3 (Skaug et al., 2009). Activation of the pathway by ligation of members of the TNFR superfamily, in particular CD40, LTβR and BAFFR, results in TRAF3 recruitment to the cell-surface receptor and its subsequent degradation (Vallabhapurapu et al., 2008), thus allowing NIK accumulation and p52 generation.

The non-canonical NF-κB pathway has primarily been studied in B cells, where it plays a major role in regulating development and maturation (Claudio et al., 2002; Hahn et al., 2016; Jellusova et al., 2013). In B cell cancers, such as diffuse large B cell lymphoma and some types of leukaemia, non-canonical NF-κB signalling can be oncogenic (De Donatis et al., 2015; Park et al., 2006; Vallabhapurapu et al., 2015).

There is some evidence to suggest that this pathway may be important in atherosclerosis too. Firstly, expression of *NFKB2* (the gene encoding p100) was identified as being upregulated at the inner curvature of the porcine aortic arch in a microarray study (Passerini et al., 2004), and phosphorylated RelB was found to be increased at the same site in mice (Jhaveri et al., 2012). In addition, TRAF3 has been found to be elevated in ECs following exposure to high shear stress, and *in vivo* overlying areas of plaques corresponding to higher shear stress (Urbich et al., 2001). Lastly, CD40 signalling has

been shown to be increased at sites prone to atherosclerosis. ApoE mutant mice also lacking the CD40 gene were found to have significantly less lesion coverage, with a decreased macrophage content and increased collagenisation (Lutgens et al., 1999). Furthermore, delivery of CD40L-containing microparticles to ECs stimulated proliferation *in vitro* and neovessel formation *in vivo* (Leroyer et al., 2008).

The expression of canonical NF-κB subunits are increased at sites of atherosclerosis, as a result of the haemodynamic conditions, however whether non-canonical NF-κB activity is regulated by shear stress has not been tested. Increased endothelial turnover has been associated with areas of atherosclerosis and exposure to low shear stress (Chaudhury et al., 2010; Dardik et al., 2005; Davies et al., 1986). As non-canonical NF-κB signalling can control endothelial proliferation in lymphatic vessels (Vondenhoff et al., 2009) it may function to carry out this role in ECs and therefore play a critical role in regulating the development of disease.

5.2 Hypothesis and aims

Hypothesis: The expression and activity of the non-canonical NF-κB pathway in ECs is regulated by shear stress and responsible for modulating endothelial phenotype at sites prone to atherosclerosis.

Aim 1: Determine the expression pattern and activity of non-canonical NF-κB pathway components in ECs exposed to shear stress.

Aim 2: Determine the function of this pathway in ECs exposed to shear stress.

5.3 Non-canonical NF-κB subunits are expressed at the inner curvature of the porcine aortic arch

The expression of *NFKB2* – the gene encoding the p100 subunit of NF-κB – has been highlighted in a microarray study as a gene potentially induced in ECs at the atheroprone region of the porcine aortic arch (Passerini et al., 2004), while phosphorylated RelB was found at the same region in mice (Jhaveri et al., 2012). To validate the expression changes of p100 and its binding partner RelB (*RELB* gene), ECs were isolated from the inner and outer curvatures of the porcine aortic arch and qPCR carried out for these genes on cDNA isolated from these regions. (Figure 5.1). Porcine aortas obtained from a local abattoir were cleaned and regions of the inner and outer curvatures of the aortic arch dissected. ECs were scraped from these sections and total RNA isolated and converted to cDNA by reverse transcription. Assessment of endothelial purity was carried out by determining the ratio of PECAM-1 to α-smooth muscle actin by qPCR (Figure 5.1a). The expression of *NFKB2* and *RELB* were also measured by qPCR (Figure 5.1b), using the expression of the housekeeper β2 microglobulin (*B2M*) to normalise cDNA quantity. The expression of both *NFKB2* and *RELB* were found to be significantly increased in ECs from the inner curvature of the aortic arch compared to the outer curvature, with approximately a four-fold increase in expression of each gene. This confirms the expression change found in the previous microarray study (Passerini et al., 2004), and also shows that *RELB* expression is similarly regulated. The underlying mechanism resulting in this expression change is not known, nor whether an alteration in mRNA expression causes a similar change in protein expression or non-canonical NF-κB activity.

5.4 Components of the non-canonical NF-κB signalling pathway are downregulated under high shear stress.

The differential expression of p100 and RelB between the two sites of the porcine aortic arch (Figure 5.1) may be due to the shear stress patterns exerted on ECs. To investigate whether shear stress can affect the expression of non-canonical NF-κB subunits, human ECs were exposed to different shear stress patterns *in vitro* using both the ibidi® and orbital shaker systems. HUVECs were exposed to shear stress for 72 hours using these systems before lysis and protein isolation. The expression of p100/p52 and RelB were determined using Western blotting, using the housekeeper PDHX for normalisation. The expression of p100, p52 and RelB were found to be significantly reduced by high shear stress in the orbital shaker system, compared to cells under low shear stress (Figure 5.2); the expression levels of cells under either condition was not significantly different to static cells. The expression of these proteins was also found to be significantly lower in

a

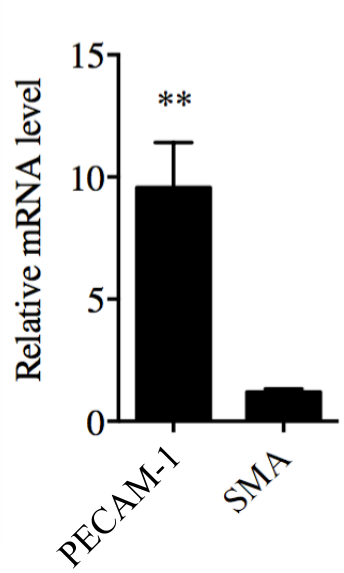

b

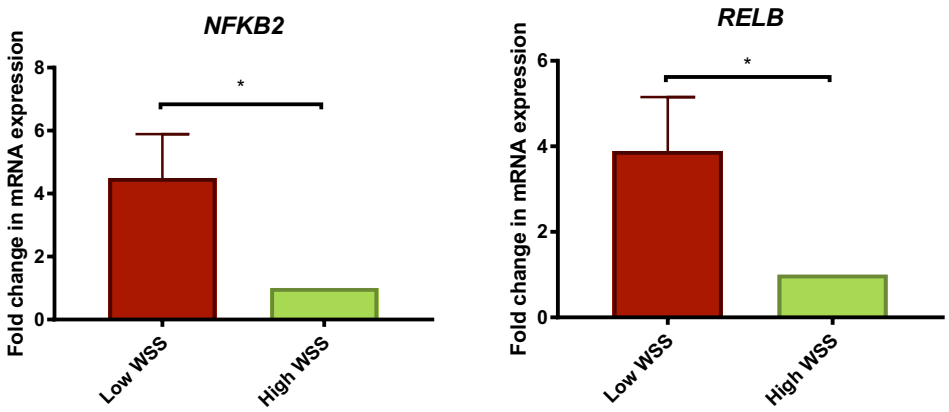

Figure 5.1: The expression of *NFKB2* and *RELB* mRNA was elevated in ECs from the inner curvature of the porcine aortic arch. Porcine aortas were obtained from a local abattoir. The aortas were then dissected and cleaned, before a scalpel was used to isolate a 1 cm^2 section from both low and high shear stress sites as previously determined by computational fluid dynamics. These sections were incubated endothelial side down in collagenase to free ECs, which were then scraped into PBS and pelleted. RNA was then isolated from these cell pellets using a commercial kit. The RNA was then converted to cDNA by reverse transcription and gene expression tested by qPCR. **(a)** The expression of the EC marker PECAM-1 and the VSMC marker α smooth muscle actin (SMA) were determined in samples from each condition, normalised to the housekeeping gene β-2 microglobulin (B2M) to ensure EC purity. Samples with a ratio lower than 3:1 PECAM-1 to α-SMA were rejected. **(b)** The expression of non-canonical NF-κB subunits *NFKB2* and *RELB* were measured in both samples, normalised to B2M.
n=4; $p<0.05$; paired t-test
The data from (a) were gathered by Dr. Ismael Gauci and used with permission.

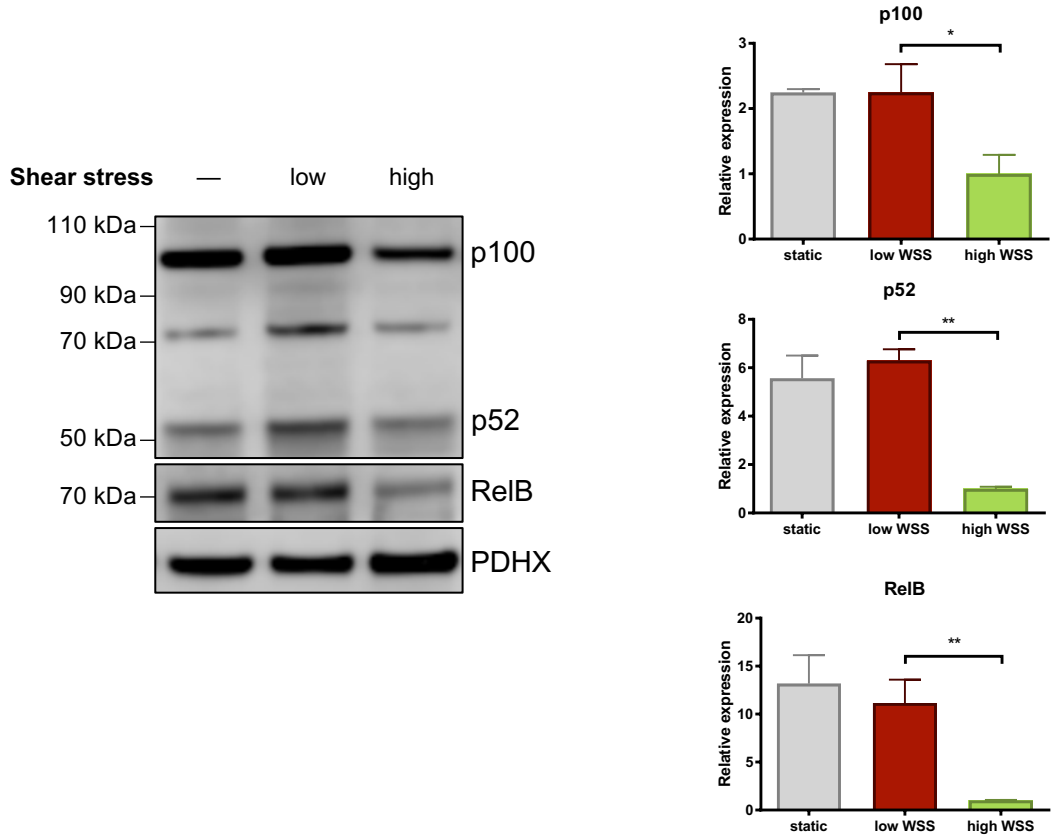

Figure 5.2: Expression of non-canonical NF-κB subunits were decreased in ECs exposed to high shear stress. HUVECs were seeded into six-well plates and exposed to shear stress for 72 hours using the orbital shaker system, or left static for the same period. Cells were then scraped from the centre (low shear stress) and periphery (high shear stress) of orbited wells, and from the entire well of static. Lysates were then generated and expression of p100/p52 and RelB determined by Western blotting, normalising to the housekeeper PDHX.
n=4; $p<0.05$; one-way ANOVA with Tukey's post test analysis.

cells exposed to high shear stress compared to low shear stress in the ibidi® system (Figure 5.3). In combination, these data confirm that shear stress alone is not sufficient to alter the expression of components of the non-canonical signalling pathway, but that low shear stress resulted in enhanced expression compared to high shear stress.

5.5 Exposure to low shear stress results in an increase in p100 processing.

While expression of components of the non-canonical NF-κB pathway was found to be decreased under high shear stress, the proportion of active p52 was relatively low. To test whether the change in expression resulted in an alteration in the processing of p100 to active p52 in response to stimulus, the non-canonical NF-κB pathway was stimulated by the addition of CD40L. HUVECs were seeded onto six-well plates and exposed to shear stress using the orbital shaker system for 72 hours. CD40L was added to samples for the final 2 hours of orbiting before cells were lysed and protein samples isolated from each condition. Levels of p100 and p52 were quantified by Western blotting, normalised to the housekeeper PDHX (Figure 5.4). The processing of p100 to p52 was found to be strongly induced by the addition of CD40L in cells exposed to low shear stress (compare lanes 1 and 3). Levels of p52 were significantly increased by CD40L stimulation in these conditions, and p100 tended to decrease. While not statistically significant, p52 expression was also found to increase in cells exposed to high shear stress, but notably the level following stimulation was less than 50% of the expression in low shear stress (compare lanes 3 and 4). Thus, it was concluded that p100 processing to p52 in response to CD40L is elevated under low compared to high shear stress.

5.6 Non-canonical NF-κB signalling promotes endothelial proliferation under low shear stress

A higher level of expression and increased capacity for activation under low shear stress indicated that the non-canonical NF-κB pathway may play a role in regulating the phenotype of ECs exposed to this mechanical environment. Non-canonical NF-κB has been previously reported to regulate B cell and lymphoid proliferation (Sun, 2011), and CD40L stimulation has been shown to induce proliferation in ECs (Leroyer et al., 2008). In addition, EC proliferation is regulated by shear stress, with unidirectional high shear stress inhibiting proliferation (Akimoto et al., 2000). In order to understand the role non-canonical NF-κB signalling may play in controlling endothelial proliferation, small interfering RNA was used to deplete *NFKB2* mRNA, then EC proliferation was measured following the application of low or high shear stress using the orbital shaker system (Figure 5.5). A subset of cells from each condition were collected for Western blotting to confirm knockdown (Figure 5.5a). The remainder of the samples were fixed in

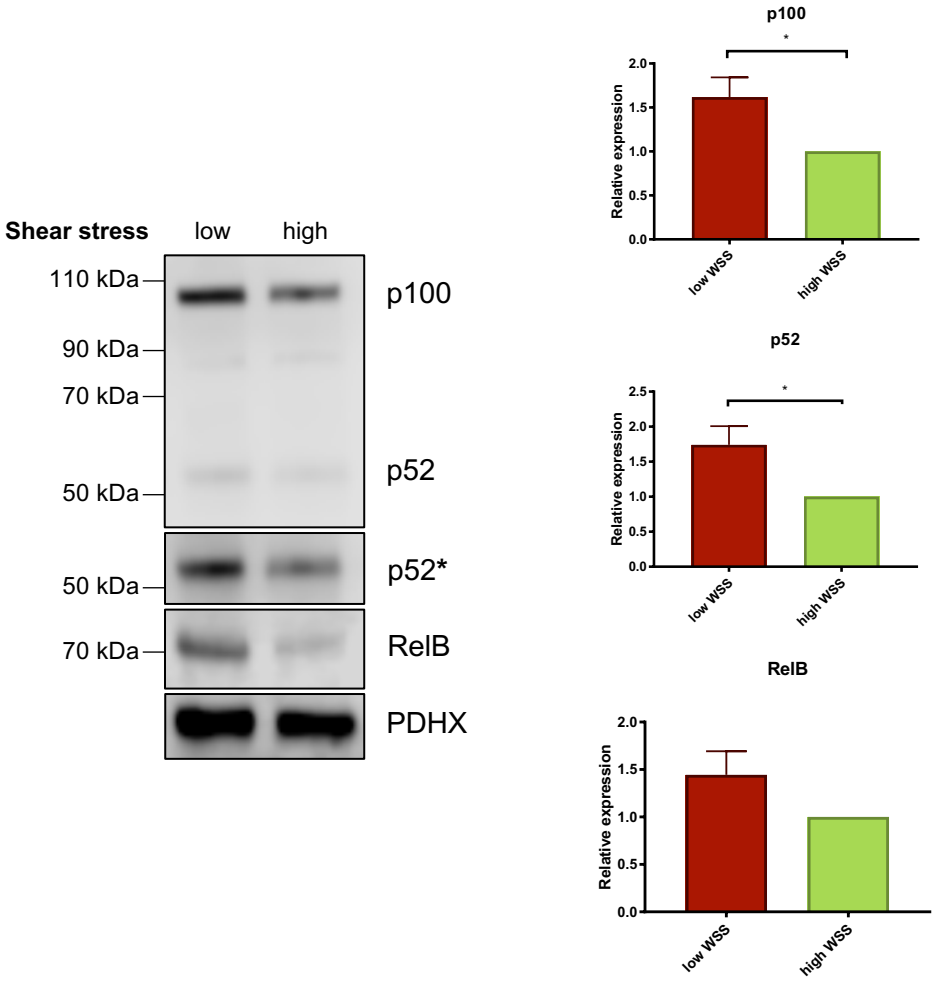

Figure 5.3: Expression of non-canonical NF-κB subunits were decreased in ECs exposed to high shear stress in the ibidi system. HUVECs were seeded into chamber slides, and once adherent, exposed to low (±4 dyn/cm^2) or high (13 dyn/cm^2) shear stress for 72 hours using the ibidi® system. Cells were then lysed and the expression of p100, p52 and RelB determined by Western blotting, normalising to the housekeeper PDHX.
n=3; $p<0.05$; paired t-test

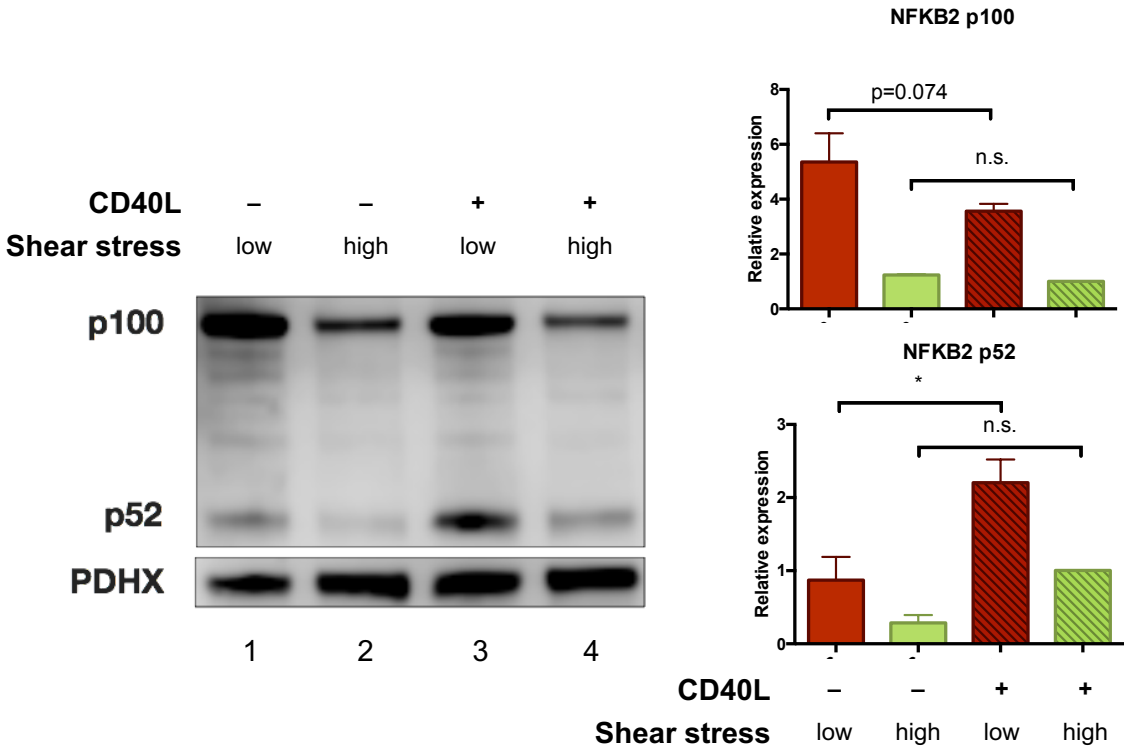

Figure 5.4: Processing of p100 in response to CD40L is increased in endothelial cells exposed to low shear stress. HUVECs were exposed to shear stress for 72 hours using the orbital shaker system. CD40L (100 ng/ml) was added to a proportion of the wells for the final 2 hours of shear stress, with the remaining wells left untreated. Following treatment, cells were scraped from both shear stress regions of each condition and lysed separately. Protein concentration was determined using a BCA assay and samples normalised accordingly. The expression of p100 and p52 were determined by Western blotting, normalising to the housekeeper PDHX. Densitometry was carried out using ImageJ software. Data are presented as mean ± SD.
n=3; *p<0.05; Two-way ANOVA with Tukey's post test analysis.

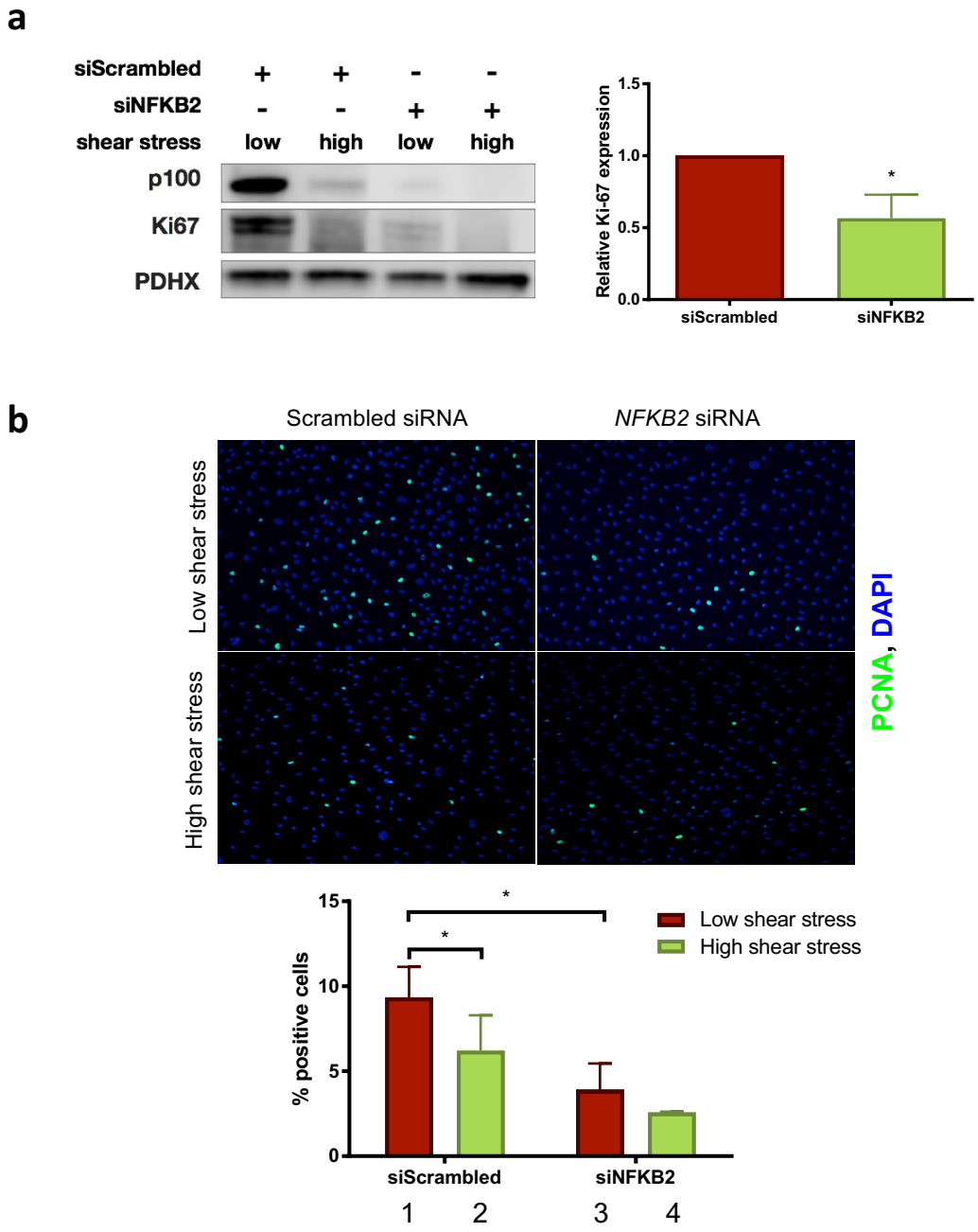

Figure 5.5: Non-canonical NF-κB subunits promote EC proliferation under low shear stress. HUVECs were transfected with *NFKB2* siRNA or a scrambled siRNA control using electroporation, then seeded onto six-well plates. Following adherence, cells were exposed to shear stress for 72 hours using the orbital shaker system. **(a)** After exposure to shear stress, cells were scraped from the centre (low shear stress) and periphery (high shear stress) of each well and lysed. Expression of p100/p52 was determined to confirm knockdown, as well as the proliferation marker Ki-67. The housekeeper PDHX was used for normalisation. **(b)** Following exposure to shear stress, cells were washed with PBS, fixed with 4% formaldehyde, permeabilised using 0.1% Triton-X100 and blocked with 5% BSA. Samples were stained for the proliferation marker PCNA and the nuclear stain DAPI. n=3; *p<0.05; (a) paired t test, carried out on raw data; (b) Two-way ANOVA.

formaldehyde for further immunofluorescence staining for proliferating cell nuclear antigen (PCNA) (Figure 5.5b). As previously reported, EC proliferation was significantly elevated in cells under low shear stress (Figure 5.5b, compare 1 and 2)). Knockdown of *NFKB2* resulted in a significant decrease in proliferating cells from the low shear stress site (compare 1 and 3), but had no effect on cells under high shear stress (compare 2 and 4).

5.7 *Nfkb2*$^{-/-}$ mice display reduced endothelial proliferation at the inner curvature of the aortic arch

To determine whether the effect on endothelial proliferation seen with knockdown of non-canonical NF-κB *in vitro* was an accurate assessment of the role of this pathway *in vivo*, studies were carried out using aortas from *Nfkb2*$^{-/-}$ mice. Aortic arches from 10-week old female *Nfkb2*$^{-/-}$ mice and C57BL/6J wild-type controls were dissected and EC proliferation assessed by immunofluorescence staining for Ki-67 in cells from the inner and outer curvatures of the arch, exposed to low and high shear stress respectively (Figure 5.6). Imaging with confocal microscopy revealed that EC proliferation in the aortic arch in C57BL/6J animals was significantly higher at the inner curvature in comparison to the outer curvature, with almost no detectable proliferating cells in the latter region (Figure 5.6, compare 1 and 2). In the *Nfkb2*$^{-/-}$ animals, the percentage of proliferating cells as identified by Ki-67 was significantly lower than in the wild-type control group (compare 1 and 3), while there was no significant difference in proliferation at the outer curvature (compare 2 and 4). Thus, it was concluded that *Nfkb2* expression is required for EC proliferation at low shear stress regions of arteries.

5.8 ICAM-1 expression at the inner curvature of the aortic arch is unchanged between wild-type and *Nfkb2*$^{-/-}$ mice.

Previous studies found that CD40 signalling can alter multiple cellular processes in ECs. In addition to its role in promoting proliferation, stimulation with CD40L also promotes an inflammatory response, with activation of p38, Akt and NF-κB and upregulation of MCP-1, ICAM-1 and other inflammatory cytokine and adhesion molecule expression (Chakrabarti et al., 2007; Henn et al., 1998). As the non-canonical NF-κB pathway can be activated by exposure to CD40L, it is possible that inflammation is also being promoted by its activity. To determine whether p100/p52 depletion was regulating inflammatory signalling in addition to proliferation in cells exposed to low shear stress, expression of ICAM-1 was measured by immunofluorescence staining in aortic arches from both wild-type and *Nfkb2*$^{-/-}$ mice in a pilot study (Figure 5.7). Analysis of fluorescence intensity by *en face* confocal microscopy showed that ICAM-1 was strongly

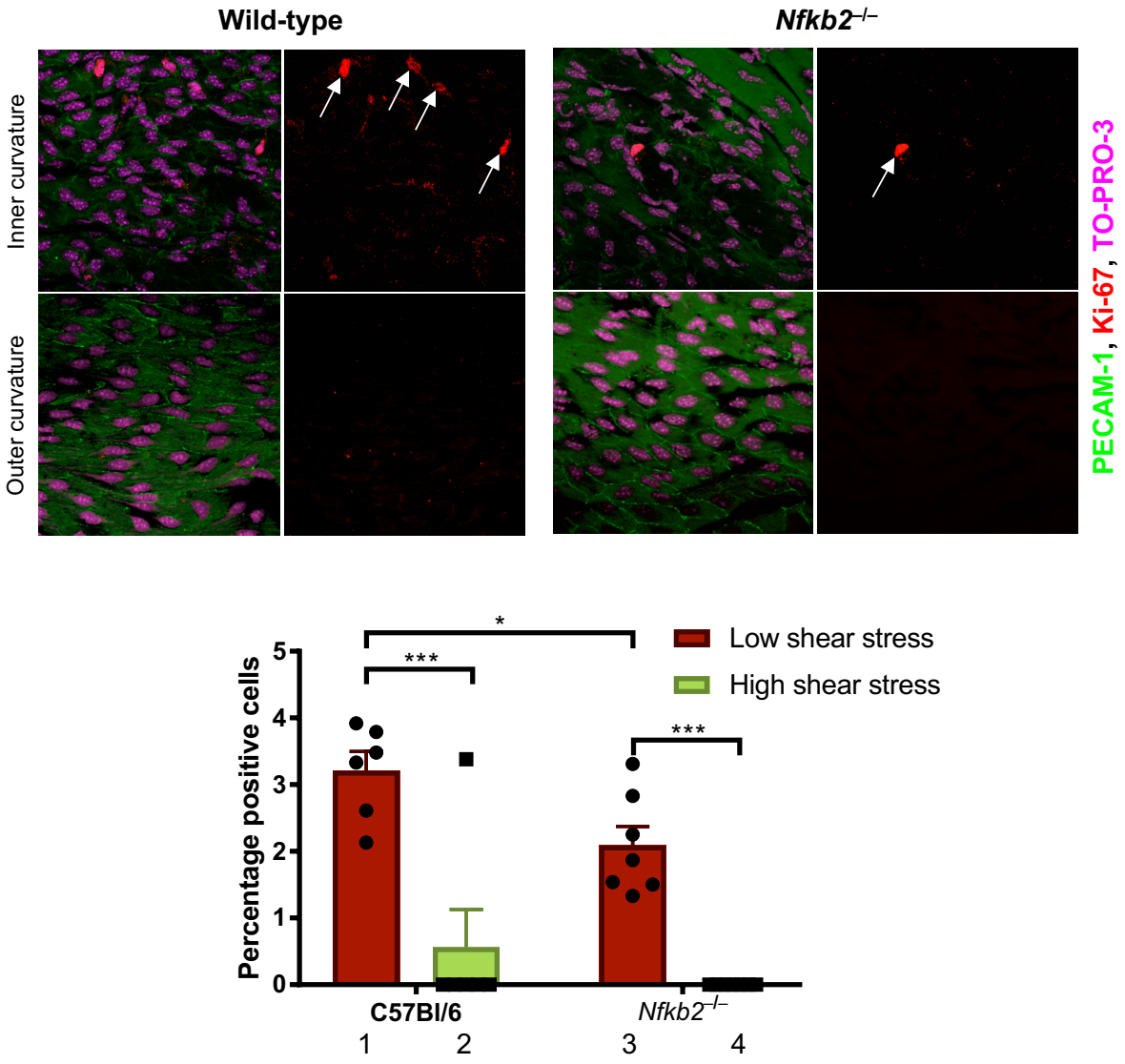

Figure 5.6: *Nfkb2*$^{-/-}$ mice display less EC proliferation at the low shear stress site of the aortic arch. Ten week old female *Nfkb2*$^{-/-}$ and matched C57BL/6J control mice were culled by intraperitoneal injection of pentobarbitone. The vasculature was then perfusion fixed with 4% formaldehyde and aortic arches dissected and opened longitudinally. These tissue samples were stained for Ki-67 to mark proliferating cells, as well as PECAM-1 as an EC marker and TO-PRO-3 to label nuclei. Sections were mounted on cover slips *en face* and imaged using confocal microscopy. Proliferation was quantified using ImageJ software to count the number of Ki-67 positive cells compared to the total number of cells per field and expressed as a percentage.
n=7; *p<0.05; ***p; 0.005; Two-way ANOVA.

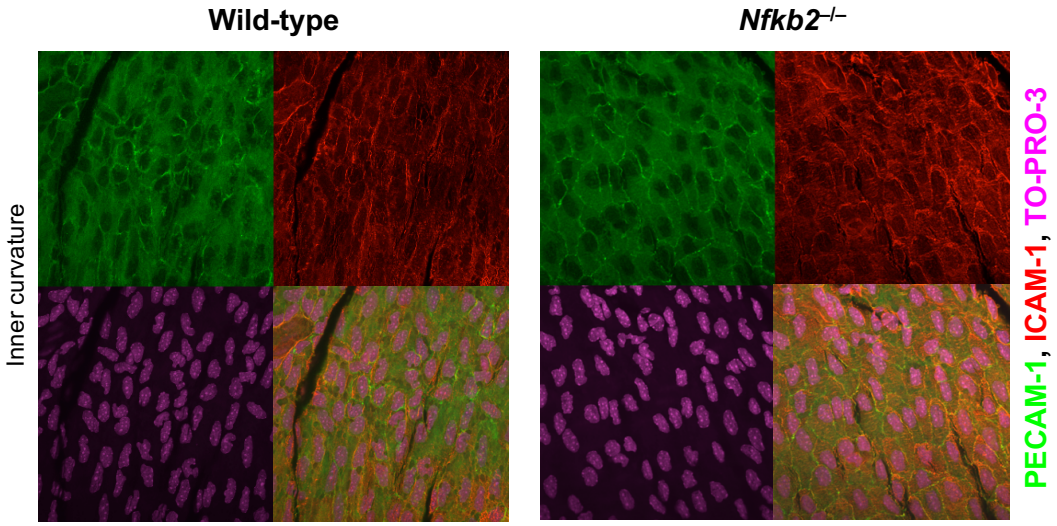

Figure 5.7: *Nfkb2*$^{-/-}$ aortic arches do not show altered ICAM-1 expression. Ten week old female *Nfkb2*$^{-/-}$ and matched C57BL/6J control mice were culled by intraperitoneal injection of pentobarbitone. The vasculature was then perfusion fixed with 4% formaldehyde and aortic arches dissected and opened longitudinally. These tissue samples were stained for ICAM-1, as well as PECAM-1 as an EC marker and TO-PRO-3 to label nuclei. Sections were mounted on cover slips *en face* and imaged using confocal microscopy.
Images are from a single experiment.

expressed on EC junctions at the inner curvature of the aortic arch in both wild-type and *Nfkb2*$^{-/-}$ animals, fitting with previous work (Iiyama et al., 1999), and indicating that there was an upregulation of inflammation at this site. Preliminary analysis suggests ICAM-1 expression was not altered, however, between the aortic arches of the wild-type and *Nfkb2*$^{-/-}$ mice. This observation suggests that p100/p52 does not function to regulate endothelial inflammation at sites of low shear stress.

5.9 The expression of p21 is negatively regulated by p100/p52 under low shear stress.

With both *in vitro* and *in vivo* results indicating that non-canonical NF-κB signalling plays an important role in the negative regulation of EC proliferation specifically at sites of low shear stress, a crucial further issue is to determine the mechanism or pathway involved in this regulation. Both p52 and RelB have been previously implicated in controlling the expression of several genes which are important in regulating cell-cycle progression (Burkitt et al., 2015; Ramachandiran et al., 2015; Rocha et al., 2003; Schumm et al., 2006), however which, if any, genes are being controlled in ECs is unclear.

To assess this, *NFKB2* or *RELB* were silenced in HUVECs by transfection with siRNA. The ECs were then plated onto six-well plates and exposed to shear stress using the orbital shaker system, before isolation of RNA. A list of putative genes which may affect proliferation were chosen based on their regulation by non-canonical NF-κB in the literature (Burkitt et al., 2015; Ramachandiran et al., 2015; Rocha et al., 2003; Schumm et al., 2006), in addition to several inflammatory genes which were also tested. The mRNA expression of these genes was tested by qPCR in samples from cells exposed to low shear stress and transfected with either scrambled, *NFKB2* or *RELB* siRNA (Figure 5.8). The results show that the expression of only one gene in the panel, p21, was affected by silencing of a non-canonical NF-κB subunit. The expression of p21 was found to be significantly elevated in cells exposed to low shear stress following silencing of *NFKB2*, and showed a trend towards elevation following *RELB* silencing.

To further investigate this phenomenon, p21 protein expression was also tested by Western blotting in lysates from sheared HUVECs transfected with *NFKB2* siRNA (Figure 5.9). The expression of p21 was also found to be significantly increased in cells transfected with *NFKB2* siRNA in comparison to scrambled siRNA control samples. This observation further verifies the result from the qPCR and shows that p21 expression at both mRNA and protein level is inhibited by p52 in cells exposed to low shear stress. As p21 is a negative regulator of proliferation, through its inhibition of cyclin-dependent

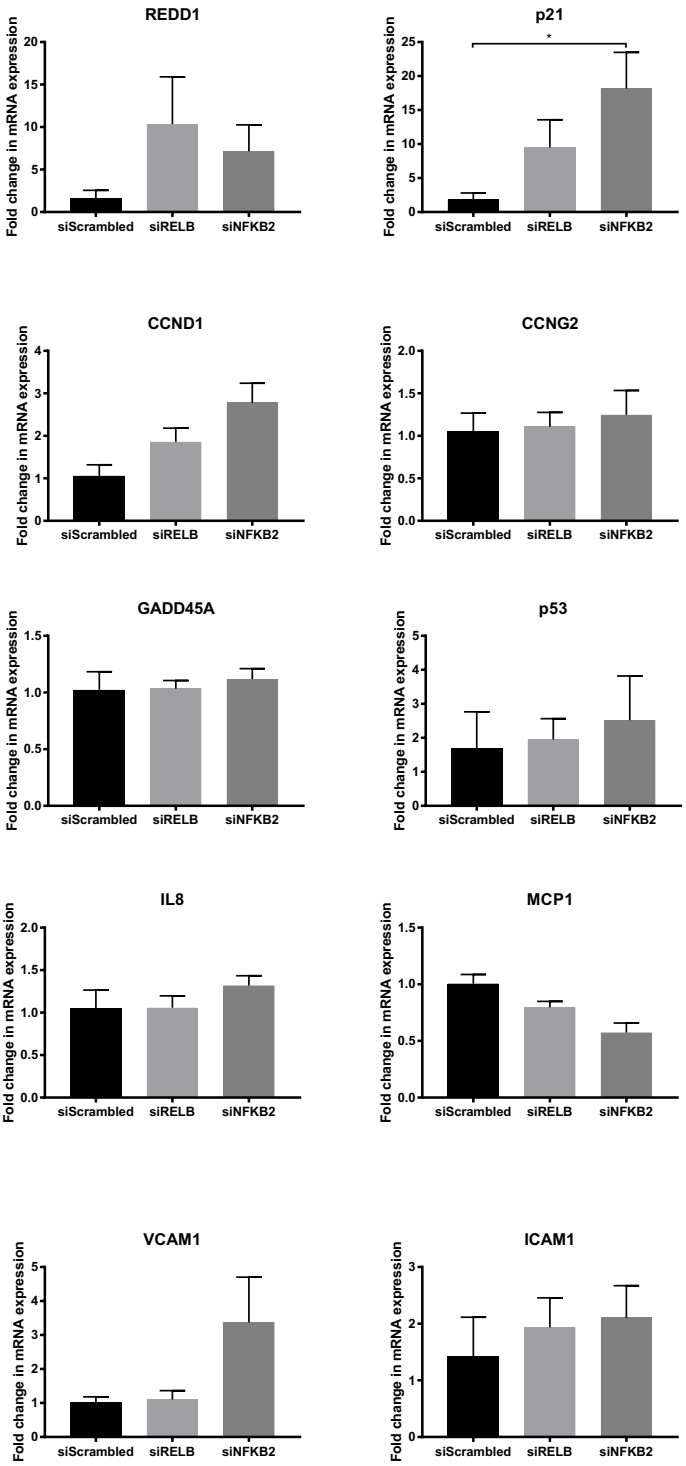

Figure 5.8: Silencing of *NFKB2* results in enhanced p21 expression in cells exposed to low shear stress. HUVECs were transfected with *NFKB2*, *RELB* or scrambled control siRNA by electroporation before being seeded onto six well plates. Once adherent, cells were exposed to shear stress for 72 hours using the orbital shaker system. Next, cells were scraped from the centre of each well (low shear stress), RNA isolated using a commercial kit and converted to cDNA by reverse transcription. The expression of a panel of putative non-canonical NF-κB target genes were tested by qPCR, normalising to the housekeeping gene HPRT.
n=3; *p<0.05; One-way ANOVA.

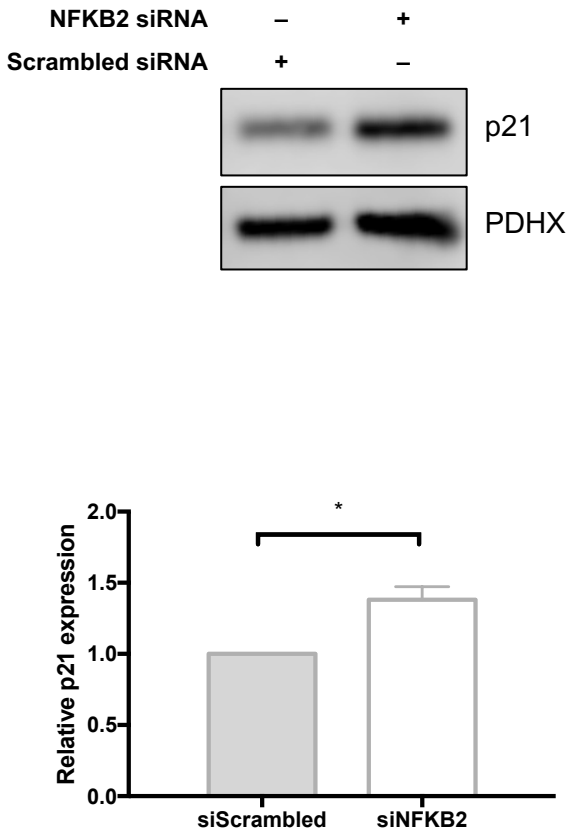

Figure 5.9: Silencing of *NFKB2* enhances p21 protein expression in ECs exposed to low shear stress. Gene silencing was carried out in HUVECs by electroporation, transfecting with either NFKB2 siRNA or non-targeting scrambled control siRNA. Transfected cells were plated into six-well plates, allowed to adhere, then exposed to shear stress for 72 hours using the orbital shaker system. Next, cells from the low shear stress region at the centre of each well were isolated and lysed. The expression of p21 was tested in these samples by Western blotting, normalising to the expression of the housekeeper PDHX. Densitometry analysis was performed using Image Studio Digits software.
n=5; $p<0.05$; paired t-test. Statistical analysis was carried out prior to normalisation.

kinases this suggests that elevated expression of non-canonical NF-κB subunits in cells exposed to low shear stress results in an enhancement of proliferation through inhibition of p21 expression. This is potentially a major pathway which controls the difference in EC proliferation between sites of the vasculature protected from and prone to atherosclerosis, and may have a role in regulating atherogenesis.

5.10 Cezanne expression in *Nfkb2*$^{-/-}$ mice

An important experiment that was not carried out during the course of this PhD was testing Cezanne expression in either cells transfected with *NFKB2* siRNA or in the aortas of *Nfkb2*$^{-/-}$ mice. An unanswered question about the upregulation of Cezanne expression by low shear stress is the mechanism behind it. Future work should include investigation that the effect of non-canonical NF-κB loss has on Cezanne.

5.11 Conclusions

The experiments described in this chapter provide an insight into the role of the non-canonical branch of NF-κB signalling in regulating endothelial responses to the haemodynamic environment they inhabit. The expression of the non-canonical NF-κB subunits p100/p52 and RelB were found to be enhanced by exposure to low shear stress both *in vitro* in HUVECs exposed to shear stress in two complimentary systems, and *in vivo* in ECs isolated from the aortic arch of healthy pigs. The mechanism of expression change was not investigated in detail but likely involved downregulation by high shear stress, as static and low shear stress samples possessed similar quantities.

The expression of these subunits was responsible for promoting EC proliferation. Silencing of the subunits *in vitro* revealed a significant decrease in Ki-67 and PCNA positivity specifically in ECs exposed to low shear stress. Analysis of aortic arches from *Nfkb2*$^{-/-}$ mice showed a similar result. There were significantly fewer Ki-67 positive cells at the inner curvature when compared to the same region in wild-type mice.

A potential mechanism was identified, involving p52 inhibition of p21 expression. Silencing of *NFKB2* resulted in a significant increase in both mRNA and protein expression of p21 in cells exposed to low shear stress. As a cyclin-dependent kinase inhibitor, p21 is responsible for stalling the cell-cycle and preventing proliferation. Its expression is known to be elevated in ECs exposed to high shear stress, and this inhibition by non-canonical NF-κB under low shear stress may be a mechanism for this difference, resulting in enhanced EC proliferation at atheroprone sites and potentially regulating the development of atherosclerosis.

5.12 Discussion

NF-κB signalling is known to play an important role in the development of atherosclerosis. Studies have primarily focused on the canonical pathway, which is upregulated at sites of low shear stress and drives expression of inflammatory cytokines and adhesion molecules, leading to monocyte recruitment and the development of atherosclerosis. The data presented in this chapter demonstrate that the non-canonical NF-κB pathway is also important in regulating endothelial phenotype by promoting EC proliferation specifically at sites of low shear stress, which may be important in mediating the development of atherosclerosis.

5.12.1 The expression of non-canonical NF-κB subunits were regulated by shear stress.

Previous studies have suggested that the expression of the non-canonical NF-κB subunits p100 and RelB are enhanced at regions of atherosclerosis. Passerini et al. (2004) carried out a microarray on porcine ECs from different regions of the aortic arch, with the *NFKB2* gene (p100 subunit) on the list of genes more highly expressed at the inner curvature of the aorta. Phosphorylated RelB has also been noted to be increased at the same site in mice (Jhaveri et al., 2012).

The experiments presented in this chapter confirm these observations, and suggest that the presence of low shear stress at the inner curvature is responsible for the differences. Expression analysis of *NFKB2* and *RELB* mRNA from ECs scraped from the inner and outer curvatures of the porcine aortic arch revealed a significant difference in expression between the two regions, with approximately four times more expression in cells from the inner curvature than the outer. This difference was likely caused by a decrease in expression at sites of high shear stress, as further *in vitro* studies compared expression in ECs exposed to low or high shear stress compared to static cells. This showed that there was no difference in protein expression of p100, p52 or RelB between static and low shear stress, but a significant decrease in high shear stress conditions.

This expression pattern is similar to that of both *NFKB1* (p105/p50) and *RELA* (Hajra et al., 2000; Passerini et al., 2004), suggesting that there could be a common mechanism controlling the induction of canonical and non-canonical components. RelA upregulation under low shear stress has been found to be controlled by the activity of JNK (Cuhlmann et al., 2011), and indeed there is some evidence that RelB expression is also affected by this pathway. Pharmacological inhibition of JNK was found to ablate induction of RELB transcription in response to a cytomegalovirus protein (Wang and Sonenshein, 2005). Thus, JNK may control expression of both canonical and non-

canonical NF-κB. Another potential explanation is that expression of the non-canonical NF-κB subunits are regulated by canonical NF-κB transcriptional activity. The promoter regions of both *NFKB2* and *RELB* contain κB binding sites (Liptay et al., 1994; Wang and Sonenshein, 2005), and their transcription has been found to be responsive to various canonical NF-κB activating factors including TNFα, LPS and IL-1β (Bren et al., 2001; de Wit et al., 1998). Induction of non-canonical NF-κB subunit expression via canonical NF-κB activity would explain the localisation to sites of low shear stress while also providing useful information on how inflammatory signalling in ECs may be responsible for other phenotypic changes.

5.12.2 CD40L mediated processing of p100 to p52 was more rapid in cells exposed to low shear stress

Exposure of sheared HUVECs to CD40L was carried out to test whether p100 processing could occur in this context. Stimulation for 2 hours revealed a significant increase in p52 generation in cells exposed to low shear stress. This may have been due simply to the elevated expression of p100 seen in these cells allowing more p52 to be generated, however another mechanism may have been involved. TRAF3 has been shown to be dampened in ECs exposed to low shear stress in previous studies (Urbich et al., 2001). It was found to inhibit CD40L signalling by blocking AP-1 DNA binding, but expression of p100 was not tested. In principle, decreased TRAF3 expression under low shear stress may result in a higher basal expression of NIK due to reduced proteasomal degradation (Figure 1.7). Upon stimulation with CD40L, as TRAF3 is degraded, enhanced NIK expression under low shear stress may allow these cells to begin p100 processing more rapidly. Antibody specificity issues prohibited the analysis of TRAF3 expression here, but if its expression was enhanced under high shear stress it may indicate a mechanism of negative regulation of non-canonical NF-κB at these sites.

CD40 signalling has been implicated in lesion development for some time; CD40L knockout mice have been found to have significantly decreased lesion size (Lutgens et al., 1999). The function of CD40 signalling has been identified as being involved in inflammatory responses. CD40L activation of ECs has been shown to induce expression of several inflammatory genes including IL-8, E-selectin and ICAM-1 (Henn et al., 1998; Urbich et al., 2001). Interestingly, in the present study, ICAM-1 expression was unchanged at the inner curvature of *Nfkb2*$^{-/-}$ mice compared to wild-type controls, suggesting that non-canonical NF-κB is not involved in this process. My data offer an alternative mechanism since non-canonical NF-κB drives excessive EC proliferation at atheroprone sites. Thus, CD40L may promote atherosclerosis by activating p52-dependent proliferation. Consistent with this, VEGF – an important regulator of EC

proliferation – can be induced by CD40L (Dormond et al., 2008; Leroyer et al., 2008; Melter et al., 2000).

5.12.3 Non-canonical NF-κB promotes EC proliferation under low shear stress

The application of low shear stress to ECs generates endothelial dysfunction, characterised by elevated inflammation, apoptosis and proliferation. The increase in both proliferation and apoptosis leads to higher EC turnover in cells exposed to these haemodynamics (Davies et al., 1986). This creates a disparity in EC turnover between sites prone to and protected from atherosclerosis and may be an important factor in regulating the development of disease.

In this study, EC proliferation was also found to be elevated in cells exposed to low shear stress at the inner curvature of the aortic arch *in vivo*, as measured by immunofluorescence staining for Ki-67. Analysis of ECs exposed to shear stress *in vitro* using the orbital shaker system recapitulated this difference in proliferation, with a significantly higher percentage of cells from the centre of each well displaying positive staining for PCNA, as well as showing an increase in Ki-67 expression by Western blotting. Examination of *Nfkb2*$^{-/-}$ mice or HUVECs transfected with *NFKB2* siRNA revealed a significant reduction in these markers specifically at the inner curvature of the aortic arch *in vivo* and cells exposed to low shear stress *in vitro*.

In the orbital shaker system, both the percentage of positive PCNA cells and total Ki-67 expression under low shear stress were reduced by *NFKB2* silencing to the levels seen in cells exposed to high shear stress. This suggests that p52 may play an important role in regulating the switch in proliferation phenotype between cells exposed to different physiological shear stress patterns. Ki-67 staining *in vivo* was not decreased to the same extent in *Nfkb2*$^{-/-}$ aortic arches, which may be due to the influence of signalling from other cell types or stimuli present *in vivo* which may also alter endothelial proliferation.

The effect of *NFKB2* silencing on the two markers *in vitro* may provide additional information about the mechanism by which proliferation is being reduced. Both Ki-67 and PCNA are expressed specifically by actively proliferating cells, but each display maximal expression at different stages of the cell cycle (Figure 5.10). The similar reduction in both PCNA and Ki-67 suggests that non-canonical NF-κB signalling acts to promote proliferation either independently of cell cycle regulation or at a cell cycle checkpoint prior to S phase entry.

In order to investigate the mechanism by which non-canonical NF-κB could be enhancing proliferation, the expression of several genes was tested by qPCR in ECs exposed to low shear stress following silencing of either *NFKB2* or *RELB*. These genes

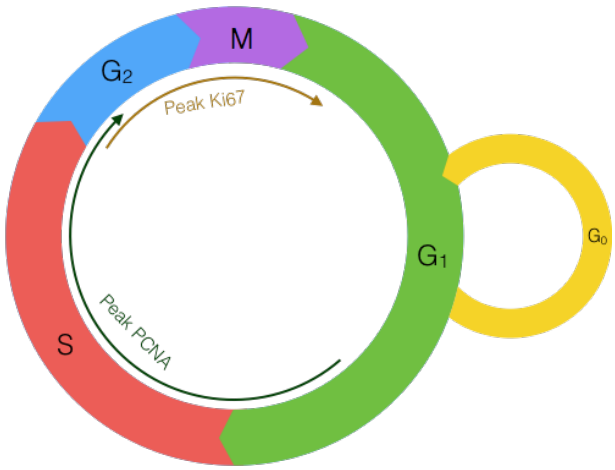

Figure 5.10: Expression of Ki-67 and PCNA proliferation markers over the cell cycle. A schematic of the cell cycle showing the relative lengths of each phase along with the peak expression two markers of proliferation. Ki-67 peaks during G_2 and M phase, while PCNA is increased in late G_1 and S phase.

were chosen due to their previous association with non-canonical NF-κB signalling in the literature (Burkitt et al., 2015; Ramachandiran et al., 2015; Rocha et al., 2003; Schumm et al., 2006), and do not represent an exhaustive list of proliferation genes. Nevertheless, these data showed a significant increase in the expression of p21, a negative regulator of proliferation, upon silencing of *NFKB2*. A second negative regulator, *REDD1*, trended towards an increase, but was not statistically significant. Western blotting for p21 in knockdown samples confirmed this observation, with a significant increase in p21 protein following silencing of *NFKB2*. REDD1 levels were not tested due to issues with antibody specificity.

While non-canonical NF-κB signalling has not been previously studied in the context of endothelial dysfunction, several published papers provide further evidence which combined lend support to the conclusion that p100/p52 can drive proliferation by negatively regulating p21 expression in cells exposed to low shear stress. Firstly, p21 expression is known to be regulated by shear stress in ECs. Exposure of HUVECs to unidirectional high shear stress leads to a gradual increase in p21 protein expression over a period of hours, resulting in a suppression of proliferation (Akimoto et al., 2000).

The anti-proliferative protein p21 is a cyclin-dependent kinase (CDK) inhibitor, responsible for suppressing proliferation by inhibiting several CDKs at various points in the cell-cycle and thus stalling checkpoint progression. In particular p21 has been shown to inhibit G_1 to S phase progression, maintain cells in the quiescent G_0 phase, and act alongside p53 to promote senescence (Dutto et al., 2014). This is consistent with the functional effect seen *in vitro*; loss of PCNA positivity and Ki-67 expression can be explained by ECs being blocked in either G_0 or G_1 phase, or being senescent upon p21 induction. Enhanced EC proliferation under low shear stress coincides with a shift from G_0/G_1 to G_2/M phase cells (Guo et al., 2007), supporting the idea that loss of p21 at these sites is causative of this change. Thus, enhanced non-canonical NF-κB signalling may be a key factor in dampening p21 expression under low shear stress, leading to elevated proliferation.

Additionally, non-canonical NF-κB signalling has been shown to be an inducer of proliferation in other contexts. Knockdown of *NFKB2* or *MAP3K14* (NIK) resulted in reduced cell number and increased senescence in melanoma cells (De Donatis et al., 2015), while silencing of RelB reduced embryonic stem cell proliferation and differentiation (Yang et al., 2010). Moreover, exposure of HUVECs to microparticles containing CD40L isolated from human carotid endarterectomy samples stimulated EC proliferation in a CD40-dependent manner (Leroyer et al., 2008), suggesting that non-canonical NF-κB signalling could play a role. The role of non-canonical NF-κB subunits

in the regulation of p21 has also been previously studied. While in complex with HDAC1 and p53, p52 has been shown to bind to the p21 promoter, repressing its expression (Schumm et al., 2006). Additionally, *RELB* silencing has been shown to induce p21 protein expression in fibroblasts, though interestingly in that study, *NFKB2* silencing had no effect on p21 protein, and neither knockdown altered mRNA expression (Iannetti et al., 2014).

Studies which have investigated mechanisms of p21 regulation by shear stress have also found mechanisms involving the same molecules, although these run opposed by implicating p53 as an initiator of p21 transcription under high shear stress through HDAC1 or HDAC3-mediated deacetylation and activation (Zeng et al., 2003, 2006). Investigation of the role of HDACs in the putative non-canonical NF-κB regulation of p21 is important to understand the pathway. The conflicting roles for these proteins may suggest a context dependent regulation of p21 expression depending on potential p53 activity. Interestingly, p53 expression has also been shown to be differentially regulated within the aortic arch, with higher expression at the inner curvature. Levels of expression were found to be heterogeneous between cells exposed to shear stress *in vitro* but strongly correlated with p21 expression, lending evidence to the suggestion that they may act within the same pathway (Warboys et al., 2011).

5.12.4 Implications for atherogenesis

Non-canonical NF-κB signalling has been shown here to be an important regulator of EC proliferation specifically in cells exposed to low shear stress. As the development of atherosclerosis is also predominantly localised to regions of the vasculature exposed to this haemodynamic environment, speculation about the role of this pathway can be put forward.

Some studies have found a correlation between altered low shear stress proliferation and the development of atherosclerosis, although its effect is unclear. Schober et al. (2014) identified a micro-RNA (miR-126-5p) responsible for repressing the anti-proliferative protein Dlk1 (delta-like 1 homolog), which was downregulated by low shear stress resulting in a net increase in proliferation at sites prone to atherosclerosis. Deletion of this micro-RNA in mice was found to impede EC repair in response to denudation, as well as lead to increased lesion size in *Mir126*$^{-/-}$*Apoe*$^{-/-}$ double knockout animals. The authors conclude that EC proliferation at sites of low shear stress protects from atherogenesis by maintaining a pool of replicative cells which can replace dead or injured cells quickly. In contrast, we have observed an opposing role; analysis of endothelial specific *Gata4* or *Twist1* knockout mice revealed a loss of proliferation at the inner curvature of the aortic arch, and a decrease in lesion size (Mahmoud et al., 2016). This

suggests that proliferation at low shear stress is pathogenic, and is supported by *in vitro* data showing loss of proliferation by overexpression of p21 in ECs exposed to low shear stress corresponded with a significant reduction in monocyte adhesion (Obikane et al., 2010) and that excessive proliferation increases endothelial permeability to LDL (Cancel and Tarbell, 2011). These studies do not directly investigate the effect of proliferation on the development of atherosclerosis, instead proliferation is correlated with protection or disease. Thus, the role of non-canonical NF-κB regulated proliferation in atherogenesis is as yet unclear. Further study could focus on determining whether the induction of proliferation conferred by non-canonical NF-κB signalling in ECs exposed to low shear stress results in an increase or decrease in lesion size or an alteration in plaque composition.

5.12.5 Summary

In summary, the expression of NF-κB subunits p100, p52 and RelB, which are known to be involved in the non-canonical pathway of NF-κB activation, are regulated by exposure to different shear stress environments. Expression both *in vivo* and *in vitro* is decreased by exposure to high shear stress, and activity was also found to follow the same pattern. This may be due to the role of JNK or TRAF3 activity, although this was untested. Silencing of *NFKB2* in HUVECs exposed to shear stress and analysis of the aortic arches of *Nfkb2*$^{-/-}$ mice revealed that EC proliferation was significantly reduced specifically in cells exposed to low shear stress. An upregulation of the antiproliferative genes p21 and *REDD1* following silencing of *NFKB2* or *RELB* suggests this is the mechanism for this reduction in proliferation, and as p21 is known to be increased at atheroprotected sites of the vasculature this suggests that non-canonical NF-κB signalling may play an important role in controlling the difference in EC proliferation between sites exposed to low and high shear stress. EC proliferation has been identified as being altered as a consequence of gene knockout in other studies which involve changes in atherosclerotic lesion size, thus non-canonical NF-κB signalling may be an important signalling mechanism which can control atherogenesis by modulating the proliferation of ECs.

6. General discussion

The research carried out during this PhD has focused on the role of NF-κB signalling in controlling EC phenotype and gene expression in the context of atherosclerosis. I have investigated the contribution that biomechanical forces have on regulating both canonical and non-canonical NF-κB and how these pathways can regulate EC gene expression to alter the development of atherosclerosis. The two main projects are discussed here.

6.1 Investigation into the regulation and function of Cezanne in vascular endothelium.

Prior to the completion of this PhD, the function of the deubiquitinase Cezanne had not been studied in the context of atherosclerosis. It was known to be a negative regulator of both canonical (Enesa et al., 2008a; Luong et al., 2013) and non-canonical (Hu et al., 2013) NF-κB signalling, in ECs and B cells respectively, as well as an enhancer of HIF-1α and HIF-2α (Bremm et al., 2014; Moniz et al., 2015). Its expression had also been found to be elevated by treatment with several NF-κB activating molecules, (Enesa et al., 2008a; Hu et al., 2013), by exposure to hypoxia (Luong et al., 2013) and in ECs exposed to high shear stress both *in vivo* (Passerini et al., 2004) and in culture (Enesa et al., 2008a). However, whether these factors were important for controlling Cezanne expression *in vivo* at sites prone to or protected from atherosclerosis was not known, nor was the function of Cezanne in controlling NF-κB in EC dysfunction and atherogenesis.

This study tested the hypotheses that Cezanne expression was differentially regulated in ECs from regions of the vasculature with a predilection to atherosclerosis development, that this regulation was as a result of the differences in shear stress, cytokines or oxygen availability experienced by these cells, and that the function of Cezanne was to inhibit both branches of NF-κB signalling, thus resulting in a dampening of atherosclerotic lesion development at the regions in which it was expressed.

The expression of Cezanne in ECs was determined *in vivo* at sites prone to and protected from atherosclerosis, as well as *in vitro* following the application of shear stress combined with NF-κB-activating stimuli or hypoxia. Cezanne function was probed by investigating NF-κB activity and target gene expression *in vitro* in cells depleted of Cezanne by gene silencing. Its role *in vivo* was also investigated, using Cezanne knockout mice to investigate adhesion molecule expression and EC phenotype, and double knockout mice also lacking the LDL receptor were used as a model for atherosclerosis development to probe Cezanne contribution to disease.

The main conclusions were that Cezanne expression was elevated in ECs from atheroprone regions of the vasculature as a result of the effects of low shear stress. Exposure to low shear stress *in vitro* enhanced Cezanne expression, but the addition of NF-κB-activating molecules or hypoxia did not further increase Cezanne expression indicating that low shear stress is the primary regulator of its elevation. Its function *in vitro* was found to be inhibition of NF-κB activity, measured by phosphorylation at serine 536 of RelA, although interestingly this did not alter gene expression of several NF-κB target genes. Processing of p100 to p52, or HIF stability was also found to be unaffected. In Cezanne knockout mice, the expression of the NF-κB target gene VCAM-1 was also not changed from wild-type, and neither was EC proliferation. Analysis of lesion size in *Otud7b*$^{-/-}$*Ldlr*$^{-/-}$ mice fed a high-fat diet for six weeks, revealed no difference in comparison to *Ldlr*$^{-/-}$ controls. Thus, it was concluded that Cezanne is not responsible for controlling the development of atherosclerosis.

These conclusions point to a model (Figure 6.1) where low shear stress activates expression of RelA in ECs, leading to inflammation and thus atherosclerosis, but in addition the expression of Cezanne is also enhanced. Cezanne acts to suppress phosphorylation of RelA at serine 536, which does not alter the expression of adhesion molecules or inflammatory cytokines important in atherogenesis, but may alter other cellular pathways which have not been identified.

6.2 Discovery of the role of non-canonical NF-κB in ECs exposed to shear stress

While testing the role of Cezanne in regulating p100 processing to p52 in ECs exposed to shear stress, an interesting additional finding was that the expression of non-canonical NF-κB subunits p100, p52 and RelB were also strongly induced by exposure to low shear stress *in vitro*. Surprisingly, when searching the literature, the expression of *NFKB2* had been identified as being expressed at an atheroprone site in an *in vivo* microarray study (Passerini et al., 2004), but no further research had been done to identify the regulation by shear stress, nor the function of this pathway in the endothelium.

The primary focus of most non-canonical NF-κB research is in B cell development, lymphoid organogenesis and cancer where it can regulate cellular proliferation (Sun, 2011), while studies in other cell types remain limited. However, activation of the pathway by processing of p100 to p52 is known to be under the regulation of cytokines such as CD40L, which are important in atherogenesis (Lutgens et al., 1999). The hypothesis to be tested was that non-canonical NF-κB components were elevated in

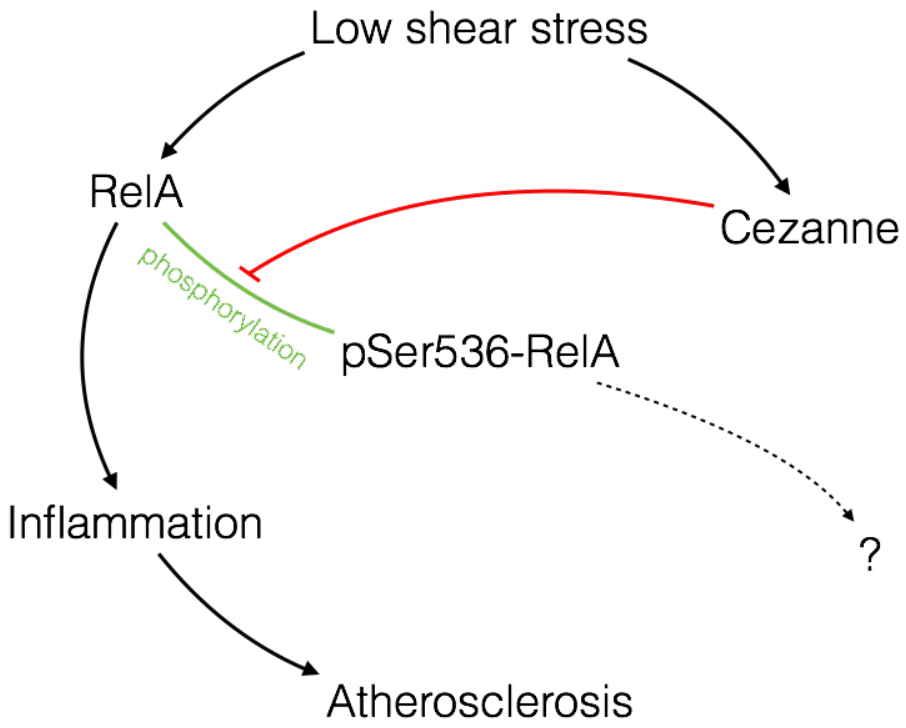

Figure 6.1: A model for the regulation and function of Cezanne in atherosclerosis. Low shear stress results in the induction of RelA expression, which enhances transcription of inflammatory cytokines and adhesion molecules and drives the initiation of atherosclerosis. Cezanne is also induced by low shear stress, and inhibits the phosphorylation of RelA at serine 536. This phosphorylation does not alter NF-κB activation of inflammatory genes but may have another role which has not been discovered.

expression by low shear stress, and this was responsible for enhancing EC proliferation at these sites.

This was tested by measuring the expression of *NFKB2* and *RELB in vivo* at sites of low and high shear stress, as well as in ECs exposed to shear stress *in vitro*. Silencing of *NFKB2 in vitro* was found to specifically reduce proliferation in ECs exposed to low shear stress, and this was recapitulated *in vivo* in the aortic arches of *Nfkb2*$^{-/-}$ mice. Analysis of putative non-canonical NF-κB target genes by qPCR in ECs depleted of *NFKB2* or *RELB* revealed enhanced p21 expression when *NFKB2* was silenced.

p21 is a CDK inhibitor responsible for stalling the cell cycle and preventing proliferation (Dutto et al., 2014). Thus, these conclusions suggest a model (Figure 6.2) where enhanced EC proliferation at sites of low shear stress is as a result of p21 loss, mediated by inhibition of transcription by p52 and/or RelB. This conclusion is supported by previous research observing that p21 expression is enhanced under high shear stress in ECs (Akimoto et al., 2000; Zeng et al., 2003, 2006), by evidence that CD40 ligation can induce EC proliferation (Dormond et al., 2008; Melter et al., 2000) and observations that p52 can act to repress p21 expression in complex with HDACs and p53 (Schumm et al., 2006). These findings shed new light on the importance of non-canonical NF-κB signalling in EC dysfunction, and suggests the pathway is important in regulating the initiation of atherosclerosis, as aberrant proliferation has been associated with disease previously (Cancel and Tarbell, 2011; Mahmoud et al., 2016; Obikane et al., 2010).

6.3 NF-κB signalling regulates many cellular functions in ECs exposed to shear stress.

ECs play a critical role in regulating the initiation of atherogenesis and further lesion development. At regions of the vasculature prone to atherosclerosis, EC sensing of low magnitude oscillating shear stress leads to dysfunction of these cells. Inflammatory activity is enhanced, with elevated expression of secreted chemokines and cell-surface adhesion molecules which collaborate to attract circulating monocytes and other leukocytes to the vessel wall and promote their transmigration into the subendothelial space where they can begin to take up LDL from the bloodstream (Warboys et al., 2011). Furthermore, this process is enhanced by increased proliferation and apoptosis of ECs at sites of low shear; cells undergoing mitosis or apoptosis increase the permeability of the endothelial monolayer and allow further transport of leukocytes and LDL, exacerbating disease (Cancel and Tarbell, 2011; Weinbaum et al., 1985).

Previous work has demonstrated that NF-κB signalling is a central regulator of many of these events. Upon exposure to the haemodynamics found at sites prone to

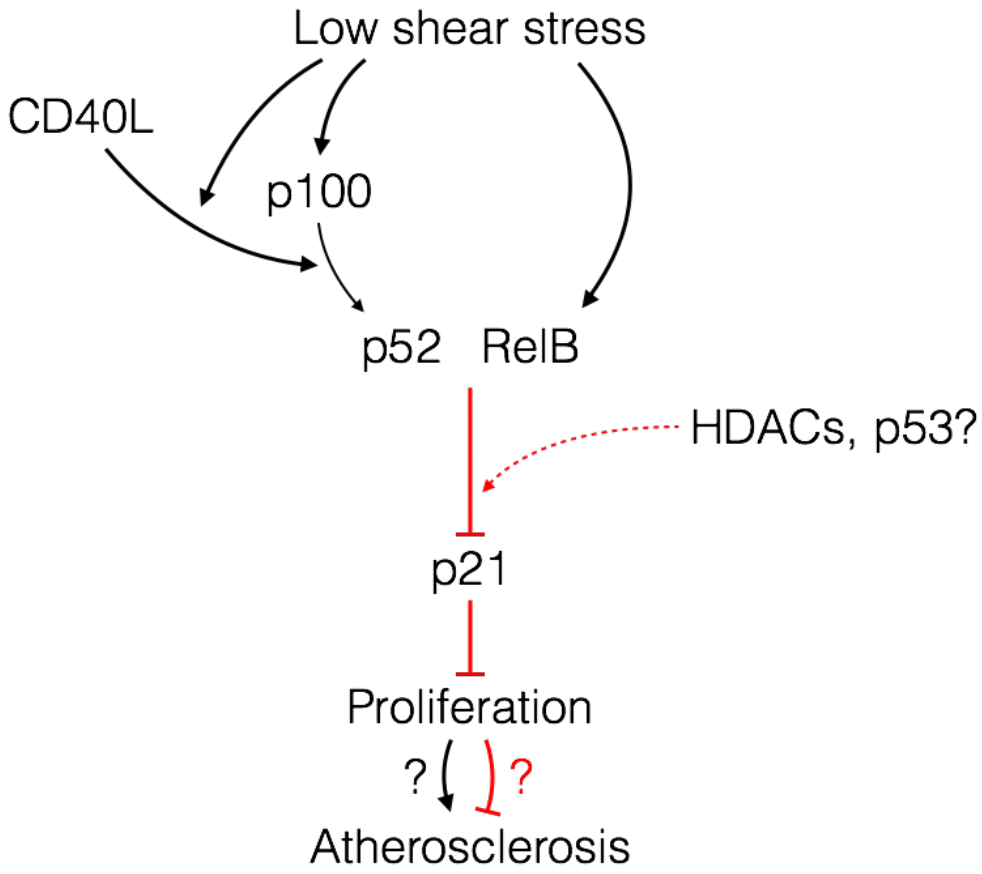

Figure 6.2: A diagram explaining the mechanism by which non-canonical NF-κB induces EC proliferation at sites of low shear stress. Low shear stress promotes expression of non-canonical NF-κB subunits p100 and RelB. Processing of the inactive p100 subunit to active p52 proceeds basally, and is enhanced by low shear stress and stimulation with CD40L. Active p52 is capable of inhibiting the transcription of p21, by a mechanism which may involve HDACs or p53. Lower p21 expression at low shear stress sites leads to enhanced proliferation by removing a negative regulator of cell cycle progression. This increased proliferation may be responsible for positively or negatively regulating the development of atherosclerosis.

atherosclerosis, expression of the NF-κB subunit RelA is enhanced, priming cells here for an inflammatory response (Cuhlmann et al., 2011; Hajra et al., 2000). Transcriptional targets of NF-κB in ECs include the secreted cytokines MCP-1 and IL-8, as well as adhesion molecules VCAM-1, ICAM-1 and E-selectin (Van der Heiden et al., 2010). Expression of these targets are all enhanced under low shear stress. Furthermore, there is evidence to suggest that NF-κB signalling can also be involved in cytoprotective activity by suppressing apoptosis. Transcription of antiapoptotic genes such as GADD45β is controlled by NF-κB signalling (Partridge et al., 2007; De Smaele et al., 2001), and inhibition of NF-κB has also been shown to increase apoptosis in response to vascular endothelial growth inhibitor (Grimaldo et al., 2009).

The experiments presented in this thesis do not show a role for Cezanne in regulating these pathways, nor on atherosclerotic lesion size. However, unpublished data recently generated by the lab has uncovered a novel mechanism by which Cezanne can regulate EC proliferation via NF-κB and HIF-1α. While, silencing of Cezanne did not confer an effect on HIF stability (Figure 4.6), overexpression of a dominant negative mutant Cezanne (possessing a cysteine to serine substitution within its active site (Enesa et al., 2008a)) in ECs resulted in a marked reduction in HIF-1α protein levels. NF-κB activity was found to be responsible for low shear stress induction of HIF, which consequently led to increased proliferation and inflammation (Feng S, Bowden N, Fragiadaki M and Evans PC, unpublished). It is likely that the discrepancy between the dominant negative Cezanne and silencing is due to residual levels of Cezanne protein following siRNA treatment that can still function to stabilise HIF, whereas the dominant negative Cezanne resulted in a complete abolition of function. This mechanism links canonical NF-κB signalling to EC proliferation at low shear stress sites and further underlines the importance of the pathway in EC dysfunction (Figure 6.3).

These functions of NF-κB are associated with the canonical pathway, primarily involving the action of RelA. In this thesis, I have identified an additional role for NF-κB in the regulation of EC dysfunction. Upregulation of non-canonical NF-κB at sites of low shear stress was responsible for enhanced proliferation in these regions. This finding sheds light on the importance of understanding the additional role of the previously unstudied non-canonical pathway in the initiation of atherosclerosis. Non-canonical NF-κB has also been attributed to enhanced apoptosis (Burkitt et al., 2015; Saxon et al., 2016) and cellular senescence (De Donatis et al., 2015; Iannetti et al., 2014), which may also contribute to EC dysfunction, but were not tested in this study.

Combined, both branches of NF-κB signalling influence a broad range of endothelial processes involved in the initiation of atherosclerosis. This thesis contributes knowledge

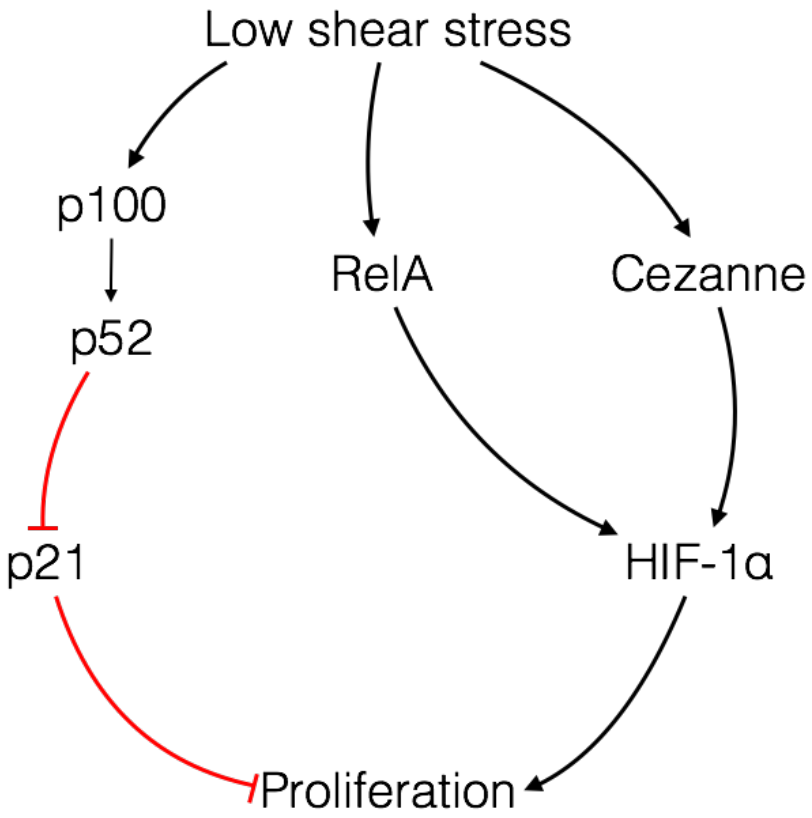

Figure 6.3: A diagram explaining how canonical and non-canonical NF-κB signalling can combine to enhance EC proliferation at sites of low shear stress. Non-canonical NF-κB signalling can contribute to EC proliferation by downregulating the CDK inhibitor p21 at sites of low shear. In addition, HIF-1α expression is driven by canonical NF-κB signalling at sites of low shear stress and stabilised by Cezanne. This pathway drives proliferation by inducing glycolysis genes.

of the function of non-canonical NF-κB into this regulatory network, while also raising questions about the unknown role of Cezanne and phosphorylated RelA in regulating cellular mechanisms other than inflammatory gene expression in ECs.

6.4 Future work

In order to possess a full picture of the roles of Cezanne and non-canonical NF-κB signalling in EC dysfunction and atherosclerosis, further experiments are required to test additional hypotheses which have been raised by the stated conclusions.

6.4.1 The function of Cezanne-dependent inhibition of RelA phosphorylation.

Perhaps the most difficult conclusion to explain was Cezanne inhibition of RelA phosphorylation conferring no discernible effect on NF-κB target gene expression as measured by qPCR. However, limitations in the study design meant that only a limited number of genes were tested, and at a single time-point after 72 hours of exposure to shear stress. Phosphorylation of serine 536 of RelA has been implicated in having several effects on NF-κB activity, including altering the dynamics of nuclear import, reducing the time spent bound to DNA and altering its target genes (Bohuslav et al., 2004; Lawrence et al., 2005; Moles et al., 2013; Sasaki et al., 2005). Thus, full elucidation of the role of Cezanne in regulating canonical NF-κB signalling in low shear stress may require more detailed analysis of NF-κB kinetics. Time-lapse microscopy in conjunction with fluorescently tagged RelA has previously been employed to study NF-κB nuclear oscillations (Nelson et al., 2004). Utilising this technique to study the effect of Cezanne silencing and shear stress on RelA transport may reveal differences in the dynamics of NF-κB that could inform its function.

In addition, unbiased screening approaches could be utilised to determine whether the expression of genes which were not included in the study were altered by Cezanne silencing or phosphorylation of RelA. Microarray or RNA sequencing analysis of transcripts from Cezanne depleted ECs in culture may be used for this, or RNA from the carotid arteries of *Otud7b*$^{-/-}$ mice after undergoing partial carotid ligation (Ni et al., 2010). This approach will allow the discovery of novel targets and avoid the technical limitations of primer design for specific targets.

6.4.2 The role of Cezanne in the development of atherosclerosis.

From the lack of difference in atherosclerotic lesion size seen between *Otud7b*$^{-/-}$*Ldlr*$^{-/-}$ and *Ldlr*$^{-/-}$ animals, I concluded that Cezanne did not function to alter the development of plaques. However, there are some reasons why this may not be the complete story, and further experiments could be used to clarify the results. Firstly, this study used a relatively short period of high-fat diet feeding at only six weeks. This served to test

whether Cezanne regulates early atherogenesis, but the effect of enhanced RelA phosphorylation may not be seen until later in plaque development. Maintaining these animals on a high-fat diet for longer periods may show an effect on later stages of lesion development. Secondly, lesion size as measured in flat tissue was the only metric used to assess the function of Cezanne in regulating the severity of atherosclerosis. Many genes are known to influence the development of atherosclerosis by altering plaque composition and not necessarily absolute lesion coverage. Histological analysis of the difference in lesion composition between *Otud7b*$^{-/-}$*Ldlr*$^{-/-}$ and *Ldlr*$^{-/-}$ animals may reveal a previously undetected effect of Cezanne loss on atherosclerosis.

6.4.3 Investigating the molecular mechanism behind p52 mediated p21 inhibition.

While previous studies have also shown inhibition of p21 by non-canonical NF-κB, it is not clear whether these mechanisms are at play in ECs exposed to shear stress. Elevated p21 under high shear stress has been found to occur as a result of HDACs and p53 promoting transcription (Zeng et al., 2003, 2006), but transcriptional repression of p21 has also been seen with these molecules in combination with p52 (Schumm et al., 2006). Immunoprecipitation studies would help to understand whether this inhibition was as a result of direct DNA binding, and which other molecules were involved. ChIP could be used with cells exposed to shear stress and silencing of HDACs or p53 to test whether p52 binds directly to the p21 promoter and if this binding is dependent on these molecules. Moreover, if ChIP-sequencing was utilized, many novel DNA binding sites of p52/RelB could be elucidated and help to inform further research into the function of non-canonical NF-κB, perhaps in apoptosis or inflammation

6.4.4 Determining the function of non-canonical NF-κB in atherosclerosis.

An unanswered question about non-canonical NF-κB signalling in ECs is what role does the pathway play in regulating the development of atherosclerosis. Enhanced proliferation at low shear stress has been associated with both increased and decreased lesion development (Cancel and Tarbell, 2011; Mahmoud et al., 2016; Schober et al., 2014), which may be due to differences in the mechanism controlling the change in proliferation. Aside from enhancing proliferation, non-canonical NF-κB signalling may also regulate other pathways involved in atherogenesis. To test the effects of the pathway on the lesion development, *Nfkb2*$^{-/-}$ mice could be crossed with *Ldlr*$^{-/-}$ or *Apoe*$^{-/-}$ mice, generating double knockouts. Alternatively, recent advances have resulted in the development of an adenoviral vector expressing a gain of function mutant of proprotein convertase subtilisin/kexin type 9 (PCSK9) which can be used to infect mice and confer susceptibility to atherosclerosis by directing LDLR for degradation (Bjørklund et al.,

2014). Feeding a high-fat diet to these animals and measuring plaque development and composition will provide valuable information about the role of the non-canonical NF-κB pathway.

6.4.5 Modulation of non-canonical NF-κB activity as a potential therapeutic strategy.

Upon determining the positive or negative effects that non-canonical NF-κB has on the development of atherosclerosis, the pathway may be an appropriate target for clinical intervention in the prevention of disease. If protective, treatment strategy may involve stimulation of p100 processing by a natural ligand. CD40L and LT-β have been shown to have inflammatory effects on ECs (Chakrabarti et al., 2007; Gene et al., 2008), so may not be suitable, however other non-canonical NF-κB stimuli may not confer the same response. If the non-canonical NF-κB pathway drives atherogenesis, then chemical inhibition of the pathway could be employed. SN52 is a small peptide inhibitor of p52/RelB nuclear import, through competitive binding of the nuclear import proteins (Xu et al., 2008). This could be employed to specifically block non-canonical NF-κB signalling and alleviate its effects. As NF-κB signalling is crucial in the normal function of immune cells, off-target effects could be minimised by targeting delivery to ECs at sites of low shear stress (Chung et al., 2016).

6.5 Closing remarks.

Signalling to and from NF-κB involves a large network of interacting members, with multiple levels of complexity. From the variety of cell surface receptors, signals are channelled into two main branches of signalling, which can initiate the transcription of numerous target genes depending on context. From the experiments in this thesis and previous work, it is clear that NF-κB signalling plays a key role in the alteration of many aspects of endothelial cell physiology which can promote the development of atherosclerosis, although there are still many important unanswered questions about the function of the pathway which can hopefully be addressed in the coming years.

7. Appendix

Reagent	Company	Volume (ml)	Stock Concentration	Final Concentration
Sterile H_2O	N/A	425		
10X M199	Life Technologies	50		
NaHCO3	Sigma	10	75 mg/ml	1.5 mg/ml
L-glutamine	Lonza	5	200 mM	2 mM
Penicillin/streptomycin	Life Technologies	5	100 U/ml & 100 µg/ml	1 U/ml & 1 µg/ml
Amphotericin B	Fisher Scientific	5	250 µg/ml	2.5 µg/ml

Appendix 7.1: Components of incomplete M199.

Reagent	Company	Volume (ml)	Stock Concentration	Final Concentration
Incomplete M199	Appendix 8.1	160		
Foetal bovine serum	Life Technologies	20		10%
Newborn calf serum	Life Technologies	20		10%
Heparin sodium salt	Sigma	0.2	90 mg/ml	90 µg/ml
EC growth supplement	Millipore	0.1	10 mg/ml	5 µg/ml

Appendix 7.2: Components of complete M199.

Target gene	Sequence
Non-targeting “scrambled” control	UGGUUUACAUGUCGACUAA
	UGGUUUACAUGUUGUGUGA
	UGGUUUACAUGUUUUCUGA
	UGGUUUACAUGUUUUCCUA
OTUD7B	CCGAUUGGCCAGUGUAAUU
	CCGAGUGGCUGAUUCCUAU
	GCAUCUAGGUACCAAUGGA
	UAACGGAGGGAGCAAGUAU
NFKB2	CGAACAGCCUUGCAUCUAG
	GUAGACACGUACCGACAGA
	AGACGAGUGUGGUGAGCUU
	GAUCUGCGCCGUUUCUGUG
RELB	CUGCGGAUUUGCCGAAUUA
	GCACAGAUGAAUUGGAGAU
	CCAUUGAGCGGAAGAUUCA
	GCCCGUCUAUGACAAGAAA

Appendix 7.3: List of siRNA molecules used.

Gene	Sense sequence	Antisense sequence
OTUD7B (Cezanne)	GAGTTGAGAAGGAAGCGTT	CACTCCTTCTGCCATTCATC
VCAM-1	CATTGACTTGCAGCACCACA	AGATGTGGTCCCCTCATTCG
ICAM-1	CACAAGCCACGCCTCCCTGAACCTA	TGTGGGCCTTTGTGTTTTGATGCTA
E-selectin	GCTCTGCAGCTCGGACAT	GAAAGTCCAGCTACCAAGGGAAT
SOD2	CATCAGCGGTAGCACCAGCA	GCGTGGTGCTTGCTGTGGTG
BCL2	GCTGCACCTGACGCCCTTCA	CCGTACAGTTCCACAAAGGC
GADD45B	TGGAGGAGCTTTTGGTGGC	AAGTGGATTTGCAGGGCGAT
CCND1	ATGAACTACCTGGACCGCTT	TTCAATGAAATCGTGCGGGG
CCNG2	GAAAGCTTGCAACTGCCGAC	CAAATTGAGAAGGCACAAGGCT
REDD1	GTTCATCAGCAAACGCCCTG	GACACCCCATCCAGGTAAGC
p21	GATGTCCGTCAGAACCCATG	TTAGGGCTTCCTCTTGGAGA
GADD45A	GCTGGTGACGAATCCACAT	ATCCATGTAGCGACTTTCCC
IL-8	TGCCAAGGAGTGCTAAAG	CTCCACAACCCTCTGCAC
p53	GCCCCCAGGGAGCACTA	GGGAGAGGAGCTGGTGTTG
HPRT	TTGGTCAGGCAGTATAATCC	GGGCATATCCTACAACAAAC
MCP1	GCAGAAGTGGGTTCAGGATT	TGGGTTGTGGAGTGAGTGTT
eNOS	TGAAGCACCTGGAGAATGAG	TTGACCATCTCCTGATGGAA
(Sus scrofa) NFKB2	CTGAAGCCGGTTATCTCCCA	ATAAACCTCATCTCCACCCCG
(Sus scrofa) RELB	GACAGCTACGGAGTGGACAAG	CGTCGTTTGCTCTCGATGC
(Sus scrofa) B2M	GGTTCAGGTTTACTCACGCCAC	CTTAACTATCTTGGGCTATTCG
NFKB2	GCCGAAAGACCTATCCCACT	TTAGTCACATGCAGGACACCC
RELB	ATTGACCCCTACAACGCTGG	AAGTGGATTTGCAGGGCGAT

Appendix 7.4: List of primers used.

Antibody	Company	Use	Concentration
Cezanne	ProteinTech	WB	1/3000
		EF	5 µg/ml
Cezanne (C terminal)	Human Protein Atlas	WB	1/1000
RelA	Santa Cruz Biotechnology	WB	1/5000
		IF	1/1000
pSer536-RelA	Cell Signaling	WB	1/1000
p100/p52	Millipore	WB	1/3000
RelB	Cell Signaling	WB	1/1000
PDHX	Santa Cruz Biotechnology	WB	1/6000
PCNA	Abcam	IF	1/500
VE-cadherin	BD Pharmingen	IF	1/500
VCAM-1	Abcam	EF	5 µg/ml
ICAM-1	ProteinTech	EF	5 µg/ml
Ki-67	Abcam	WB	1/1000
		EF	5 µg/ml
Goat anti-rabbit Alexa Fluor 488	Life Technologies	IF	variable
Goat anti-rabbit Alexa-Fluor 568	Life Technologies	IF	variable
Goat anti-rat Alexa Fluor 568	Life Technologies	IF	variable
Goat anti-rabbit horse radish peroxidase	Dako	WB	variable
Goat anti-mouse horse radish peroxidase	Dako	WB	variable

Appendix 7.5: Antibodies used.
WB = Western blotting;
IF = immunofluorescence staining;
EF = en face immunofluorescence staining.

Reagent	Volume (ml)
Distilled H_2O	180
1 M Tris-HCl (pH 8.5)	10
10% Tween-20	10
0.5 M EDTA (pH 8.0)	0.4

Appendix 7.6: Composition of ear-clip lysis buffer.

Reagent	Company	Volume per reaction (µl)
Ear-clip DNA	N/A	10
H_2O	N/A	8
Q5 Reaction Buffer	New England Biolabs	5
Sense primer	Appendix 8.4	0.625
Anti-sense primer	Appendix 8.4	0.625
dNTPs	Thermo Scientific	0.5
Q5 DNA polymerase	New England Biolabs	0.25

Appendix 7.7: Components of the PCR reaction used for genotyping.

Ingredient	Percentage (w/w)
Sucrose	33.94
Anhydrous milk fat	20.00
Casein	19.50
Maltodextrin	10.00
Corn starch	5.00
Cellulose	5.00
Corn oil	1.00
Calcium carbonate	0.40
L-cysteine	0.30
Choline bitartrate	0.20
Cholesterol	0.15
Antioxidant	0.01
AIN-76A-MX	3.50
AIN-76A-VX	1.00

Appendix 7.8: Composition of Western diet.

8. References

Agewall, S. (2006). Matrix metalloproteinases and cardiovascular disease. Eur. Heart J. *27*, 121–122.

Akhtar, S., Hartmann, P., Karshovska, E., Rinderknecht, F.A., Subramanian, P., Gremse, F., Grommes, J., Jacobs, M., Kiessling, F., Weber, C., Steffens, S., and Schober, A. (2015). Endothelial Hypoxia-Inducible Factor-1α Promotes Atherosclerosis and Monocyte Recruitment by Upregulating MicroRNA-19a. Hypertension *66*, 1220–1226.

Akimoto, S., Mitsumata, M., Sasaguri, T., and Yoshida, Y. (2000). Laminar Shear Stress Inhibits Vascular Endothelial Cell Proliferation by Inducing Cyclin-Dependent Kinase Inhibitor p21Sdi1/Cip1/Waf1. Circ. Res. *86*, 185–190.

Amir, R.E., Haecker, H., Karin, M., and Ciechanover, A. (2004). Mechanism of processing of the NF-kappa B2 p100 precursor: identification of the specific polyubiquitin chain-anchoring lysine residue and analysis of the role of NEDD8-modification on the SCF(beta-TrCP) ubiquitin ligase. Oncogene *23*, 2540–2547.

Arenzana-Seisdedos, F., Turpin, P., Rodriguez, M., Thomas, D., Hay, R.T., Virelizier, J.L., and Dargemont, C. (1997). Nuclear localization of I kappa B alpha promotes active transport of NF-kappa B from the nucleus to the cytoplasm. J. Cell Sci. *110*, 369–378.

Baldwin, A.S. (2012). Regulation of cell death and autophagy by IKK and NF-??B: Critical mechanisms in immune function and cancer. Immunol. Rev. *246*, 327–345.

Bando, M., Yamada, H., Kusunose, K., Fukuda, D., Amano, R., Tamai, R., Torii, Y., Hirata, Y., Nishio, S., Yamaguchi, K., Soeki, T., Wakatsuki, T., and Sata, M. (2015). Comparison of carotid plaque tissue characteristics in patients with acute coronary syndrome or stable angina pectoris: assessment by iPlaque, transcutaneous carotid ultrasonography with integrated backscatter analysis. Cardiovasc. Ultrasound *13*, 34.

Basak, S., Kim, H., Kearns, J.D., Tergaonkar, V., O'Dea, E., Werner, S.L., Benedict, C. a, Ware, C.F., Ghosh, G., Verma, I.M., and Hoffmann, A. (2007). A fourth IkappaB protein within the NF-kappaB signaling module. Cell *128*, 369–381.

Baumeister, W., Walz, J., Zühl, F., and Seemüller, E. (1998). The proteasome: paradigm of a self-compartmentalizing protease. Cell *92*, 367–380.

Beinke, S., and Ley, S.C. (2004). Functions of NF-κB1 and NF-κB2 in immune cell biology. Biochem. J. *382*, 393–409.

Bénézech, C., Mader, E., Desanti, G., Khan, M., White, A., Ware, C.F., Anderson, G., and

Caamaño, J.H. (2013). NIH Public Access. *37*.

Bennett, M.R., Sinha, S., and Owens, G.K. (2016). Vascular Smooth Muscle Cells in Atherosclerosis. Circ. Res. *118*, 692–702.

Vanden Berghe, W., De Bosscher, K., Plaisance, S., Boone, E., and Haegeman, G. (1999). The Nuclear Factor-kappa B engages CBP/p300 and Histone Acetyltransferase Activity for Transcriptional Activation of the Interleukin-6 Gene Promoter. J Biol Chem *274*, 32091–32098.

Bertrand, M.J.M., Milutinovic, S., Dickson, K.M., Ho, W.C., Boudreault, A., Durkin, J., Gillard, J.W., Jaquith, J.B., Morris, S.J., and Barker, P.A. (2008). cIAP1 and cIAP2 facilitate cancer cell survival by functioning as E3 ligases that promote RIP1 ubiquitination. Mol. Cell *30*, 689–700.

Biggs, P., Wooster, R., Ford, D., Chapman, P., Mangion, J., Quirk, Y., Easton, D.F., Burn, J., and Stratton, M.R. (1995). Familial cylindromatosis (turban tumour syndrome) gene localised to chromosome 16q12-q13: evidence for its role as a tumour suppressor gene. Nat. Genet. *11*, 441–443.

Bjørklund, M.M., Hollensen, A.K., Hagensen, M.K., Dagnæs-Hansen, F., Christoffersen, C., Mikkelsen, J.G., and Bentzon, J.F. (2014). Induction of atherosclerosis in mice and hamsters without germline genetic engineering. Circ. Res. *114*, 1684–1689.

Bohuslav, J., Chen, L.F., Kwon, H., Mu, Y., and Greene, W.C. (2004). p53 induces NF-κB activation by an IκB kinase-independent mechanism involving phosphorylation of p65 by ribosomal S6 kinase 1. J. Biol. Chem. *279*, 26115–26125.

Bond, M., Fabunmi, R., Baker, A., and Newby, A. (1998). Synergistic upregulation of metalloproteinase-9 by growth factors and inflammatory cytokines: an absolute requirement for transcription factor NF-κB. FEBS Lett. *435*, 29–34.

Boon, B. (2009). Leonardo da Vinci on atherosclerosis and the function of the sinuses of Valsalva. Netherlands Hear. J. *17*, 496–499.

Boonyasrisawat, W., Eberle, D., Bacci, S., Zhang, Y.-Y., Nolan, D., Gervino, E. V., Johnstone, M.T., Trischitta, V., Shoelson, S.E., and Doria, A. (2007). Tag polymorphisms at the A20 (TNFAIP3) locus are associated with lower gene expression and increased risk of coronary artery disease in type 2 diabetes. Diabetes *56*, 499–505.

Brand, K., Page, S., Rogler, G., Bartsch, a, Brandl, R., Knuechel, R., Page, M., Kaltschmidt, C., Baeuerle, P. a, and Neumeier, D. (1996). Activated transcription factor nuclear factor-kappa B is present in the atherosclerotic lesion. J. Clin. Invest. *97*, 1715–

1722.

Bremm, A., Freund, S.M. V, and Komander, D. (2010). Lys11-linked ubiquitin chains adopt compact conformations and are preferentially hydrolyzed by the deubiquitinase Cezanne. Nat. Struct. Mol. Biol. *17*, 939–947.

Bremm, A., Moniz, S., Mader, J., Rocha, S., and Komander, D. (2014). Cezanne (OTUD 7 B) regulates HIF- 1 a homeostasis in a proteasome-independent manner. 1–11.

Bren, G.D., Solan, N.J., Miyoshi, H., Pennington, K.N., Pobst, L.J., and Paya, C. V (2001). Transcription of the RelB gene is regulated by NF-kappaB. Oncogene *20*, 7722–7733.

Brummelkamp, T.R., Nijman, S.M.B., Dirac, A.M.G., and Bernards, R. (2003). Loss of the cylindromatosis tumour suppressor inhibits apoptosis by activating NF-kappaB. Nature *424*, 797–801.

Burkitt, M.D., Hanedi, A.F., Duckworth, C. a, Williams, J.M., Tang, J.M., O'Reilly, L. a, Putoczki, T.L., Gerondakis, S., Dimaline, R., Caamano, J.H., and Pritchard, D.M. (2015). NF-κB1, NF-κB2 and c-Rel differentially regulate susceptibility to colitis-associated adenoma development in C57BL/6 mice. J. Pathol. *236*, 326–336.

Caamaño, J., and Hunter, C. a (2002). NF-kappaB family of transcription factors: central regulators of innate and adaptive immune functions. Clin. Microbiol. Rev. *15*, 414–429.

Caamaño, J.H., Rizzo, C.A., Durham, S.K., Barton, D.S., Raventós-Suárez, C., Snapper, C.M., and Bravo, R. (1998). Nuclear Factor (NF)-κB2 (p100/p52) Is Required for Normal Splenic Microarchitecture and B Cell-mediated Immune Responses. J. Exp. Med. *187*, 185–196.

Cancel, L.M., and Tarbell, J.M. (2011). The role of mitosis in LDL transport through cultured endothelial cell monolayers. Am. J. Physiol. Heart Circ. Physiol. *300*, H769-76.

Cardozo, T., and Pagano, M. (2004). The SCF ubiquitin ligase: insights into a molecular machine. Nat. Rev. Mol. Cell Biol. *5*, 739–751.

Carmeliet, P., Dor, Y., Herbert, J.-M., Fukumura, D., Brusselmans, K., Dewerchin, M., Neeman, M., Bono, F., Abramovitch, R., Maxwell, P., Koch, C.J., Ratcliffe, P., Moons, L., Jain, R.K., Collen, D., and Keshert, E. (1998). Role of HIF-1A inhypoxia- mediated apoptosis, cell proliferation and tumour angiogenesis. Nature *394*, 485–490.

Caro, C.G., Fitz-Gerald, J.M., and Schroter, R.C. (1969). Arterial Wall Shear and Distribution of Early Atheroma in Man. Nature *223*, 1159–1161.

Caro, C.G., Fitz-Gerald, J.M., and Schroter, R.C. (1971). Atheroma and Arterial Wall

Shear Observation, Correlation and Proposal of a Shear Dependent Mass Transfer Mechanism for Atherogenesis. Proc. R. Soc. B Biol. Sci. *177*, 109–133.

Catz, S.D., and Johnson, J.L. (2001). Transcriptional regulation of bcl-2 by nuclear factor kappa B and its significance in prostate cancer. Oncogene *20*, 7342–7351.

Chakrabarti, S., Blair, P., and Freedman, J.E. (2007). CD40-40L signaling in vascular inflammation. J. Biol. Chem. *282*, 18307–18317.

Chappell, D.C., Varner, S.E., Nerem, R.M., Medford, R.M., and Alexander, R.W. (1998). Oscillatory Shear Stress Stimulates Adhesion Molecule Expression in Cultured Human Endothelium. Circ. Res. *82*, 532–539.

Chatzizisis, Y.S., Baker, A.B., Sukhova, G.K., Koskinas, K.C., Papafaklis, M.I., Beigel, R., Jonas, M., Coskun, A.U., Stone, B. V, Maynard, C., Shi, G.-P., Libby, P., Feldman, C.L., Edelman, E.R., and Stone, P.H. (2011). Augmented expression and activity of extracellular matrix-degrading enzymes in regions of low endothelial shear stress colocalize with coronary atheromata with thin fibrous caps in pigs. Circulation *123*, 621–630.

Chaudhury, H., Zakkar, M., Boyle, J., Cuhlmann, S., Van Der Heiden, K., Luong, L.A., Davis, J., Platt, A., Mason, J.C., Krams, R., Haskard, D.O., Clark, A.R., and Evans, P.C. (2010). C-Jun N-terminal kinase primes endothelial cells at atheroprone sites for apoptosis. Arterioscler. Thromb. Vasc. Biol. *30*, 546–553.

Chen, Z.J., Bhoj, V., and Seth, R.B. (2006). Ubiquitin, TAK1 and IKK: is there a connection? Cell Death Differ. *13*, 687–692.

Cheng, C., Haperen, R. Van, Waard, M. De, Damme, L.C. a Van, Tempel, D., Hanemaaijer, L., Cappellen, G.W. a Van, Bos, J., Slager, C.J., Duncker, D.J., Steen, A.F.W. Van Der, Crom, R. De, and Krams, R. (2005). Shear stress affects the intracellular distribution of eNOS : direct demonstration by a novel in vivo technique Plenary paper Shear stress affects the intracellular distribution of eNOS : direct demonstration by a novel in vivo technique. Blood *106*, 3691–3698.

Cheng, C., Tempel, D., Van Haperen, R., Van Der Baan, A., Grosveld, F., Daemen, M.J. a P., Krams, R., and De Crom, R. (2006). Atherosclerotic lesion size and vulnerability are determined by patterns of fluid shear stress. Circulation *113*, 2744–2753.

Chiu, J., and Chien, S. (2011). Effects of Disturbed Flow on Vascular Endothelium: Pathophysiological Basis and Clinical Perspectives. Physiol. Rev. *91*.

Chiu, J.-J., Chen, L.-J., Chang, S.-F., Lee, P.-L., Lee, C.-I., Tsai, M.-C., Lee, D.-Y., Hsieh,

H.-P., Usami, S., and Chien, S. (2005). Shear Stress Inhibits Smooth Muscle Cell–Induced Inflammatory Gene Expression in Endothelial Cells. Arterioscler. Thromb. Vasc. Biol. *25*, 963–969.

Choy, J.C., Granville, D.J., Hunt, D.W., and McManus, B.M. (2001). Endothelial cell apoptosis: biochemical characteristics and potential implications for atherosclerosis. J. Mol. Cell. Cardiol. *33*, 1673–1690.

Chung, J., Shim, H., Kim, K., Lee, D., Kim, W.J., Kang, D.H., Kang, S.W., Jo, H., and Kwon, K. (2016). Discovery of novel peptides targeting pro-atherogenic endothelium in disturbed flow regions -Targeted siRNA delivery to pro-atherogenic endothelium in vivo. Sci. Rep. *6*, 25636.

Cildir, G., Low, K.C., and Tergaonkar, V. (2016). Noncanonical NF-??B Signaling in Health and Disease. Trends Mol. Med. *22*, 414–429.

Claudio, E., Brown, K., Park, S., Wang, H., and Siebenlist, U. (2002). BAFF-induced NEMO-independent processing of NF-kappa B2 in maturing B cells. Nat. Immunol. *3*, 958–965.

Collins, T., Read, M.A., Neish, A.S., Whitley, M.Z., Thanos, D., and Maniatis, T. (1995). Transcriptional regulation of endothelial cell adhesion molecules: NF-κB and cytokine-inducible enhancers. FASEB J. *9*, 899–909.

Cominacini, L., Pasini, A.F., Garbin, U., Davoli, A., Tosetti, M., Campagnola, M., Rigoni, A., Pastorino, A., Lo Cascio, V., and Sawamura, T. (2000). Oxidized Low Density Lipoprotein (ox-LDL) Binding to ox-LDL Receptor-1 in Endothelial Cells Induces the Activation of NF-kappa B through an Increased Production of Intracellular Reactive Oxygen Species. J. Biol. Chem. *275*, 12633–12638.

Csordas, A., and Bernhard, D. (2013). The biology behind the atherothrombotic effects of cigarette smoke. Nat. Rev. Cardiol. *10*, 219–230.

Cuhlmann, S., Van der Heiden, K., Saliba, D., Tremoleda, J.L., Khalil, M., Zakkar, M., Chaudhury, H., Luong, L.A., Mason, J.C., Udalova, I., Gsell, W., Jones, H., Haskard, D.O., Krams, R., and Evans, P.C. (2011). Disturbed blood flow induces RelA expression via c-Jun N-terminal kinase 1: a novel mode of NF-κB regulation that promotes arterial inflammation. Circ. Res. *108*, 950–959.

Cunningham, K.S., and Gotlieb, A.I. (2005). The role of shear stress in the pathogenesis of atherosclerosis. Lab. Investig. *85*, 9–23.

Dardik, A., Chen, L., Frattini, J., Asada, H., Aziz, F., Kudo, F. a, and Sumpio, B.E. (2005).

Differential effects of orbital and laminar shear stress on endothelial cells. J. Vasc. Surg. *41*, 869–880.

David, Y., Ziv, T., Admon, A., and Navon, A. (2010). The E2 ubiquitin-conjugating enzymes direct polyubiquitination to preferred lysines. J. Biol. Chem. *285*, 8595–8604.

Davies, P., Remuzzi, A., Gordon, E.J., Dewey, C.F., and Gimbrone, M.A. (1986). Turbulent fluid shear stress induces vascular endothelial cell turnover in vitro. Proc. Natl. Acad. Sci. U. S. A. *83*, 2114–2117.

Delhase, M., Hayakawa, M., Chen, Y., and Karin, M. (1999). Positive and Negative Regulation of IB Kinase Activity Through IKK Subunit Phosphorylation. Science (80-.). *284*, 309–313.

Deshaies, R.J., and Joazeiro, C. a P. (2009). RING domain E3 ubiquitin ligases. Annu. Rev. Biochem. *78*, 399–434.

Dimmeler, S., Haendeler, J., Rippmann, V., Nehls, M., and Zeiher, a M. (1996). Shear stress inhibits apoptosis of human endothelial cells. FEBS Lett. *399*, 71–74.

Djuric, Z., Kashif, M., Fleming, T., Muhammad, S., Piel, D., von Bauer, R., Bea, F., Herzig, S., Zeier, M., Pizzi, M., Isermann, B., Hecker, M., Schwaninger, M., Bierhaus, A., and Nawroth, P.P. (2012). Targeting Activation of Specific NF-κB Subunits Prevents Stress-Dependent Atherothrombotic Gene Expression. Mol. Med. *18*, 1.

Dod, H.S., Bhardwaj, R., Sajja, V., Weidner, G., Hobbs, G.R., Konat, G.W., Manivannan, S., Gharib, W., Warden, B.E., Nanda, N.C., Beto, R.J., Ornish, D., and Jain, A.C. (2010). Effect of intensive lifestyle changes on endothelial function and on inflammatory markers of atherosclerosis. Am. J. Cardiol. *105*, 362–367.

De Donatis, G.M., Pape, E.L., Pierron, A., Cheli, Y., Hofman, V., Hofman, P., Allegra, M., Zahaf, K., Bahadoran, P., Rocchi, S., Bertolotto, C., Ballotti, R., and Passeron, T. (2015). NF-kB2 induces senescence bypass in melanoma via a direct transcriptional activation of EZH2. Oncogene *35*, 1–11.

Döring, Y., Drechsler, M., Soehnlein, O., and Weber, C. (2015). Neutrophils in atherosclerosis: From mice to man. Arterioscler. Thromb. Vasc. Biol. *35*, 288–295.

Doriot, P., Dorsaz, P., Dorsaz, L., De Benedetti, E., Chatelain, P., and Delafontaine, P. (2000). In-vivo measurements of wall shear stress in human coronary arteries. Coron. Artery Dis. *11*, 495–502.

Dormond, O., Contreras, A.G., Meijer, E., Datta, D., Flynn, E., Pal, S., and Briscoe, D.M.

(2008). CD40-Induced Signaling in Human Endothelial Cells Results in mTORC2- and Akt-Dependent Expression of Vascular Endothelial Growth Factor In Vitro and In Vivo. J. Immunol. *181*, 8088–8095.

Dunn, J., Qiu, H., Kim, S., Jjingo, D., Hoffman, R., Kim, C.W., Jang, I., Son, D.J., Kim, D., Pan, C., Fan, Y., Jordan, I.K., and Jo, H. (2014). Flow-dependent epigenetic DNA methylation regulates endothelial gene expression and atherosclerosis. J. Clin. Invest. *124*, 3187–3199.

Dutto, I., Tillhon, M., Cazzalini, O., Stivala, L.A., and Prosperi, E. (2014). Biology of the cell cycle inhibitor p21CDKN1A: molecular mechanisms and relevance in chemical toxicology. Arch. Toxicol. *89*, 155–178.

Dynek, J.N., Goncharov, T., Dueber, E.C., Fedorova, A. V, Izrael-Tomasevic, A., Phu, L., Helgason, E., Fairbrother, W.J., Deshayes, K., Kirkpatrick, D.S., and Vucic, D. (2010). c-IAP1 and UbcH5 promote K11-linked polyubiquitination of RIP1 in TNF signalling. EMBO J. *29*, 4198–4209.

Ea, C.-K., Deng, L., Xia, Z.-P., Pineda, G., and Chen, Z.J. (2006). Activation of IKK by TNFalpha requires site-specific ubiquitination of RIP1 and polyubiquitin binding by NEMO. Mol. Cell *22*, 245–257.

Enesa, K., Zakkar, M., Chaudhury, H., Luong, L. a, Rawlinson, L., Mason, J.C., Haskard, D.O., Dean, J.L.E., and Evans, P.C. (2008a). NF-kappaB suppression by the deubiquitinating enzyme Cezanne: a novel negative feedback loop in pro-inflammatory signaling. J. Biol. Chem. *283*, 7036–7045.

Enesa, K., Ito, K., Luong, L. a, Thorbjornsen, I., Phua, C., To, Y., Dean, J., Haskard, D.O., Boyle, J., Adcock, I., and Evans, P.C. (2008b). Hydrogen peroxide prolongs nuclear localization of NF-kappaB in activated cells by suppressing negative regulatory mechanisms. J. Biol. Chem. *283*, 18582–18590.

Evans, P.C., Taylor, E.R., Coadwell, J., Heyninck, K., Beyaert, R., and Kilshaw, P.J. (2001). Isolation and characterization of two novel A20-like proteins. Biochem. J. *357*, 617–623.

Evans, P.C., Smith, T.S., Lai, M.-J., Williams, M.G., Burke, D.F., Heyninck, K., Kreike, M.M., Beyaert, R., Blundell, T.L., and Kilshaw, P.J. (2003). A novel type of deubiquitinating enzyme. J. Biol. Chem. *278*, 23180–23186.

Evans, P.C., Ovaa, H., Hamon, M., Kilshaw, P.J., Hamm, S., Bauer, S., Ploegh, H.L., and Smith, T.S. (2004). Zinc-finger protein A20, a regulator of inflammation and cell

survival, has de-ubiquitinating activity. Biochem. J. *378*, 727–734.

Feaver, R.E., Gelfand, B.D., and Blackman, B.R. (2013). Human haemodynamic frequency harmonics regulate the inflammatory phenotype of vascular endothelial cells. Nat. Commun. *4*, 1525.

Feintuch, A., Ruengsakulrach, P., Lin, A., Zhang, J., Zhou, Y.-Q., Bishop, J., Davidson, L., Courtman, D., Foster, F.S., Steinman, D.A., Henkelman, R.M., and Ethier, C.R. (2007). Hemodynamics in the mouse aortic arch as assessed by MRI, ultrasound, and numerical modeling. Am. J. Physiol. Heart Circ. Physiol. *292*, 884–892.

Fong, A., and Sun, S.-C. (2002). Genetic evidence for the essential role of beta-transducin repeat-containing protein in the inducible processing of NF-kappa B2/p100. J. Biol. Chem. *277*, 22111–22114.

Fusco, A.J., Huang, D.-B., Miller, D., Wang, V.Y.-F., Vu, D., and Ghosh, G. (2009). NF-kappaB p52:RelB heterodimer recognizes two classes of kappaB sites with two distinct modes. EMBO Rep. *10*, 152–159.

Fütterer, A., Mink, K., Luz, A., Kosco-Vilbois, M.H., and Pfeffer, K. (1998). The lymphotoxin β receptor controls organogenesis and affinity maturation in peripheral lymphoid tissues. Immunity *9*, 59–70.

Ganguli, A., Persson, L., Palmer, I.R., Evans, I., Yang, L., Smallwood, R., Black, R., and Qwarnstrom, E.E. (2005). Distinct NF-??B regulation by shear stress through ras-dependent I??B?? oscillations: Real-time analysis of flow-mediated activation in live cells. Circ. Res. *96*, 626–634.

Gao, L., Chen, Q., Zhou, X., and Fan, L. (2012). The role of hypoxia-inducible factor 1 in atherosclerosis. J. Clin. Pathol. *65*, 872–876.

Gareus, R., Kotsaki, E., Xanthoulea, S., van der Made, I., Gijbels, M.J.J., Kardakaris, R., Polykratis, A., Kollias, G., de Winther, M.P.J., and Pasparakis, M. (2008). Endothelial cell-specific NF-kappaB inhibition protects mice from atherosclerosis. Cell Metab. *8*, 372–383.

Gene, N.N.B.P., Madge, L. a, Kluger, M.S., Orange, J.S., and May, M.J. (2008). Lymphotoxin- ⎵ 1 ␋ 2 and LIGHT Induce Classical and Noncanonical NF- B-Dependent Proinflammatory Gene Expression in Vascular Endothelial Cells 1. J. Immunol. *180*, 15–20.

Grimaldo, S., Tian, F., and Li, L.Y. (2009). Sensitization of endothelial cells to VEGI-induced apoptosis by inhibiting the NF-κB pathway. Apoptosis *14*, 788–795.

Guo, D., Chien, S., and Shyy, J.Y.J. (2007). Regulation of endothelial cell cycle by laminar versus oscillatory flow: Distinct modes of interactions of AMP-activated protein kinase and akt pathways. Circ. Res. *100*, 564–571.

Haas, T.L., Emmerich, C.H., Gerlach, B., Schmukle, A.C., Cordier, S.M., Rieser, E., Feltham, R., Vince, J., Warnken, U., Wenger, T., Koschny, R., Komander, D., Silke, J., and Walczak, H. (2009). Recruitment of the Linear Ubiquitin Chain Assembly Complex Stabilizes the TNF-R1 Signaling Complex and Is Required for TNF-Mediated Gene Induction. Mol. Cell *36*, 831–844.

Hahn, M., Macht, A., Waisman, A., and H??velmeyer, N. (2016). NF-??B-inducing kinase is essential for B-cell maintenance in mice. Eur. J. Immunol. *46*, 732–741.

Hajra, L., Evans, a I., Chen, M., Hyduk, S.J., Collins, T., and Cybulsky, M.I. (2000). The NF-kappa B signal transduction pathway in aortic endothelial cells is primed for activation in regions predisposed to atherosclerotic lesion formation. Proc. Natl. Acad. Sci. U. S. A. *97*, 9052–9057.

Hayden, M.S., and Ghosh, S. (2008). Shared principles in NF-kappaB signaling. Cell *132*, 344–362.

Van der Heiden, K., Cuhlmann, S., Luong, L. a, Zakkar, M., and Evans, P.C. (2010). Role of nuclear factor kappaB in cardiovascular health and disease. Clin. Sci. (Lond). *118*, 593–605.

Hellings, W.E., Peeters, W., Moll, F.L., Piers, S., Van Setten, J., Van Der Spek, P.J., De Vries, J.P.P.M., Seldenrijk, K.A., De Bruin, P.C., Vink, A., Velema, E., De Kleijn, D.P. V, and Pasterkamp, G. (2010). Composition of carotid atherosclerotic plaque is associated with cardiovascular outcome: A prognostic study. Circulation *121*, 1941–1950.

Henn, V., Slupsky, J.R., Gräfe, M., Anagnostopoulos, I., Förster, R., Müller-Berghaus, G., and Kroczek, R.A. (1998). CD40 ligand on activated platelets triggers an inflammatory reaction of endothelial cells. Nature *391*, 591–594.

Heo, K., Fujiwara, K., and Abe, J. (2011). Disturbed-Flow-Mediated Vascular Reactive Oxygen Species Induce Endothelial Dysfunction. Circ. J. *75*, 2722–2730.

Hjermann, I., Holme, I., Byre, K., and Leren, P. (1981). Effect of diet and smoking intervention on the incidence of coronary heart disease: report from the Oslo Study Group of a randomised trial in healthy men. Lancet *318*, 1303–1310.

Hoffmann, a, Natoli, G., and Ghosh, G. (2006). Transcriptional regulation via the NF-kappaB signaling module. Oncogene *25*, 6706–6716.

Hopkins, P.N. (2013). Molecular biology of atherosclerosis. Physiol. Rev. *93*, 1317–1542.

Hsu, H., Xiong, J., and Goeddel, D. (1995). The TNF Receptor 1-Associated Protein TRADD Signals Cell Death and NF-KB Activation. Cell *81*, 495–504.

Hsu, H., Shu, H.B., Pan, M.G., and Goeddel, D. V (1996a). TRADD-TRAF2 and TRADD-FADD interactions define two distinct TNF receptor 1 signal transduction pathways. Cell *84*, 299–308.

Hsu, H., Huang, J., Shu, H.B., Baichwal, V., and Goeddel, D. V (1996b). TNF-dependent recruitment of the protein kinase RIP to the TNF receptor-1 signaling complex. Immunity *4*, 387–396.

Hu, H., Brittain, G.C., Chang, J.-H., Puebla-Osorio, N., Jin, J., Zal, A., Xiao, Y., Cheng, X., Chang, M., Fu, Y.-X., Zal, T., Zhu, C., and Sun, S.-C. (2013). OTUD7B controls non-canonical NF-κB activation through deubiquitination of TRAF3. Nature *494*, 371–374.

Hu, H., Wang, H., Xiao, Y., Jin, J., Chang, J.-H., Zou, Q., Xie, X., Cheng, X., and Sun, S.-C. (2016). Otud7b facilitates T cell activation and inflammatory responses by regulating Zap70 ubiquitination. J. Exp. Med. jem.20151426.

Huxford, T., and Ghosh, G. (2009). A structural guide to proteins of the NF-κB signaling module. Cold Spring Harb. Perspect. … *1*, a000075.

Iannetti, A., Ledoux, A.C., Tudhope, S.J., Sellier, H., Zhao, B., Mowla, S., Moore, A., Hummerich, H., Gewurz, B.E., Cockell, S.J., Jat, P.S., Willmore, E., and Perkins, N.D. (2014). Regulation of p53 and Rb Links the Alternative NF-κB Pathway to EZH2 Expression and Cell Senescence. PLoS Genet. *10*, e1004642.

Iiyama, K., Hajra, L., Iiyama, M., Li, H., DiChiara, M., Medoff, B.D., and Cybulsky, M.I. (1999). Patterns of vascular cell adhesion molecule-1 and intercellular adhesion molecule-1 expression in rabbit and mouse atherosclerotic lesions and at sites predisposed to lesion formation. Circ. Res. *85*, 199–207.

Ishibashi, S., Brown, M.S., Goldstein, J.L., Gerard, R.D., Hammer, R.E., and Herz, J. (1993). Hypercholesterolemia in low density lipoprotein receptor knockout mice and its reversal by adenovirus-mediated gene delivery. J. Clin. Invest. *92*, 883–893.

Ishibashi, S., Goldstein, J.L., and Michael, S. (1994). Massive Xanthomatosis and Atherosclerosis in Cholesterol-fed Low Density Lipoprotein Receptor-negative Mice. J. Clin. Invest. *93*, 1885–1893.

Ishikawa, H., Carrasco, D., Claudio, E., Ryseck, R.P., and Bravo, R. (1997). Gastric

hyperplasia and increased proliferative responses of lymphocytes in mice lacking the COOH-terminal ankyrin domain of NF-kappaB2. J. Exp. Med. *186*, 999–1014.

Jacobs, M.D., and Harrison, S.C. (1998). Structure of an IκBα/NF-κB Complex. Cell *95*, 749–758.

Jaipersad, A.S., Lip, G.Y., Silverman, S., and Shantsila, E. (2013). The role of monocytes in angiogenesis and atherosclerosis. J. Am. Coll. Cardiol.

Jellusova, J., Miletic, A. V., Cato, M.H., Lin, W.W., Hu, Y., Bishop, G.A., Shlomchik, M.J., and Rickert, R.C. (2013). Context-Specific BAFF-R Signaling by the NF-κB and PI3K Pathways. Cell Rep. *5*, 1022–1035.

Jeong, S.J., Pise-Masison, C. a., Radonovich, M.F., Hyeon, U.P., and Brady, J.N. (2005). A novel NF-??B pathway involving IKK??and p65/RelA Ser-536 phosphorylation results in p53 inhibition in the absence of NF-??B transcriptional activity. J. Biol. Chem. *280*, 10326–10332.

Jhaveri, K., Debnath, P., Chernoff, J., Sanders, J., and Schwartz, M. (2012). The role of p21-activated kinase in the initiation of atherosclerosis. BMC Cardiovasc. Disord. *12*, 55.

Kanki, K., Akechi, Y., Ueda, C., Tsuchiya, H., Shimizu, H., Ishijima, N., Toriguchi, K., Hatano, E., Endo, K., Hirooka, Y., and Shiota, G. (2013). Biological and clinical implications of retinoic acid-responsive genes in human hepatocellular carcinoma cells. J. Hepatol. *59*, 1037–1044.

Kaplanski, G., Porat, R., Aiura, K., Erban, J.K., Gelfand, J. a, and Dinarello, C. a (1993). Activated platelets induce endothelial secretion of interleukin-8 in vitro via an interleukin-1-mediated event. Blood *81*, 2492–2495.

Kogan, M., Haine, V., Ke, Y., Wigdahl, B., Fischer-Smith, T., and Rappaport, J. (2012). Macrophage colony stimulating factor regulation by nuclear factor kappa B: a relevant pathway in human immunodeficiency virus type 1 infected macrophages. DNA Cell Biol. *31*, 280–289.

Komander, D., and Barford, D. (2008). Structure of the A20 OTU domain and mechanistic insights into deubiquitination. Biochem. J. *409*, 77–85.

Komander, D., and Rape, M. (2012). The ubiquitin code. Annu. Rev. Biochem. *81*, 203–229.

Komander, D., Clague, M.J., and Urbé, S. (2009). Breaking the chains: structure and function of the deubiquitinases. Nat. Rev. Mol. Cell Biol. *10*, 550–563.

Kovalenko, A., Chable-Bessia, C., Cantarella, G., Israël, A., Wallach, D., and Courtois, G. (2003). The tumour suppressor CYLD negatively regulates NF-κB signalling by deubiquitination. Nature *424*, 801–805.

Krappmann, D., Hatada, E.N., Tegethoff, S., Li, J., Klippel, a, Giese, K., Baeuerle, P. a, and Scheidereit, C. (2000). The I kappa B kinase (IKK) complex is tripartite and contains IKK gamma but not IKAP as a regular component. J. Biol. Chem. *275*, 29779–29787.

Kuchan, M.J., and Frangos, J. a (1994). Role of calcium and calmodulin in flow-induced nitric oxide production in endothelial cells. Am. J. Physiol. *266*, C628-36.

Lamothe, B., Besse, A., and Campos, A. (2007). Site-specific Lys-63-linked tumor necrosis factor receptor-associated factor 6 auto-ubiquitination is a critical determinant of IκB kinase activation. J. Biol. Chem. *282*, 4102–4112.

Lantz, J., Gårdhagen, R., and Karlsson, M. (2012). Quantifying turbulent wall shear stress in a subject specific human aorta using large eddy simulation. Med. Eng. Phys. *34*, 1139–1148.

Lawrence, T., Bebien, M., Liu, G.Y., Nizet, V., and Karin, M. (2005). IKKalpha limits macrophage NF-kappaB activation and contributes to the resolution of inflammation. Nature *434*, 1138–1143.

Lee, S.-H., and Hannink, M. (2002). Characterization of the nuclear import and export functions of Ikappa B(epsilon). J. Biol. Chem. *277*, 23358–23366.

Lee, D.-Y., Lee, C.-I., Lin, T.-E., Lim, S.H., Zhou, J., Tseng, Y.-C., Chien, S., and Chiu, J.-J. (2012). Role of histone deacetylases in transcription factor regulation and cell cycle modulation in endothelial cells in response to disturbed flow. Proc. Natl. Acad. Sci. U. S. A. *109*, 1967–1972.

Lee, T.H., Shank, J., Cusson, N., and Kelliher, M. a (2004). The kinase activity of Rip1 is not required for tumor necrosis factor-alpha-induced IkappaB kinase or p38 MAP kinase activation or for the ubiquitination of Rip1 by Traf2. J. Biol. Chem. *279*, 33185–33191.

Leroyer, A.S., Rautou, P.E., Silvestre, J.S., Castier, Y., Lesèche, G., Devue, C., Duriez, M., Brandes, R.P., Lutgens, E., Tedgui, A., and Boulanger, C.M. (2008). CD40 Ligand+ Microparticles From Human Atherosclerotic Plaques Stimulate Endothelial Proliferation and Angiogenesis. A Potential Mechanism for Intraplaque Neovascularization. J. Am. Coll. Cardiol. *52*, 1302–1311.

Liao, G., Zhang, M., Harhaj, E.W., and Sun, S.-C. (2004). Regulation of the NF-kappaB-inducing kinase by tumor necrosis factor receptor-associated factor 3-induced

degradation. J. Biol. Chem. *279*, 26243–26250.

Libby, P. (2002). Inflammation in atherosclerosis. Arterioscler. Thromb. Vasc. Biol. *32*, 2045–2051.

Ling, L., Cao, Z., and Goeddel, D. V (1998). NF-kappaB-inducing kinase activates IKK-alpha by phosphorylation of Ser-176. Proc. Natl. Acad. Sci. U. S. A. *95*, 3792–3797.

Liptay, S., Schmid, R.M., Nabel, E.G., and Nabel, G.J. (1994). Transcriptional Regulation of NF-κB2: Evidence for κB-Mediated Positive and Negative Autoregulation. Mol. Cell. Biol. *14*, 7695–7703.

Lopes, J., Adiguzel, E., Gu, S., Liu, S.L., Hou, G., Heximer, S., Assoian, R.K., and Bendeck, M.P. (2013). Type VIII collagen mediates vessel wall remodeling after arterial injury and fibrous cap formation in atherosclerosis. Am. J. Pathol. *182*, 2241–2253.

Luong, L. a, Fragiadaki, M., Smith, J., Boyle, J., Lutz, J., Dean, J.L.E., Harten, S., Ashcroft, M., Walmsley, S.R., Haskard, D.O., Maxwell, P.H., Walczak, H., Pusey, C., and Evans, P.C. (2013). Cezanne regulates inflammatory responses to hypoxia in endothelial cells by targeting TRAF6 for deubiquitination. Circ. Res. *112*, 1583–1591.

Lutgens, E., Gorelik, L., Daemen, M.J., de Muinck, E.D., Grewal, I.S., Koteliansky, V.E., and Flavell, R. a (1999). Requirement for CD154 in the progression of atherosclerosis. Nat. Med. *5*, 1313–1316.

Luttun, A., Lutgens, E., Manderveld, A., Maris, K., Collen, D., Carmeliet, P., and Moons, L. (2004). Loss of matrix metalloproteinase-9 or matrix metalloproteinase-12 protects apolipoprotein E-deficient mice against atherosclerotic media destruction but differentially affects plaque growth. Circulation *109*, 1408–1414.

Ma, Y., Wang, W., Zhang, J., Lu, Y., Wu, W., Yan, H., and Wang, Y. (2012). Hyperlipidemia and atherosclerotic lesion development in Ldlr-deficient mice on a long-term high-fat diet. PLoS One *7*, e35835.

Mahmoud, M.M., Kim, H.R., Xing, R., Hsiao, S., Mammoto, A., Chen, J., Serbanovic-Canic, J., Feng, S., Bowden, N.P., Maguire, R., Ariaans, M., Francis, S.E., Weinberg, P.D., Van Der Heiden, K., Jones, E.A., Chico, T.J.A., Ridger, V., and Evans, P.C. (2016). TWIST1 integrates endothelial responses to flow in vascular dysfunction and atherosclerosis. Circ. Res. *119*, 450–462.

Malek, S., Chen, Y., Huxford, T., and Ghosh, G. (2001). IkappaBbeta, but not IkappaBalpha, functions as a classical cytoplasmic inhibitor of NF-kappaB dimers by masking both NF-kappaB nuclear localization sequences in resting cells. J. Biol. Chem.

276, 45225–45235.

Malinverni, C., Unterreiner, A., and Staal, J. (2010). Cleavage by MALT1 induces cytosolic release of A20. Biochem. Biophys. Res. Commun. *400*, 543–547.

Martin, L., Murphy, M., Scanlon, A., Naismith, C., Clark, D., and Farouque, O. (2014). Timely treatment for acute myocardial infarction and health outcomes: An integrative review of the literature. Aust. Crit. Care *27*, 111–118.

Matsuzawa, A., Tseng, P.-H., Vallabhapurapu, S., Luo, J.-L., Zhang, W., Wang, H., Vignali, D. a a, Gallagher, E., and Karin, M. (2008). Essential cytoplasmic translocation of a cytokine receptor-assembled signaling complex. Science (80-.). *321*, 663–668.

Melter, M., Reinders, M.E.J., Sho, M., Pal, S., Geehan, C., Denton, M.D., Mukhopadhyay, D., and Briscoe, D.M. (2000). Ligation of CD40 induces the expression of vascular endothelial growth factor by endothelial cells and monocytes and promotes angiogenesis in vivo. Blood *96*, 3801–3809.

Michiels, C. (2003). Endothelial cell functions. J. Cell. Physiol. *196*, 430–443.

Milner, J.S., Moore, J.A., Rutt, B.K., and Steinman, D.A. (1998). Hemodynamics of human carotid artery bifurcations: Computational studies with models reconstructed from magnetic resonance imaging of normal subjects. J. Vasc. Surg. *28*, 143–156.

Mohan, S., Mohan, N., and Sprague, E.A. (1997). Differential activation of NF-kappa B in human aortic endothelial cells conditioned to specific flow environments. Am. J. Physiol. *273*, C572-8.

Moles, A., Sanchez, A.M., Banks, P.S., Murphy, L.B., Luli, S., Borthwick, L., Fisher, A., O'Reilly, S., van Laar, J.M., White, S. a., Perkins, N.D., Burt, A.D., Mann, D. a., and Oakley, F. (2013). Inhibition of RelA-Ser536 phosphorylation by a competing peptide reduces mouse liver fibrosis without blocking the innate immune response. Hepatology *57*, 817–828.

Moniz, S., Bandarra, D., Biddlestone, J., and Campbell, K.J. (2015). Cezanne Regulates E2F1- dependent HIF2α expression Journal of Cell Science Accepted manuscript.

Müller, C., and Harrison, S. (1995). The structure of the NF-κB p50:DNA-complex: a starting point for analysing the Rel family. FEBS Lett. *369*, 113–117.

Nagel, T., Resnick, N., Dewey Jr., C.F., and Gimbrone Jr., M.A. (1999). Vascular endothelial cells respond to spatial gradients in fluid shear stress by enhanced activation of transcription factors. Arter. Thromb Vasc Biol *19*, 1825–34.

Nam, D., Ni, C.-W., Rezvan, A., Suo, J., Budzyn, K., Llanos, A., Harrison, D., Giddens, D., and Jo, H. (2009). Partial carotid ligation is a model of acutely induced disturbed flow, leading to rapid endothelial dysfunction and atherosclerosis. Am. J. Physiol. Heart Circ. Physiol. *297*, H1535–H1543.

Napoli, C., Armiento, F.P.D., Mancini, F.P., Postiglione, A., and Witztum, J.L. (2005). Fatty Streak Formation Occurs in Human Fetal Aortas and is Greatly Enhanced by Maternal Hypercholesterolemia. *100*, 2680–2690.

Natarajan, R., Fisher, B.J., Jones, D.G., and Fowler, A.A. (2002). Atypical mechanism of NF-??B activation during reoxygenation stress in microvascular endothelium: A role for tyrosine kinases. Free Radic. Biol. Med. *33*, 962–973.

Natoli, G., Saccani, S., Bosisio, D., and Marazzi, I. (2005). Interactions of NF-kappaB with chromatin: the art of being at the right place at the right time. Nat. Immunol. *6*, 439–445.

Nelson, D.E., Ihekwaba, a E.C., Elliott, M., Johnson, J.R., Gibney, C. a, Foreman, B.E., Nelson, G., See, V., Horton, C. a, Spiller, D.G., Edwards, S.W., McDowell, H.P., Unitt, J.F., Sullivan, E., Grimley, R., Benson, N., Broomhead, D., Kell, D.B., and White, M.R.H. (2004). Oscillations in NF-kappaB signaling control the dynamics of gene expression. Science *306*, 704–708.

Ni, C.W., Qiu, H., Rezvan, A., Kwon, K., Nam, D., Son, D.J., Visvader, J.E., and Jo, H. (2010). Discovery of novel mechanosensitive genes in vivo using mouse carotid artery endothelium exposed to disturbed flow. Blood *116*, 66–73.

Obikane, H., Abiko, Y., Ueno, H., Kusumi, Y., Esumi, M., and Mitsumata, M. (2010). Effect of endothelial cell proliferation on atherogenesis: A role of p21Sdi/Cip/Waf1 in monocyte adhesion to endothelial cells. Atherosclerosis *212*, 116–122.

Oeckinghaus, A., Hayden, M.S., and Ghosh, S. (2011). Crosstalk in NF-κB signaling pathways. Nat. Immunol. *12*, 695–708.

Onder, L., Danuser, R., Scandella, E., Firner, S., Chai, Q., Hehlgans, T., Stein, J. V, and Ludewig, B. (2013). Endothelial cell-specific lymphotoxin-β receptor signaling is critical for lymph node and high endothelial venule formation. J. Exp. Med. *210*, 465–473.

Parhami, F., Fang, Z.T., Fogelman, A.M., Andalibi, A., Territo, M.C., and Berliner, J.A. (1993). Minimally modified low density lipoprotein-induced inflammatory responses in endothelial cells are mediated by cyclic adenosine monophosphate. J. Clin. Invest. *92*, 471–478.

Park, S.G., Chung, C., Kang, H., Kim, J.-Y., and Jung, G. (2006). Up-regulation of cyclin D1 by HBx is mediated by NF-??B2/BCL3 complex through ??B site of cyclin D1 promoter. J. Biol. Chem. *281*, 31770–31777.

Partridge, J., Carlsen, H., Enesa, K., Chaudhury, H., Zakkar, M., Luong, L., Kinderlerer, A., Johns, M., Blomhoff, R., Mason, J.C., Haskard, D.O., and Evans, P.C. (2007). Laminar shear stress acts as a switch to regulate divergent functions of NF-kappaB in endothelial cells. FASEB J. *21*, 3553–3561.

Passerini, A.G., Polacek, D.C., Shi, C., Francesco, N.M., Manduchi, E., Grant, G.R., Pritchard, W.F., Powell, S., Chang, G.Y., Stoeckert, C.J., and Davies, P.F. (2004). Coexisting proinflammatory and antioxidative endothelial transcription profiles in a disturbed flow region of the adult porcine aorta. Proc. Natl. Acad. Sci. U. S. A. *101*, 2482–2487.

Peng, J., Schwartz, D., Elias, J.E., Thoreen, C.C., Cheng, D., Marsischky, G., Roelofs, J., Finley, D., and Gygi, S.P. (2003). A proteomics approach to understanding protein ubiquitination. Nat. Biotechnol. *21*, 921–926.

Perkins, N.D. (2006). Post-translational modifications regulating the activity and function of the nuclear factor kappa B pathway. Oncogene *25*, 6717–6730.

Ramachandiran, S., Adon, A., Guo, X., Wang, Y., Wang, H., Chen, Z., Kowalski, J., Sunay, U.R., Young, A.N., Brown, T., Mar, J.C., Du, Y., Fu, H., Mann, K.P., Natkunam, Y., Boise, L.H., Saavedra, H.I., Lossos, I.S., and Bernal-Mizrachi, L. (2015). Chromosome instability in diffuse large B cell lymphomas is suppressed by activation of the noncanonical NF-??B pathway. Int. J. Cancer *136*, 2341–2351.

Reidy, M. a, and Langille, B.L. (1980). The effect of local blood flow patterns on endothelial cell morphology. Exp. Mol. Pathol. *32*, 276–289.

Rocha, S., Martin, A.M., Meek, D.W., and Perkins, N.D. (2003). p53 represses cyclin D1 transcription through down regulation of Bcl-3 and inducing increased association of the p52 NF-kappaB subunit with histone deacetylase 1. Mol. Cell. Biol. *23*, 4713–4727.

Sakurai, H., Suzuki, S., Kawasaki, N., Nakano, H., Okazaki, T., Chino, A., Doi, T., and Saiki, I. (2003). Tumor necrosis factor-??-induced IKK phosphorylation of NF-??B p65 on serine 536 is mediated through the TRAF2, TRAF5, and TAK1 signaling pathway. J. Biol. Chem. *278*, 36916–36923.

Samady, H., Eshtehardi, P., McDaniel, M.C., Suo, J., Dhawan, S.S., Maynard, C., Timmins, L.H., Quyyumi, A.A., and Giddens, D.P. (2011). Coronary artery wall shear

stress is associated with progression and transformation of atherosclerotic plaque and arterial remodeling in patients with coronary artery disease. Circulation *124*, 779–788.

Santilli, S.M., Stevens, R.B., Anderson, J.G., Payne, W.D., and Caldwell, M. de F. (1995). Transarterial wall oxygen gradients at the dog carotid bifurcation. Am. J. Physiol. *268*, H155–H161.

Sasaki, C.Y., Barberi, T.J., Ghosh, P., and Longo, D.L. (2005). Phosphorylation of Re1A/p65 on serine 536 defines an I??B??- independent NF-??B pathway. J. Biol. Chem. *280*, 34538–34547.

Sata, M., Saiura, A., Kunisato, A., Tojo, A., Okada, S., Tokuhisa, T., Hirai, H., Makuuchi, M., Hirata, Y., and Nagai, R. (2002). Hematopoietic stem cells differentiate into vascular cells that participate in the pathogenesis of atherosclerosis. Nat.Med *8*, 403–409.

Saxon, J.A., Cheng, D.-S., Han, W., Polosukhin, V. V., McLoed, A.G., Richmond, B.W., Gleaves, L.A., Tanjore, H., Sherrill, T.P., Barham, W., Yull, F.E., and Blackwell, T.S. (2016). p52 Overexpression Increases Epithelial Apoptosis, Enhances Lung Injury, and Reduces Survival after Lipopolysaccharide Treatment. J. Immunol. *196*, 1891–1899.

Schober, A., Nazari-Jahantigh, M., Wei, Y., Bidzhekov, K., Gremse, F., Grommes, J., Megens, R.T.A., Heyll, K., Noels, H., Hristov, M., Wang, S., Kiessling, F., Olson, E.N., and Weber, C. (2014). MicroRNA-126-5p promotes endothelial proliferation and limits atherosclerosis by suppressing Dlk1. Nat. Med. *20*, 368–376.

Schulman, B., and Harper, J. (2009). Ubiquitin-like protein activation by E1 enzymes: the apex for downstream signalling pathways. Nat. Rev. Mol. Cell Biol. *10*, 319–331.

Schumm, K., Rocha, S., Caamano, J., and Perkins, N.D. (2006). Regulation of p53 tumour suppressor target gene expression by the p52 NF-kappaB subunit. EMBO J. *25*, 4820–4832.

Seimon, T., and Tabas, I. (2009). Mechanisms and consequences of macrophage apoptosis in atherosclerosis. J. Lipid Res. *50*, S382–S387.

Semenza, G.L. (1996). Molecular Mechanisms of Oxygen Homeostasis TranscriptionalRegulation by Hypoxia-InducibleFactor I. Science (80-.). *6*, 151–157.

Sen, R., and Smale, S.T. (2009). Selectivity of the NF- B Response. Cold Spring Harb. Perspect. Biol. *2*, a000257–a000257.

Serbanovic-Canic, J., de Luca, A., Warboys, C., Ferreira, P., Luong, L.A., Hsiao, S., Gauci, I., Mahmoud, M., Feng, S., Souilhol, C., Bowden, N., Ashton, J., Walczak, H., Firmin, D.,

Krams, R., Mason, J., Haskard, D., Sherwin, S., Ridger, V., Chico, T., and Evans, P. (2016). Zebrafish Model for Functional Screening of Flow-Responsive Genes. Arterioscler. Thromb. Vasc. Biol. 100.

Shyy, Y.J., Hsieh, H.J., Usami, S., and Chien, S. (1994). Fluid shear stress induces a biphasic response of human monocyte chemotactic protein 1 gene expression in vascular endothelium. Proc. Natl. Acad. Sci. U. S. A. *91*, 4678–4682.

Skaug, B., Jiang, X., and Chen, Z.J. (2009). The role of ubiquitin in NF-kappaB regulatory pathways. Annu. Rev. Biochem. *78*, 769–796.

De Smaele, E., Zazzeroni, F., Papa, S., Nguyen, D.U., Jin, R., Jones, J., Cong, R., and Franzoso, G. (2001). Induction of gadd45beta by NF-kappaB downregulates pro-apoptotic JNK signalling. Nature *414*, 308–313.

Solan, N.J., Miyoshi, H., Carmona, E.M., Bren, G.D., and Paya, C. V (2002). RelB cellular regulation and transcriptional activity are regulated by p100. J. Biol. Chem. *277*, 1405–1418.

Staughton, T.J., Lever, M.J., and Weinberg, P.D. (2001). Effect of altered flow on the pattern of permeability around rabbit aortic branches. Am. J. Physiol. Heart Circ. Physiol. *281*, H53-9.

Stone, G.W., Maehara, A., Lansky, A.J., de Bruyne, B., Cristea, E., Mintz, G.S., Mehran, R., McPherson, J., Farhat, N., Marso, S.P., Parise, H., Templin, B., White, R., Zhang, Z., and Serruys, P.W. (2011). A Prospective Natural-History Study of Coronary Atherosclerosis. N. Engl. J. Med. *364*, 226–235.

Sun, S.-C. (2011). Non-canonical NF-κB signaling pathway. Cell Res. *21*, 71–85.

Sun, S.-C., and Ley, S.C. (2008). New insights into NF-kappaB regulation and function. Trends Immunol. *29*, 469–478.

Sun, S., Tang, Y., Lou, X., Zhu, L., Yang, K., Zhang, B., Shi, H., and Wang, C. (2007). UXT is a novel and essential cofactor in the NF-??B transcriptional enhanceosome. J. Cell Biol. *178*, 231–244.

Suo, J., Ferrara, D.E., Sorescu, D., Guldberg, R.E., Taylor, W.R., and Giddens, D.P. (2007). Hemodynamic shear stresses in mouse aortas: implications for atherogenesis. Arterioscler. Thromb. Vasc. Biol. *27*, 346–351.

Surapisitchat, J., Hoefen, R.J., Pi, X., Yoshizumi, M., Yan, C., and Berk, B.C. (2001). Fluid shear stress inhibits TNF-alpha activation of JNK but not ERK1/2 or p38 in human

umbilical vein endothelial cells: Inhibitory crosstalk among MAPK family members. Proc. Natl. Acad. Sci. U. S. A. *98*, 6476–6481.

Tarbell, J.M. (2003). Mass transport in arteries and the localization of atherosclerosis. Annu. Rev. Biomed. Eng. *5*, 79–118.

Tirziu, D., Jaba, I.M., Yu, P., Larrivée, B., Coon, B.G., Cristofaro, B., Zhuang, Z.W., Lanahan, A.A., Schwartz, M.A., Eichmann, A., and Simons, M. (2012). Endothelial nuclear factor-??B-dependent regulation of arteriogenesis and branching. Circulation *126*, 2589–2600.

Tokunaga, F. (2013). Linear ubiquitination-mediated NF-κB regulation and its related disorders. J. Biochem. *154*, 313–323.

Townsend, N., Bhatnagar, P., Wilkins, E., Wickramasinghe, K., and Rayner, M. (2015). Cardiovascular Disease Statistics, 2015 (British Heart Foundation: London).

Trompouki, E., Hatzivassiliou, E., Tsichritzis, T., Farmer, H., Ashworth, A., and Mosialos, G. (2003). CYLD is a deubiquitinating enzyme that negatively regulates NF-kappaB activation by TNFR family members. Nature *424*, 793–796.

Tzima, E., Irani-Tehrani, M., Kiosses, W.B., Dejana, E., Schultz, D. a, Engelhardt, B., Cao, G., DeLisser, H., and Schwartz, M.A. (2005). A mechanosensory complex that mediates the endothelial cell response to fluid shear stress. Nature *437*, 426–431.

Urbich, C., Mallat, Z., Tedgui, A., Clauss, M., Zeiher, A.M., and Dimmeler, S. (2001). Upregulation of TRAF-3 by shear stress blocks CD40-mediated endothelial activation. J. Clin. Invest. *108*, 1451–1458.

Vallabhapurapu, S., and Karin, M. (2009). Regulation and function of NF-kappaB transcription factors in the immune system. Annu. Rev. Immunol. *27*, 693–733.

Vallabhapurapu, S., Matsuzawa, A., Zhang, W., Tseng, P.-H., Keats, J.J., Wang, H., Vignali, D. a a, Bergsagel, P.L., and Karin, M. (2008). Nonredundant and complementary functions of TRAF2 and TRAF3 in a ubiquitination cascade that activates NIK-dependent alternative NF-kappaB signaling. Nat. Immunol. *9*, 1364–1370.

Vallabhapurapu, S.D., Noothi, S.K., Pullum, D.A., Lawrie, C.H., Pallapati, R., Potluri, V., Kuntzen, C., Khan, S., Plas, D.R., Orlowski, R.Z., Chesi, M., Kuehl, W.M., Bergsagel, P.L., Karin, M., and Vallabhapurapu, S. (2015). Transcriptional repression by the HDAC4–RelB–p52 complex regulates multiple myeloma survival and growth. Nat. Commun. *6*, 8428.

VanderLaan, P. a, Reardon, C. a, and Getz, G.S. (2004). Site specificity of atherosclerosis: site-selective responses to atherosclerotic modulators. Arterioscler. Thromb. Vasc. Biol. *24*, 12–22.

Vijay-Kumar, S., Bugg, C.E., and Cook, W.J. (1987). Structure of ubiquitin refined at 1.8 A resolution. J. Mol. Biol. *194*, 531–544.

Vince, J.E., Pantaki, D., Feltham, R., Mace, P.D., Cordier, S.M., Schmukle, A.C., Davidson, A.J., Callus, B. a, Wong, W.W.-L., Gentle, I.E., Carter, H., Lee, E.F., Walczak, H., Day, C.L., Vaux, D.L., and Silke, J. (2009). TRAF2 must bind to cellular inhibitors of apoptosis for tumor necrosis factor (tnf) to efficiently activate nf-{kappa}b and to prevent tnf-induced apoptosis. J. Biol. Chem. *284*, 35906–35915.

Vondenhoff, M.F., Greuter, M., Goverse, G., Elewaut, D., Dewint, P., Ware, C.F., Hoorweg, K., Kraal, G., and Mebius, R.E. (2009). LT R Signaling Induces Cytokine Expression and Up-Regulates Lymphangiogenic Factors in Lymph Node Anlagen. J. Immunol. *182*, 5439–5445.

Wada, S., and Karino, T. (2002). Theoretical Prediction of Low-Density Lipoproteins Concentration at the Luminal Surface of an Artery with a Multiple Bend. Ann. Biomed. Eng. *30*, 778–791.

Walsh, M.C., Kim, G.K., Maurizio, P.L., Molnar, E.E., and Choi, Y. (2008). TRAF6 autoubiquitination-independent activation of the NFkappaB and MAPK pathways in response to IL-1 and RANKL. PLoS One *3*, e4064.

Wang, X., and Sonenshein, G.E. (2005). Induction of the RelB NF- κ B Subunit by the Cytomegalovirus IE1 Protein Is Mediated via Jun Kinase and c-Jun / Fra-2 AP-1 Complexes Induction of the RelB NF- □ B Subunit by the Cytomegalovirus IE1 Protein Is Mediated via Jun Kinase and c-Jun / Fra-2 AP-1. *79*, 95–105.

Wang, Y., and Sheibani, N. (2006). PECAM-1 isoform-specific activation of MAPK/ERKs and small GTPases: Implications in inflammation and angiogenesis. J. Cell. Biochem. *98*, 451–468.

Wang, C., Baker, B.M., Chen, C.S., and Schwartz, M.A. (2013a). Endothelial cell sensing of flow direction. Arterioscler. Thromb. Vasc. Biol. *33*, 2130–2136.

Wang, L., Wu, X., Shi, T., and Lu, L. (2013b). Epidermal growth factor (EGF)-induced corneal epithelial wound healing through nuclear factor κB subtype-regulated CCCTC binding factor (CTCF) activation. J. Biol. Chem. *288*, 24363–24371.

Warboys, C.M., Amini, N., de Luca, A., and Evans, P.C. (2011). The role of blood flow in

determining the sites of atherosclerotic plaques. F1000 Med. Rep. *3*, 5.

Warboys, C.M., de Luca, A., Amini, N., Luong, L., Duckles, H., Hsiao, S., White, A., Biswas, S., Khamis, R., Chong, C.K., Cheung, W.-M., Sherwin, S.J., Bennett, M.R., Gil, J., Mason, J.C., Haskard, D.O., and Evans, P.C. (2014). Disturbed Flow Promotes Endothelial Senescence via a p53-Dependent Pathway. Arterioscler. Thromb. Vasc. Biol. *34*, 985–995.

Weber, C., and Noels, H. (2011). Atherosclerosis: current pathogenesis and therapeutic options. Nat. Med. *17*, 1410–1422.

Weinbaum, S., Tzeghai, G., Ganatos, P., Pfeffer, R., and Chien, S. (1985). Effect of cell turnover and leaky junctions on arterial macromolecular transport. Am. J. Physiol. *248*, H945-60.

Wertz, I., O'Rourke, K., Zhou, H., and Eby, M. (2004). De-ubiquitination and ubiquitin ligase domains of A20 downregulate NF-κB signalling. Nature *430*.

Wilson, P.W.F., D'Agostino, R.B., Levy, D., Belanger, a. M., Silbershatz, H., and Kannel, W.B. (1998). Prediction of Coronary Heart Disease Using Risk Factor Categories. Circulation *97*, 1837–1847.

de Winther, M.P.J., Kanters, E., Kraal, G., and Hofker, M.H. (2005). Nuclear factor kappaB signaling in atherogenesis. Arterioscler. Thromb. Vasc. Biol. *25*, 904–914.

de Wit, H., Dokter, W.H., Koopmans, S.B., Lummen, C., van der Leij, M., Smit, J.W., and Vellenga, E. (1998). Regulation of p100 (NFKB2) expression in human monocytes in response to inflammatory mediators and lymphokines. Leuk. Off. J. Leuk. Soc. Am. Leuk. Res. Fund, U.K *12*, 363–370.

Xiao, G., Harhaj, E., and Sun, S. (2001). NF-κB-Inducing Kinase Regulates the Processing of NF-κB2 p100. Mol. Cell *7*, 401–409.

Xu, Y., Fang, F., St Clair, D.K., Sompol, P., Josson, S., and St Clair, W.H. (2008). SN52, a novel nuclear factor-kappaB inhibitor, blocks nuclear import of RelB:p52 dimer and sensitizes prostate cancer cells to ionizing radiation. Mol. Cancer Ther. *7*, 2367–2376.

Xu, Z., Pei, L., Wang, L., Zhang, F., Hu, X., and Gui, Y. (2014). Snail1-dependent transcriptional repression of Cezanne2 in hepatocellular carcinoma. Oncogene *33*, 2836–2845.

Yamada, T., Mitani, T., Yorita, K., Uchida, D., Matsushima, a, Iwamasa, K., Fujita, S., and Matsumoto, M. (2000). Abnormal immune function of hemopoietic cells from

alymphoplasia (aly) mice, a natural strain with mutant NF-kappa B-inducing kinase. J. Immunol. *165*, 804–812.

Yang, C., Atkinson, S.P., Vilella, F., Lloret, M., Armstrong, L., Mann, D.A., and Lako, M. (2010). Opposing putative roles for canonical and noncanonical NF??B signaling on the survival, proliferation, and differentiation potential of human embryonic stem cells. Stem Cells *28*, 1970–1980.

Yang, Y., Fang, S., Jensen, J., Weissman, A., and Ashwell, J. (2000). Ubiquitin Protein Ligase Activity of IAPs and Their Degradation in Proteasomes in Response to Apoptotic Stimuli. Science (80-.). *288*, 874–877.

Ye, Y., and Rape, M. (2009). Building ubiquitin chains: E2 enzymes at work. Nat. Rev. Mol. Cell Biol. *10*, 755–764.

Yoshida, H., and Kisugi, R. (2010). Mechanisms of LDL oxidation. Clin. Chim. Acta *411*, 1875–1882.

Yu, X.H., Fu, Y.C., Zhang, D.W., Yin, K., and Tang, C.K. (2013). Foam cells in atherosclerosis. Clin. Chim. Acta *424*, 245–252.

Yusuf, S., Hawken, S., Ôunpuu, S., Dans, T., Avezum, A., Lanas, F., McQueen, M., Budaj, A., Pais, P., Varigos, J., and Lisheng, L. (2004). Effect of potentially modifiable risk factors associated with myocardial infarction in 52 countries in a case-control study based on the INTERHEART study. Lancet *364*, 937–952.

Zakkar, M., Chaudhury, H., Sandvik, G., Enesa, K., Luong, L.A., Cuhlmann, S., Mason, J.C., Krams, R., Clark, A.R., Haskard, D.O., and Evans, P.C. (2008). Increased endothelial mitogen-activated protein kinase phosphatase-1 expression suppresses proinflammatory activation at sites that are resistant to atherosclerosis. Circ. Res. *103*, 726–732.

Zakkar, M., Van der Heiden, K., Luong, L.A., Chaudhury, H., Cuhlmann, S., Hamdulay, S.S., Krams, R., Edirisinghe, I., Rahman, I., Carlsen, H., Haskard, D.O., Mason, J.C., and Evans, P.C. (2009). Activation of Nrf2 in endothelial cells protects arteries from exhibiting a proinflammatory state. Arterioscler. Thromb. Vasc. Biol. *29*, 1851–1857.

Zambon, A.C. (2011). NIH Public Access. *77*, 564–570.

Zandi, E., Rothwarf, D., and Delhase, M. (1997). The IκB Kinase Complex (IKK) Contains Two Kinase Subunits, IKKα and IKKβ, Necessary for IκB Phosphorylation and NF-κB Activation. Cell *91*, 243–252.

Zarnegar, B., Yamazaki, S., He, J.Q., and Cheng, G. (2008a). Control of canonical NF-kappaB activation through the NIK-IKK complex pathway. Proc. Natl. Acad. Sci. U. S. A. *105*, 3503–3508.

Zarnegar, B.J., Wang, Y., Mahoney, D.J., Dempsey, P.W., Cheung, H.H., He, J., Shiba, T., Yang, X., Yeh, W.-C., Mak, T.W., Korneluk, R.G., and Cheng, G. (2008b). Noncanonical NF-kappaB activation requires coordinated assembly of a regulatory complex of the adaptors cIAP1, cIAP2, TRAF2 and TRAF3 and the kinase NIK. Nat. Immunol. *9*, 1371–1378.

Zeng, L., Zhang, Y., Chien, S., Liu, X., and Shyy, J.Y.J. (2003). The Role of p53 Deacetylation in p21Waf1 Regulation by Laminar Flow. J. Biol. Chem. *278*, 24594–24599.

Zeng, L., Xiao, Q., Margariti, A., Zhang, Z., Zampetaki, A., Patel, S., Capogrossi, M.C., Hu, Y., and Xu, Q. (2006). HDAC3 is crucial in shear- and VEGF-induced stem cell differentiation toward endothelial cells. J. Cell Biol. *174*, 1059–1069.

Zhang, J., and Stirling, B. (2006). Impaired regulation of NF-κB and increased susceptibility to colitis-associated tumorigenesis in CYLD-deficient mice. J. Clin. Invest. *116*, 3042–3049.

Zhong, H., Voll, R.E., and Ghosh, S. (1998). Phosphorylation of NF-kappa B p65 by PKA stimulates transcriptional activity by promoting a novel bivalent interaction with the coactivator CBP/p300. Mol. Cell *1*, 661–671.

Zimmerman, M. (1993). The paleopathology of the cardiovascular system. Texas Hear. Inst. J. *20*, 252–257.

Author Contributions

All work was carried out by Neil Bowden apart from RNA isolation from porcine scrapes (Figure 5.1) and Western blotting for HIF-1α and its target genes (Figures 4.5 and 4.6). These were carried out by Dr Ismael Gauci and Dr Shuang Feng respectively.